EFFECT OF NON-THERMAL ATMOSPHERIC PRESSURE PLASMA ON WOUND BACTERIA AND CELL PROLIFERATION

NORHAYATI BINTI MOHD NASIR

FACULTY OF SCIENCE
UNIVERSITI MALAYA
KUALA LUMPUR

2020

EFFECT OF NON-THERMAL ATMOSPHERIC PRESSURE PLASMA ON WOUND BACTERIA AND CELL PROLIFERATION

NORHAYATI BINTI MOHD NASIR

THESIS SUBMITTED IN FULFILMENT OF THE REQUIREMENTS FOR THE DEGREE OF DOCTOR OF PHILOSOPHY

DEPARTMENT OF PHYSICS
FACULTY OF SCIENCE
UNIVERSITI MALAYA
KUALA LUMPUR

2020

UNIVERSITI MALAYA
ORIGINAL LITERARY WORK DECLARATION

Name of Candidate : **NORHAYATI BINTI MOHD NASIR**

Matric No: **SHC 150014**

Name of Degree : **DOCTOR OF PHILOSOPHY**

Title of Thesis :

EFFECT OF NON-THERMAL ATMOSPHERIC PRESSURE PLASMA JET ON WOUND BACTERIA AND CELL PROLIFERATION

Field of Study :

EXPERIMENTAL PHYSICS

I do solemnly and sincerely declare that:

(1) I am the sole author/writer of this work;

(2) This work is original;

(3) Any use of any work in which copyright exists was done by way of fair dealing and for permitted purposes and any excerpt or extract from, or reference to or reproduction of any copyright work has been disclosed expressly and sufficiently and the title of the Work and its authorship have been acknowledged in this Work;

(4) I do not have any actual knowledge nor do I ought reasonably to know that the making of this work constitutes an infringement of any copyright work;

(5) I hereby assign all and every rights in the copyright to this Work to the University of Malaya ("UM"), who henceforth shall be owner of the copyright in this Work and that any reproduction or use in any form or by any means whatsoever is prohibited without the written consent of UM having been first had and obtained;

(6) I am fully aware that if in the course of making this work I have infringed any copyright whether intentionally or otherwise, I may be subject to legal action or any other action as may be determined by UM.

Candidate's Signature Date: 13 March 2020

Subscribed and Solemnly declared before,

Witness's signature Date : 13 March 2020

Name:
Designation:

EFFECT OF NON-THERMAL ATMOSPHERIC PRESSURE PLASMA ON WOUND BACTERIA AND CELL PROLIFERATION

ABSTRACT

Non-thermal plasma produced in the plasma jet at atmospheric pressure consists of many reactive species and free radicals. The use of the atmospheric plasma jet has been expanded from surface treatment on polymers and biomaterials to the application as plasma medicine. It has been studied as a tools for wound sterilizations, enhance wound healing, topical treatment of skin diseases caused by bacteria infection and cancer therapy in recent research. The current study aims to investigate the effect of plasma on chronic wound bacteria as a supplementary to wound management particularly for compromised patients. The common practice in wound management is systemic antibiotic therapy that of poor penetration to specific region of tissues like wounds caused by burns. In the application of the non-thermal plasma in wound therapy, the antiseptic effect on bacteria inhibition is confirmed and its effect on the growth of the fibroblast cells is revealed. Two dielectric barrier discharge (DBD) configurations, planar DBD and capillary configuration powered by (AC) and direct current (DC) sources were employed to generate non-thermal plasma. The electrical characteristics was measured and emission spectroscopy was obtained. The analysis based of the current-voltage and power measurements gave the properties of the non-thermal plasma. The methicillin resistant *Staphylococcus aureus* (MRSA) and *Pseudomonas aeruginosa* (PA) isolated from chronic wound bacteria strains were treated with the non-thermal plasma for a duration of 10 mins to 60 mins. The efficacy of the plasma jet was further investigated on bacteria lawn. *E coli* lawn with short exposure from 10 s to 120 s. Fibroblast cells were also treated with plasma jet with AC powered to test the potential toxicity of plasma. The fibroblast cells were subjected to the non-thermal plasma at distant of 5 mm, 10 mm, 15 mm and 20 mm. The plasma

dosage has been calculated by using multiple linear regression. It is found that low dosage of plasma produces cell proliferation effect. This results suggests that non-thermal plasma has advantage in wound management not only by its antiseptic effects but also simulate cell proliferation thus promote healing at specified treatment conditions.

Keywords: Non-Thermal Plasma, Plasma jet, Cell Proliferation

KESAN PLASMA TEKANAN UDARA KE ATAS BAKTERIA DI KULTUR DARI LUKA DAN SEL PROLIFERASI

ABSTRAK

Plasma tanpa termal ialah gas terion yang terdiri daripada reaktif spesies dan radikal bebas. Aplikasi plasma pada tekanan udara telah berkembang dari rawatan permukaan polimer ke bio bahan dan plasma perubatan. Ia telah diiktiraf sebagai alternatif dalam dalam perindustrian, rawatan permukaan bahan dan perubatan. Kajian terkini plasma ke atas luka kronik dapat membantu dalam pengurusan luka. Di bidang perubatan, plasma telah digunakan secara meluas dalam pensterilan luka, rawatan kanser, penyembuhan luka dan juga rawatan topikal penyakit kulit. Kaedah biasa pengawalan luka adalah dengan penggunaan antibiotik. Kelemahan pada sistem tersebut ialah ianya gagal untuk menembusi tisu yang disebabkan oleh luka terbakar. Kesan plasma terhadap terapi luka telah terbukti berkesan. Kesan perkembangan sel fibroblast juga telah didedahkan. Dua konfigurasi dielektrik discaj iaitu planar DBD dan konfigurasi kapilari telah diuji keatas *Staphylococcus aureus* (MRSA) tahan metisilin dan *Pseudomonas aeruginosa* (PA) yang di isolasi daripada kultur luka kronik. Rawatan selama 10 ke 60 minit telah di buat ke atas bakteria tersebut. Keberkesanan plasma jet tersebut telah di uji seterusnya ke atas agar *E coli*. Rawatan selama 10 ke 120 saat telah di jalankan ke atas agar bakteria tersebut. Sel fibroblast juga di rawat dengan mengunakan plasma jet untuk melihat kesan ketoksikan plasma tersebut pada jarak 5 mm, 10 mm, 15 mm and 20 mm. Dos plasma telah di kira dengan menggunakan kaedah ‘Multiple Linear Regression’. Keputusan menunjukkan bahawa plasma pada dos yang rendah berupayaa untuk meningkatkan perkembangan sel fibroblast. Ia juga berpotensi untuk digunakan sebagai terapi luka dan juga mampu menggalakkan perkembangan sel pada dos yang rendah.

Kata kunci: Plasma tanpa terma, Jet Plasma, Proliferasi

ACKNOWLEDGEMENTS

Alhamdulillah all praises to Allah S.W.T for the determination, courage and strength to complete this study. I would like to give my utmost gratitude to my supervisor Associate Professor Dr. Yap Seong Ling for her guidance and help in completing this study. This project would not be possible without her consistent guidance. I also would like to acknowledge my appreciation to Associate Professor Dr. Zulhazrin for the motivation and advice given throughout. Special thanks to Dr Partha Saikia in providing technical support. To our collaborators, Prof Thong kwai lin and Dr Ronald for their assistance in biomedical parts.

I would like to dedicate special thanks to Aini, Sarah, Sarah Mizi, Lidya, Siti Sarah, Amira, and all. Thank You for this lovely friendship, helpful and delightful discussions.

Finally yet importantly, I would like to thank my husband for his devoted love and support, to my parents and siblings. Most valuable memories to my beautiful babies which bring me through this journey.

TABLE OF CONTENTS

LIST OF FIGURES

LIST OF TABLES

LIST OF SYMBOLS AND ABBREVIATIONS

A	:	The transition probability
C	:	Total Capacitance
C_{cell}	:	Cell Capacitance
C_{diel}	:	Dielectric Capacitance
C_{gap}	:	Gap Capacitance
d	:	Gap Width
E	:	Electric Field
E_1	:	Energy of the excited state for selected lines
E_2	:	Energy of the excited state for selected lines
F	:	Frequency
g	:	statistical weight
H_2O_2	:	Hydrogen Peroxide
I_{em}	:	Intensity
I	:	Discharge Current
k	:	Boltzmann constant
K	:	Temperature in Kelvin
κB	:	kappa-light-chain-enhancer of activated B cells
n	:	Number of spikes
p	:	gap pressure
Q	:	Charge across capacitor
R	:	Resistance
T	:	Discharge Time
T_e	:	Electron Temperature
T_I	:	Time of Incubation
T_T	:	Time of treatment

V_b	:	Breakdown voltage
AC	:	Alternating current
APPJ	:	Atmospheric pressure plasma jet
CFC	:	Choloflorocarbon
CFU	:	Colony forming unit
CGCD	:	Capillary guided corona discharge
DC	:	Direct current
DBD	:	Dielectric barrier discharge
FDA	:	Food drug administration
Ge	:	Germanium
IV	:	Current-voltage
LB	:	Luria Bertani
LTE	:	Local thermodynamic equilibrium
LTP	:	Low temperature plasma
N	:	Number density of gases
NIST	:	National Institute of Standards and Technology
NO	:	Nitrogen Oxide
NO_2	:	Nitric Oxide
MRSA	:	Meticilin resistant *staphylococcus aureus*
PA	:	*Pseudomonas aeruginosa*
QV	:	Charge-Voltage
RNS	:	Reactive nitrogen species
ROS	:	Reactive oxygen species
Si	:	Silicon
SiGe	:	Silicon Germanium
SO_2	:	Sulfur dioxide,

TSA	:	Tryptone Soy Agar
TSB	:	Tryptone Soy Broth
N_2	:	Nitrogen Gas
NF	:	Nuclear factor
O	:	Free oxygen atom
O_3	:	Ozone
OH	:	Hydroxide
N	:	Number density of gases
VOC	:	volatile organic compounds

LIST OF APPENDICES

CHAPTER 1: INTRODUCTION

1.1 Laboratory Plasma: Historical Perspective

Plasma is an ionized gas and is the fourth state of matter. It exist in abundance in the universe with 99 percent of it mainly in the galaxy, sun, nebula, star magnestophere and also earth magnetosphere. Plasma can be artificially generated by subjecting gas to a strong electric field or through a heating process that causes the outer electrons to escape from the atom and form positive and negative particles (ions). The rich profusion of these particles leads to its capability to react in the presence of an electromagnetic field. The recent discovery of plasma is due to the surrounding earth temperature which is too cold (300 K) for the formation of a stable plasma. It requires a special device to generate plasma where it was first established successfully in a Crookes tube by Sir William Crookes (1879). In 1879, the nature of plasma was further investigated by Sir J.J Thompson. Although the behavior of plasma is still not fully understood, plasma is extensively present in various industrial as well as scientific applications. Plasma generation has revolved around different means of production and its application. It is classified as thermal or non-thermal plasma depending on its temperature. Thermal plasma condition is achieved when electrons and heavy particles are in thermal equilibrium whereby all particles are at the same temperature. On the other hand, the non-thermal plasma condition exists when ions and neutrals are at a much lower temperature than electrons. This condition is regarded as the non-thermal equilibrium state. It occurs when electrons are unable to transfer their kinetic energy gained from the external electric field onto bigger particles, causing inequality of the temperatures. Thermal plasma is produced at a high pressure, which is more than 10 kPa, by means of a direct current (DC), alternating current (AC), radio frequency (RF) or microwave sources with temperatures around 2000 to 20,000 K. Thermal plasma is commonly initiated in DC

transferred arcs, plasma torches and radio frequency (RF) inductively coupled discharges. On the contrary, non- thermal plasma is typically established in a glow discharge, low-pressure RF discharge or a corona discharge. Non-thermal plasma is widely used in surface cleaning, etching, lighting as well as deposition.

Research on thermal plasma has undergone enormous evolutions which started at the beginning of the 20th century and its technology have been utilized in various applications. The success of the Crookes tube was followed by the expansion of theories with the article published by Langmuir titled 'Oscillations in Ionized gases' in 1928. Subsequently, the carbon arc lamp was invented by Humpry Davy in 1928 by applying arc in between two carbon electrodes and followed by the production of movie projection lamps as a radiation standard employed in spectroscopy. In the early days, there was a hypothesis stating that the cold glow discharge has the opposite nature to thermal plasma wherein it can only be generated at low temperatures. Thermal plasma underwent various types of improvements such as arc welding that has a variety of forms, making it accountable for the development of other technologies. Numerous approaches of flow and vortex arc stabilization were employed in the development of plasma torches. Subtle and rarefied experiment on non-thermal plasma designs and applications expanded at an impressive pace in the early 20th century. It was prior to the invention of generators based on dielectric barrier discharge (DBD) by German electrical engineer, Werner Von Siemens (1857). Siemens developed a DBD discharge setup which was placed in a small gap of two coaxial glass tubes. Ambient air or oxygen gas was introduced into the DBD and subjected to an alternating field at sufficient values of electric fields. According to Kogelschatz et al., (2002), the most important characteristic of DBDs is that non-equilibrium plasma conditions can be provided at an elevated pressure, for example atmospheric pressure. In DBDs, this condition can be achieved in a much simpler way as

compared to other alternative techniques such as in low-pressure discharges, fast pulsed high-pressure discharges or electron beam injection, (Kogelschatz et al., 2002). The flexibility of DBD configurations concerning the geometrical shape, operating medium and operating parameters are remarkable. In many cases, discharge conditions optimized in small laboratory experiments can be scaled up to large industrials installations. Efficient low-cost power supplies are available up to very high power levels (Kogelschatz et al., 2002). The non-thermal plasma also known as cold atmospheric plasma which has shown tremendous potential in breaking new grounds continue to attract the interest of the scientific community as well as industrial players. Atmospheric pressure discharge which was further tested on the inactivation of bacteria subsequently led to the development of a new field of applications in biomedical sciences currently known as plasma medicine. Plasma medicine is known for its therapeutic treatment on or in a human body by direct applications of cold atmospheric plasma, (Weltmann et al., 2009). DBD and atmospheric plasma jet have been introduced to be implemented in plasma medicine and further tested experimentally on biomedical samples. The first atmospheric pressure plasma jet was first produced by Koinuma et al (1992). The availability of small scale sizes and portable feature of the plasma jet makes it possible for surface materials treatment as well as in biomedical applications. Non-thermal plasma has been utilized in various medical applications and health care focusing on sterilization, (Laroussi et al., 2005), food industry and blood coagulations, (Giannini et al., 1957; Andrenucci et al., 2010); Gianinni et al., 1960; Freeman et al., 1968; Boffa et al., 1970). It has been confirmed that the usage of plasma in medicine is due to its excellent bactericidal effects as well as its capability in surpassing narrow and confined spaces, (Lu et al., 1991; Yoshie et al., 1992; Akatsuka et al., 1993; Glocker et al., 2000; Benocci et al., 2004). Plasma medicine has extensively broadened up its research area by including hospital hygine (Grundmann, 2006), antifungal treatment (Morfill et al., 2009), dental care (Klein et al.,

2004), skin diseases, chronic wounds (Fridman et al., 2008), (Etufugh et al., 2007). Its application is developed in the ability of cells proliferation in cancer treatment (Kim et al., 2009). The utilization of non-thermal plasma in medicine and healthcare are in massive non-equilibrium state (Lofty, 2017). Sterilization and metallic medical devices decontaminations require plasma with gas temperature of 100˚C-150˚C meanwhile 60˚C to 100˚C temperature is often used for blood clotting and ablation of living tissues. They are also used as decontaminator on a large number of temperature-sensitive plastic and glass medical devices, Lofty (2017). Plasma with gas temperature of 20˚C - 60˚C are often used for the treatment of living tissues without causing, or with least, damage to the surrounding healthy tissue, (Lofty, 2017). The need for simple, thermal sensitive designs which are easily operated at atmospheric pressure has further boosted the development of plasma jet. Easy and simple constructions without the need of a vacuum system makes plasma jet a better solution for medicinal use in applications involving living tissues. Over the past few years many developments and investigations were carried out on plasma jet at atmospheric pressure (Dresvin et al., 1971). The easily constructed design and ability to be operated with various working gas at different driving frequencies features enables it to solve the limitations of vacuum-based plasma. Furthermore, generating non-thermal plasma at atmospheric pressure is advantageous due to the non-toxic effect as well as the capability of the devices to be in portable or handheld devices. Different designs and configurations of plasma jet devised commonly consist of a center needle electrode, rod electrode or hollow electrode inside a glass or quartz tube. Research in connection with atmospheric plasma jet on biomedical applications marks a primary focus in this study. The effect of simple and easy configurations of plasma jet affecting parameters concerning antibacterial effect and the cells proliferation which helps wound healing process will be the main research criteria conducted in this study.

1.2 Motivation of studies

Generally, this study is motivated by the fact that plasma is ubiquitous and has unique features. The features include the capability of atmospheric pressure generation, provide a thermal sensitive exposure, low temperature which are suitable to be exposed on living tissues and coupled with its unique property of anti-bactericidal effect. This effect has become an interesting topic of study. The predominant feature of atmospheric plasma is its capability in generating a combination of biologically active agents such as Reactive Oxygen Species (ROS) and reactive Nitrogen Species (RNS). In addition, the ability to maintain ambient temperature makes it a lot safer without electrical and chemical risks. Atmospheric plasma also offers a low cost plasma generation because of its ability to be generated with less usage of working gas. A variety of studies focusing on the anti-bactericidal effects and the effect of ROS and RNS on living tissue have been conducted by researchers. Davydof et al (2004) conducted a clinical evaluation of the intraoperative application of air-plasma flow enriched by nitrogen monoxide in operations on uterus. While Shekter et al (2005) investigated the effect of gaseous nitric oxide on the healing of skin wounds resulting a better understanding in the mechanism of antibacterial. Various plasma jet with different configurations and means were designed, (Winter et al., 2015). These configurations have unlocked the possibility of using a similar approach for biomedical treatment specifically in wound healing treatment. According to Lu et al (2008), plasma jet configurations is the most appropriate design to be implemented generally in biomedical application samples and specifically for multidrug bacteria treatment as well as proliferations of wound cells. The design is achievable due to its capability of generating active species, operation under atmospheric pressure, handheld, low gas temperature without arcing and safe to be touched by human without any conducting path effects.

1.3 Research problem

Wound commonly occurs when a break or any upsetting events take place on the skin by means of thermal or heat, chemical, mechanical or due to post-surgery effects. Wound healing is a complex process and can develop into an acute or chronic wound depending on the duration of healing time. Acute wound includes mechanical abrasions, incisions, burns as well as chemical injuries. Chronic wound is commonly found in diabetic foot, pressure and leg ulcers. Normal healing would take up to 3 weeks to heal and one which requires more than 12 weeks are prone to be chronic. The common practice in wound management is systemic antibiotic therapy. Despite the development of antibiotic drug resistance and adverse side effect, this therapy is still widely used in wound management. Systemic antibiotics have poor penetration in tissues and less effective on wounds caused by burns. Mupirocin ointment has been identified as a common topical antibiotics practiced in wound management. Nevertheless, the focus of the said antibiotics has been recognized on specific target and believed to be resistant to *Staphylococcus aureus* bacteria. To date, there is no food drug administration (FDA) approvals on antibiotics which works for the wound treatment infections. New advanced technologies and latest treatment methods are very much needed and important in controlling wound infection, inflammation and promote wound healing. A promising method that has been identified as capable in improving and promoting wound healing process is cold plasma or non-thermal plasma generated in atmospheric pressure. Even though plasma jet has been successfully generated, it still intrigues interest among the Malaysian research community, especially in low-temperature plasma. Despite the success of the generation of plasma jet at atmospheric pressure, there are a few studies in this topic that dominates the interest in Malaysia. Researches focusing on low- temperature plasma in Malaysia has yet to discover the utilization of plasma jet at atmospheric pressure in various aspects.

1.4 Research Objectives

The main objectives of this research are:-

a) To generate atmospheric pressure plasma jet with Dielectric Barrier Discharge (DBD) and Capillary Guided Corona Discharge (CGCD) configurations.
b) To treat bacterial isolates from wound sample by using generated atmospheric plasma jet.
c) To investigate the effect of non-thermal plasma on fibroblast cells by using generated atmospheric plasma jet.

Generating homogenous non-thermal plasma at atmospheric pressure is still a challenge. The motivation to set up good and promising systems which are capable in intervening the said problems is becoming the topic of interest of various studies. In this study, our primary focus is to generate non-thermal plasma at atmospheric pressure. The generated plasma will be tested in biomedical applications focusing in chronic wound healing samples.

1.5 Thesis Layout

This thesis is divided into five chapters in which the first chapter presents a concise introduction of plasma in general and the main focus is in non-thermal plasma specifically in its applications. It becomes the motivation as well as the objective of the study. Chapter two provides the insight of plasma jet theory, configurations of plasma jet and, generation of plasma jet as well as the bactericidal effect. Descriptions of the experimental methodology, as well as plasma configurations are presented in chapter three. The selected configuration for plasma jet generation will be explained in detail especially the geometrical parameters and optimization of the plasma jet configuration. The explanation of the experimental setup for treatment will be discussed thoroughly in chapter three.

Chapter four will be presenting results that covers the essential concepts or the highlights of the topics as to how plasma jet can be successfully generated. The suitable parameter for plasma jet treatment and the effect of plasma jet on bacteria samples and also on cells proliferation will also be presented. The comparison between previous findings will be the main discussion in chapter five. The findings of this study will be explained in relation to latest findings from other research. In chapter six the conclusion of the findings will be presented. The objectives of this study will be concluded in chapter six. The limitation of study as well as proposed work for the enhancement of the study is also presented.

CHAPTER 2 : LITERITURE REVIEW

2.1 Introduction

Chapter two will discuss the detail explanation on non-thermal plasma at atmospheric pressure by utilizing dielectric barrier discharge (DBD) systems. Plasma breakdown mechanism is an important concept that will be discussed. The geometrical parameter, system configuration, plasma diagnostics as well as biomedical samples focusing in the wound healing process will also be included. Various applications involving DBD discharge will be presented to understand the nature of the plasma generated. This will be important in further knowledge of the plasma jet. A number of novel applications based on DBDs will be described. The development of plasma jet based on DBD configurations is another important aspect which requires proper attention for further applications, especially for biomedical sample treatment.

2.2 Non Thermal Plasma:-Dielectric Barrier Discharge (DBD)

Non-thermal plasma has been conventionally generated at low-pressures of 10^{-2} to 10^{-3} mb (Yasuda et al., 1989). Practically this is done by limiting the amount of electron and ion density in a chamber which contributes to the electrical discharge. Plasma generation at atmospheric pressure has drawn a lot of interest among researchers. It is currently widely accepted by the industry and subsequently becoming a topic of great interest (Mizuno, 2007). The plasma generated at atmospheric pressure is cost-effective and friendly due to the absence of expensive vacuum systems and vacuum compatibility issues. It requires a chamber to ensure the pressure is maintained low and thus limiting the size of treated samples without the vacuum system. Spatially uniform (diffuse plasma) can be generated in DBDs at certain operating conditions (Aldea et al., 2005; Starostin et

al., 2008; Starostin et al., 2009; Osawa et al., 2012; Osawa, 2013; Golubovskii et al., 2004; Gherardi et al., 2001). Filamentary discharge (non-homogenous) is mostly achievable for almost all of the operating condition (Stollenwerk et al., 2007). Filaments are characterized by high local electron densities of up to 10^{15} cm^{-3} and strong electric fields of up to 10^5 V/cm. The filaments are self-limiting because they charge the dielectric surface and locally negate the gap voltage until extinction occurs (Peeters, 2015). The filaments spread out over the dielectric surface. When a DBD is driven by a sinusoidal external voltage at a frequency of 100 kHz, filaments ignite for more than 3 μs (Peeters., 2015). Filamentary or microdischarge commonly observed able to sustain in range of tens of nanosecond. The maximum current of 0.1A is associated with the microdischarges.Non-thermal plasma at atmospheric pressure was produced by utilizing Dielectric Barrier Discharge (DBD) system. The DBD system has been proposed by various research in the initiation of non-thermal plasma atmospheric pressure without the need of high-cost vacuum system. Its configurations mainly consist of two metal electrodes with one of the electrode is insulated by a dielectric. The schematic diagram of the DBD configuration is shown in Figure 2.1. Plasma discharge generated between the electrodes are commonly found in filamentary mode or transient filaments (Figure 2.1).

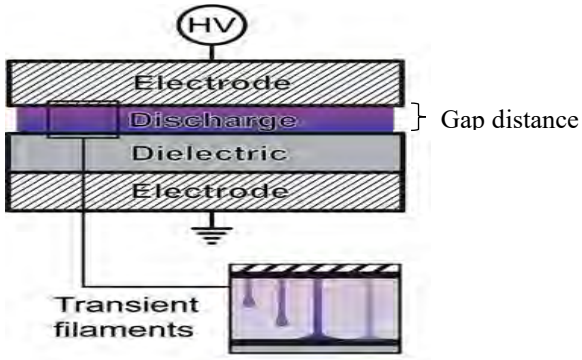

Figure 2.1 : Schematic of a DBD with one electrode covered by a dielectric.

As filamentary discharge occurs, it will spread over the whole surface of the electrodes between the gap in random or regular nature (Kogelchatz, 2002). The addition of dielectric material to any of the electrodes will prevent arc transition between the gap distances. Arc transition will be eliminated due to the accumulation of numerous amount of current by discharge between the two electrodes. When there is a huge amount of charges collected on the surface of dielectrics, it creates an electric field that has the ability to oppose the electrical field created by the discharge voltage during the filament formation (Kogelchatz, 2010). Hence, the effective field between the electrodes will be reduced and eventually the filament is quenched (Xu et al., 1998).

DBD configurations can be constructed in two ways either through volume discharge arrangement or surface arrangement (Kogelchatz, 2010). DBD electrodes are separated by a certain gap distance for volume discharge arrangement (Figure 2.1). By varying the potential difference between the electrodes, the discharge will take place when the amount of voltage is sufficient between the electrodes. The surface arrangement was first investigated by Masuda et al., (1988) in the ozone generation. This arrangement does not require any gap between the electrodes and direct contact is permitted between electrodes and dielectric surface. Plasma luminosity will be observed on the surface of the dielectric (Gibalov et al., 2000). Various materials were introduced as dielectrics including glass, alumina, mica, and quartz as well as polymer layer. The DBD is an interesting system to be investigated due to the simplicity of the setup and the convenience of conducting the experiment at atmospheric pressure. Furthermore, it can be powered by a 50 Hz AC power system without having to resort to sophisticated pulsing circuits. Hence, the possibility of multiple implementations in various applications.

2.3 Mechanisms of Plasma Discharge in DBD configurations

Discharge mechanism starts as the electrical breakdown of DBD occurs. Discharge mechanism occurs when the high voltage applied across the electrodes is greater than the required breakdown electric field between the electrodes. Stray charges (electron) in the air gap between the electrodes accelerates rapidly toward the anode. As the electron traverses the gap, it gains sufficient energy to free a second electron from the neutral atom through inelastic collision. More free electrons are created in cascading ionization (Figure 2.2) known as Townsend avalanche resulting the conduction of current.

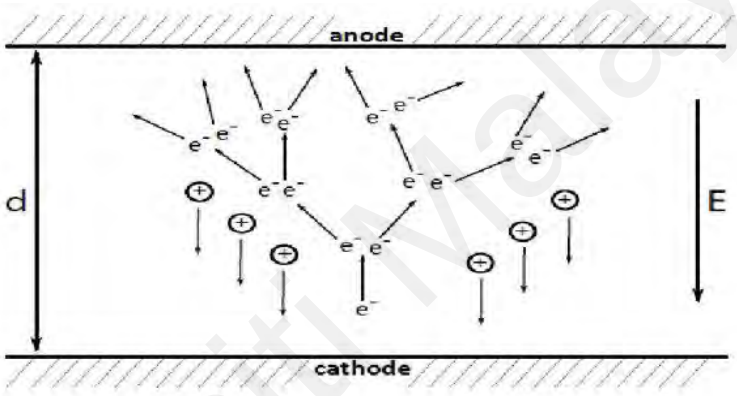

Figure 2.2: Electron avalanche on the basis of Townsend's theory

Based on Paschen's Law (1910), the value of the electric field should be sufficient enough and exceeds certain threshold value to ensure the breakdown can occur. Paschen's Law is a function product of V = f(pd), where V = breakdown voltage, p = gap pressure, d = gap width. It is sometimes written as V = f(Nd) where N is the number density of gases. The former function product is valid when the condition is under room temperature while the latter depends on the number of density and not necessarily to be under room temperature (Kogelchatz et al., 2005). Townsend breakdown is only applicable when the function product of Paschen's law product is low. When it is high as in > 200 Torr-cm, it is then best described as a streamer breakdown. Streamer breakdown happens due to a large electronic avalanche and capable in creating adequate number of ions. It gives rise

to localised space-charge field and subsequently creates a thin conducting channel across the gap known as streamers. During a streamer breakdown, the transition process from the avalanches to streamer transition is in the order of 10^8 cm/s. This transition magnitude is greater than the movement of the avalanches. It is capable of covering the gap distance in a 10 ns duration time. In figure 2.3, the schematic diagram shows streamer propagating from the anode to the cathode. Additional avalanches and micro discharges are formed by channel streamers that strike at the same place each time the polarity of applied voltage changes (Chirokov et al., 2005). The persistence of streamers to strike at the same place or spot is due to memory effect. The memory effect is associated with charges deposited on the dielectric barrier, as well as on residual charges and excited species in the microdischarge channel (Chirokov et al., 2005). The memory effect was described in detail by Eliasson et al., (1987). Streamer development started with the initial electrons initiating avalanches from anode to cathode as shown in Figure 2.3.

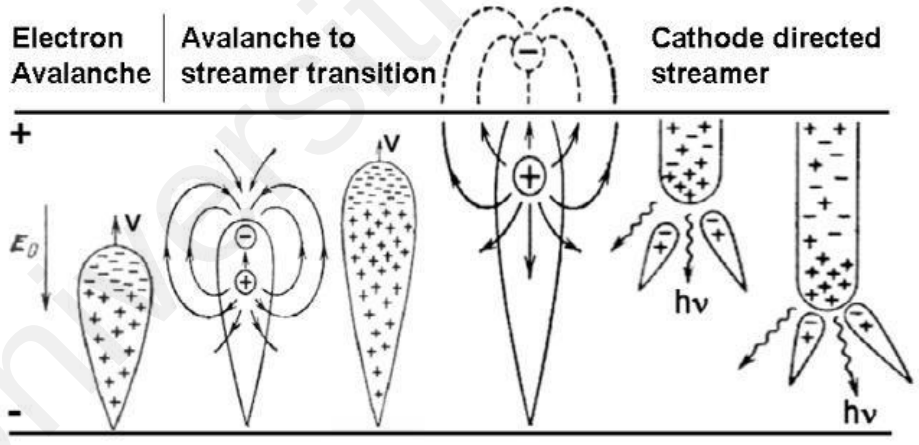

Figure 2.3 : Evolution of electron avalanche in discharge gap, showing avalanche development, avalanche to-streamer transition, and streamer propagation.

With its lighter mass and high velocity of propagation, electrons lead the avalanches while heavy ions tail behind the avalanches (Figure 2.3). As the electron reaches the anode electrode, it then dissipates rapidly within 30 ns into the metal electrode, while the heavy ions remain in between the gap for several microseconds (Chirokov et al., 2005). The deposition of electrons from the conducting channel onto the anode dielectric barrier

results in charge accumulation preventing the formation of new avalanches and streamers in the vicinity until the cathode and anode are reversed. After the voltage polarity reverses, the deposited negative charge facilitates the formation of new avalanches and streamers in the same spot (Chirokov et al., 2005).

2.4 Development of DBD : Historical Perspective

The interest in DBD discharge system started decades ago with the discovery of filamentary discharge during breakdown between the air-insulated electrodes by Buss et al., (1932). Buss also reported that DBD discharge consists of a large number of bright filaments covering the narrow space gap using photographic traces. Further explanation particularly on the individual discharge was investigated by Klemenc et al., (1937). Eventually, it was realized that the filamentary discharge or rather known as micro discharges has a number of utilization in many aspects of applications (Eliasson et al., 1987). Most of the applications involving DBD systems emphasize on the power dissipated by the system. In 1943 Manley determined the power dissipated by a DBD system using Charge –Voltage Lissajous figure (QV). It has been reported by Bartnikas, (1968) that a rather homogenous glow discharge can be generated in atmospheric pressure condition known as pseudo glow. The glow appears between the narrow gap of two parallel plane electrodes. Thus it was believed that it is possible to generate homogenous discharge at atmospheric pressure at suitable plasma condition. Method of differentiating between the glow discharge mode and filamentary mode is based on the current waveform and using high-speed photography. The current waveform of glow discharge or diffuse plasma is commonly perceived as one current peak for every voltage polarity half cycle in both of AC discharge. One of the typical signals of homogenous discharge is shown in Figure 2.4.

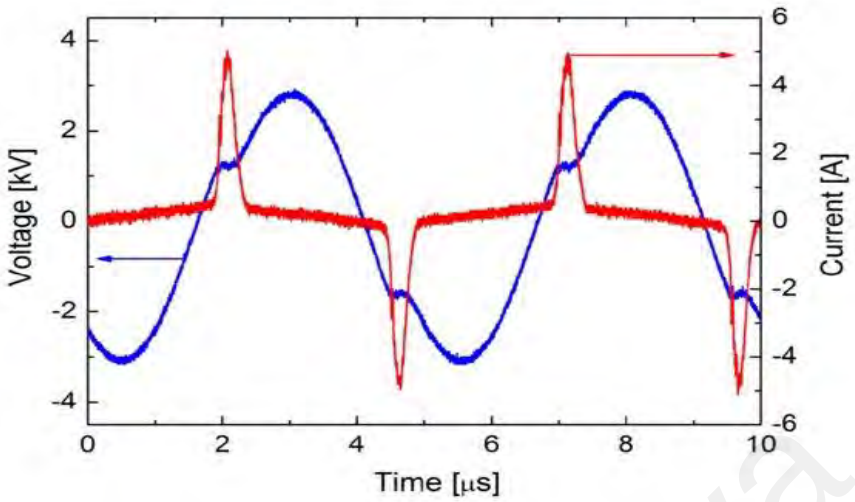

Fig. 2.4. Voltage and current waveforms of the diffuse DBD discharge in $N_2/O_2/Ar/TEOS$

Sophisticated imaging tools is required to capture the image since the development of filamentary discharge is in the order of nanoseconds. In 1993 QV Lissajous figure was proposed by Okazaki et al., (1993). The typical QV figures shown in Figure 2.5.

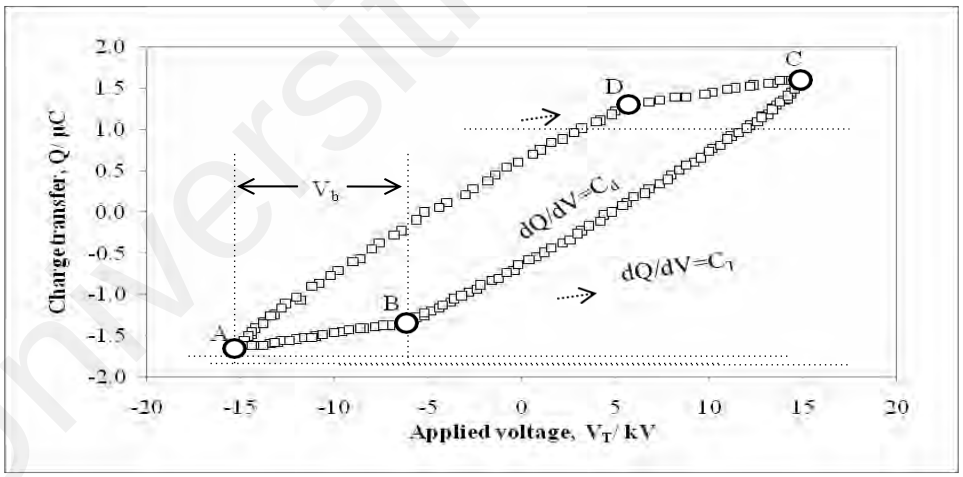

Figure 2.5: The typical QV Lissajous figure under breakdown condition

The parallelogram shape of figure 2.5 represents filamentary discharge, while the QV figure of glow discharge appears to be represented by the two voltage lines at the top and the bottom in the Lissajous figure. In industrial sectors, filamentary has been employed in various applications and commonly powers ozone reactors. The ozone reactor has led to the creation of numerous applications such as the application of ozone in wastewater

treatment, disinfection and water treatment as well as in bleaching processes. DBD discharge are also employed in air pollution control involving hazardous elements such as sulphur oxide and nitrogen oxides. These harmful elements are mainly from flue gases and volatile organic compounds (VOC) coming from hydrocarbon and chlorofluorocarbon (CFC) emitted from industrial processes and transportation causing pollution to the environment. Research have been conducted in the effort of removing the poisonous elements by using plasma DBD generated at atmospheric pressure. The effect of reactive species in the plasma for removing of this element (NO, $N0_x$ and SO_2) was investigated by (Chang, 1992; Nagai et al., 1991; Chang et al., 1991; Toda et al., 2001). This is achievable when the DBDs are set at a certain high pressure creating a condition suitable to be applied as an intense source. Excimer lamps were also employed in photo reactive polymers, photo-deposition of large area or patterned thin metal or semiconductor films, of high- and low-dielectric-constant insulating layers, photo-assisted low-temperature oxidation of Si, SiGe and Ge, polymer etching and microstructuring of polymer surfaces (Kogelschatz., 2000).

2.5 DBD in Biomedical Applications

Investigation of plasma generated by DBD involving living organisms or medicine and biomedicine was reported. In the middle of 1990s, a group of researchers conducted an experiment (Laroussi, 1996) by exposing atmospheric pressure plasma DBD discharge on bacteria. The capability of plasma in the inactivation of bacteria has expanded the scope of plasma applications into the field of biology and medicine and not only restricted to industry. Several other early reports using plasma on sterilisation and bacterial decontamination followed (Garate et al., 1998; Laroussi et al., 1999; Hernmann et al., 1999; Birmingham et al., 2000; Laroussi et al 2000; Montie et al., 2000; Laroussi et al., 2002). In early 2000, research was further enhanced in investigating the effect of plasma

discharge on eukaryotic cells. Lower doses of non-thermal plasma were exposed to the cells and it was found that it was capable in promoting cell proliferation in fibroblast cell, increasing phagocytosis and could result in apostosis (Shekter et al., 1998; Stoffels et al., 2002). The above-described groundbreaking research efforts showed that non-thermal plasma can gently interact with biological cells (prokaryotes and eukaryotes) to induce certain desired outcomes. These early achievements raised great interest and paved the way for many laboratories from around the world to investigate the biomedical applications of LTP and by the end of the first decade of the 2000s, a global scientific community was established around such research activities. The field is today known by the term plasma medicine, (Laroussi, 2018). Figure 2.6 shows the timeline of the progress of non-thermal plasma applications in biological and medicine in various scope of research in the early foundation of plasma medicine and it has grown rapidly since 2006.

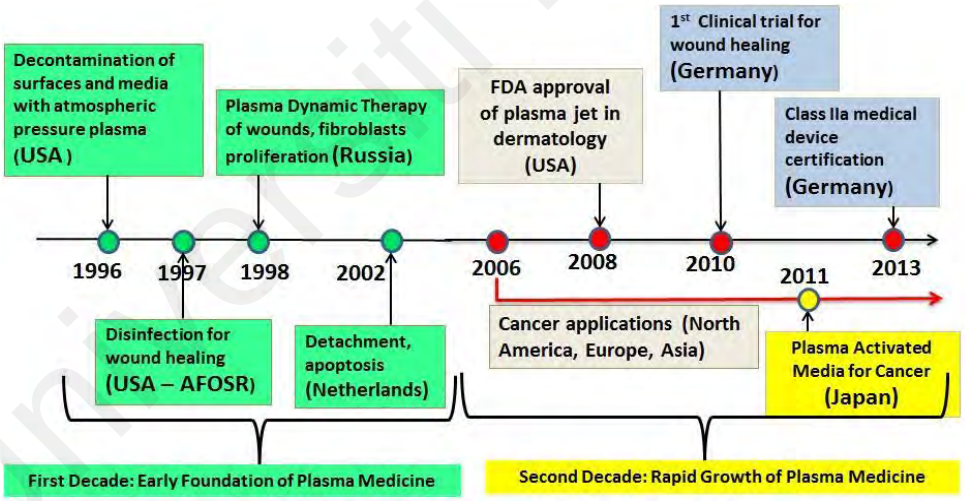

Figure 2.6: Timeline showing some major milestones of the new field do of the biomedical applications of low-temperature atmospheric pressure plasma

Various research utilizing plasma has expand rapidly in attempt to accelerate wound healing. Zhang et al., 2019 has explore the effects of an atmospheric-pressure plasma generated in helium gas through dielectric barrier discharge on skin wound healing in rats and its mechanism. The results showed that compared to that of the control group, the

size of the wound area in the CAP group significantly decreased, the contraction and re-epithelialization of the wounds were obviously speeded up, and the protein level of smooth muscle actin markedly increased. Plasma has been used to promote cell repair modulation and regeneration. Despite of remarkable usage of plasma in promoting wound healing, the underlying mechanisms and the molecular influences on human tissue has yet to be discovered. Scharf et al., 2019 has treated human S9 bronchial epithelial cells cold atmospheric pressure to study the detailed cellular adaptation reactions for a specified plasma intensity by time-resolved comparative proteome analyses. Both control and treated cells are compared to elucidate the mechanisms of the observed improved wound healing and to define potential biomarkers and networks for the evaluation of plasma effects on human epithelial cells. The development of new devices optimized for specific clinical applications is well under way the most prominent being (Boehm and Bourke, 2019).

2.6 Non-Thermal Plasma in wound healing

At the beginning of 1990s, non-thermal atmospheric pressure plasma offers great potential in biomedical applications as well as medicine. Multiple research have been conducted ever since to investigate the effect of non-thermal plasma on the wound healing process. The normal wound should heal within 2-3 weeks and the process of healing which takes more than that has the tendency to become a chronic wound. Infected wound by antibiotics resistant pathogens is the main factor which can contribute to the formation of chronic wound. It has been reported that many setbacks occur once a wound becomes chronic. It will be a major burden to public health wherein United States of America it has been reported that chronic wounds affect an estimated 2.4–4.5 million people (Brownrigg et al., 2002). Without proper attention, this situation can lead to high morbidity and high mortality. Chronic wounds which are predominantly a condition for

the elderly is becoming more prevalent and more difficult to treat and are associated with high treatment costs (Rice et al., 2014). Asian countries also suffer the same problem whereby it is estimated that there will be more than 400 million diabetics worldwide by 2025, with the greatest increases in Asia, Africa, and South America (Thomas, 2013). Non-thermal plasma has provided new and encouraging tools for promoting wound healing process. A new promising approach to overcome wound contamination, particularly infection, is with antibiotic-resistant pathogens. Thermal plasma or hot plasma which has set foot in the medicine field employs 'hot' plasma in the sterilisation of hospital equipment and to cut and cauterize tissue during operation (Heinlin et al., 2010). It has been shown by Heinlin et al., (2010) that non-thermal plasma sterilisation conducted on human skin are safe without any unpleasant effects or any thermal by product. In addition, previous studies also show that non-thermal plasma is very effective in bacteria inactivation where (Maisch, 2012; Isbary et al., 2013) conducted their research by exposing plasma to a broad spectrum of bacteria which resulted in a successful bacteria inactivation. Plasma is nontoxic with no adverse effect and promotes wound healing by promoting fibroblast proliferation cells. Fibroblasts play a key role in the proliferative and remodeling phases of wound healing. The main functions of fibroblasts include synthesis of extracellular matrix (ECM) molecules, release of multiple proteases, such as interstitial collagenases, gelatinase, and secretion of cytokines and contraction of wound (Smith et al., 1997; Li et al., 2011). Non-thermal dielectric barrier discharge plasma is currently being developed for a wide range of medical applications, including blood coagulation, malignant cell apoptosis, and wound healing (Kalghatgi et al., 2009a). However, the effect of non-thermal plasma on the vasculature is unclear. Blood vessels affected during plasma treatment of many tissues whereas the blood vessels themselves may be an important clinical plasma therapy target. Investigations have also been conducted on the effect of non-thermal plasma treatment on endothelial cells. Non-

thermal plasma treatment with short exposures (up to 30 seconds; 4 J/cm^2) was relatively non-toxic to endothelial cells (Kalghatgi et al., 2009a). They have reported that endothelial cells treated with plasma for 30 seconds demonstrated twice as much proliferation as untreated cells five days after plasma treatment. Proliferation was abrogated by a fibroblast growth factor-2 neutralizing antibody and reactive oxygen species inhibitors. This process suggests that plasma-induced endothelial cell proliferation is caused by growth factor release following reactive oxygen species. Moreover, it was suggested that low power non-thermal plasma treatment is a potential novel therapy for the promotion of endothelial cell-mediated angiogenesis (Kalghatgi et al., 2009b). Jin et al., (2017) repeated that to promote cells proliferation, a low and proper dosage is in need. Fibroblast cells treated with plasma for less than 20 s had significant increases in proliferation (Liu et al., 2017).

2.7 Plasma Mechanisms on Bacterial killing and Cell Proliferation

Plasma consists of electrons, ions, neutral particles, UV radiation, oxygen as well as nitrogen species (RONS). These plasma constituents as it interacts with microorganisms or cell/tissue, the components of plasma it will play different roles despites of its mechanism has not been fully understood (Xiong, 2018). It has been verified by Xiong, (2018) that UVB (280-320 nm) and UVC (100-280 nm) able to cross the epidermis and UVA (320-400 nm) can reach the dermis. Accumulation of charges are resulted in the generation of electrostatic force. These force has been reported by Mendis et al., (2002) which capable in rupturing the outer layer of membrane cells and lead to the bacteria inactivation. In other cases, direct treatment of samples with the plasma can caused the intensity of plasma received by the samples becomes greater. These lead to the inactivation of bacteria due to the electric field. In some other reports (Lu et al., 2008; Uhm et al., 2007; Eto et al.,2008) has reported that generated plasma in open air generated

reactive RONS such as O, O_3, NO, NO_2, OH and H_2O_2. These reactive RONS are reported to be responsible in the inactivation of bacteria. Atmospheric pressure plasma has been investigated not only has the inactivation ability but also able to promote cell proliferation. In wound repair, cell proliferation and migration together with angiogenesis are the stages involved during wound repair. Fibroblast cells and keratinocytes are among the cells which responsible in the healing process of wound (Tipa et al., 2011). It is also reported that atmospheric pressure plasma capable in stimulating the proliferation process. Ngo et al., (2014) has suggested that plasma promote proliferation of fibroblasts through simulated release of fibroblast growth factor -7. This has been reported by (Blackert et al., 2013) reported that the proliferation process due to plasma treatment is through triggering hormesis-like processes. It has been investigated that cancer cells and normal cells reaction with regards to its resistance to plasma are different. This ability makes plasma selective in killing cancer cells and normal cells (Wang et al., 2013).

2.8 Historical review of Plasma jet

Plasma jet discharge can be generated by employing different modes of power operation including alternating current (AC), direct current (DC), radio frequency (RF), and microwave discharge. A different method of generation will produce different results such as cold plasma torch, plasma pencil, microwave torch, atmospheric pressure plasma jet and also plasma needle. Plasma jet was first introduced in industrial applications and later employed by biomedical applications. The first plasma jet developed by Koinuma et al., (1992) introduced a quartz tube to place the needle electrodes and ground the anode electrode. The plasma jet system was powered by a 13.6 MHz power supply. A uniform plasma jet at atmospheric pressure was generated by employing RF mode power supply by Jeong et al., (1998) for material processing where he added oxygen to the helium gas for etching purposes. Hollow cathode configuration used by Janca et al., (1999) to be

implemented on chemical technologies, restorations and to reduce corrosion products on artefacts made from metal. The advantage of dielectric in the construction of DBD plasma jet has been verified by Hubicka et al., (2002). They were able to confirm that introducing dielectric in their plasma jet design helps reduce the effect of overheating which lead to nozzle melting. The plasma jet improvisation in increasing the plasma reactivity investigated by Kim et al., (2009) was a major achievement that resulted another design of plasma jet. They discovered that the plasma reactivity, as well as the radius of the jet, becomes thicker when a ground electrode in the form of a ring was set on the surface of a quartz wall (pin to ring configuration). In addition, the amplitude of the discharge current and the optical emission were enhanced significantly (Kim et al., 2009). Anghel et al., (2007) constructed plasma jet by using a single electrode powered by a low DC power supply. Helium gas was used as the feed gas. The non-thermal plasma is a touchable plasma jet and has been used on the human body, i.e. finger as the counter electrode (Wu et al., 2010).

2.9 Challenges with Plasma jet

The plasma discharge property is the main challenge that needs to be addressed in employing plasma jet in biomedical applications. This property especially the temperature of the gas, power transferred to the target, UV radiation and the effect of toxicity of the feed gas applied to generate the jet is crucial and requires proper attention. The focus of this study is on the effect of plasma jet atmospheric pressure in promoting wound healing process by looking at the effect of plasma jet onto microbial activity and the proliferation effects which promotes the healing process. A longer length of plasma jet will be more helpful as it enables the plasma jet to function deeper into the living tissue. The longest plasma jet plume ever detected is around 11 cm by Lu et al., (2008). They employed a 40 kHz AC high voltage to biomedical samples with a gas flow rate of

23.6 Litre/min. The jet generated is stable, low temperature and safe to the touch without any arcing effect and able to generate reactive species responsible for inactivation or proliferations. Discharge current generated by the plasma jet is another essential parameter that requires great consideration in terms of the safety issue. Lu et al., (2008) exposed the highest current carried by a room temperature plasma ever reported for biomedical applications discharge where the plasma plume recorded a peak current of 360 mA. Daeschclein et al., (2010) simulated antisepsis on wound surfaces and a handheld plasma jet were employed on the samples. It has been demonstrated that the hand-held atmospheric pressure plasma jet (APPJ) is capable to effectively inactivate the pathogens in vitro against the most encountered pathogenic species of acute and chronic wounds reaching nearly the power of antiseptics on typical wound pathogens in vitro simulating antisepsis on wound surfaces. Subsequently, the study suggested that atmospheric plasma jet is suitable and flexible enough to be administered to wound colonization in short durations and is appropriate to be used as a therapeutic treatment in therapy or colonised wound (Daeschclein et al., 2010).

Another successful non-thermal atmospheric plasma jet was reported by Isbary et al., (2012). In the study, they observed that a 5-min plasma jet treatment with argon as the feed gas shows a significantly reduced number in bacteria load in chronically infected wounds in vivo. They assessed that the plasma jet is also safe in reducing bacterial load regardless of the types of bacteria involved and also the level of resistance of the bacteria. In 2013, The kINPen MED (Leibniz Institute for Plasma Science and Technology – INP Greifswald and neoplas tools GmbH Greifswald, Germany) was introduced as the first commercialised cold atmospheric pressure plasma jet worldwide to be accredited as a medical device for the use in patients. This argon plasma jet is intended for the treatment of non-healing wounds and ulcers of the human skin. Argon atmospheric pressure plasma

jet was applied to generate LTP for treatment of murine fibroblast cell (L929) cultured in vitro to investigate the effect of NF-κB pathway on fibroblast proliferation (Jin et al., 2017). It shows that the atmospheric plasma jet promotes growth and simultaneously accelerate wound healing process. Nan et al, 2018 developed a low-cost and portable plasma device to generate atmospheric pressure non-thermal plasma. A longer jet length of 12 mm can be obtained in the full-wave breakdown discharge mode, while moderate plasma has a length of 8 mm. Currently, the study is well-known in its quest to design a portable plasma jet for better handling and simple operations. In 2019 Usta et al., designed a portable battery-powered non-thermal atmospheric plasma device and characterisation of its antibacterial efficacies without requiring external power input.

CHAPTER 3: METHODOLOGY

A suitable Dielectric Barrier Discharge (DBD) configuration was determined for chronic wound bacteria treatment. Two DBD configurations, Planar DBD and capillary configuration were employed on chronic wound bacteria samples. The capillary configuration known as capillary guided corona discharge (CGCD) and planar DBD treatment setup were prepared. The methodology is presented in this chapter. Methicillin resistant *staphylococcus aureus* (MRSA) and *Pseudomonas aeruginosa* (PA) bacteria strains were tested using both DBD configurations. The DBD configuration was found to be more suitable, thus the capillary configuration was replaced with plasma jet. The plasma jet adopted a pin to ring configuration. The detail process of constructing the plasma jet configuration is presented. Alternating current (AC) and direct current (DC) sources were applied in order to generate plasma jet. The geometrical parameter of the plasma jet configurations were recorded. Both AC and DC plasma jet electrical characteristics were determined and recorded. Diagnostic techniques were employed and the data was recorded. Efficacy of the plasma jet was identified from a treatment on *E coli* bacteria. AC plasma jet was further tested on fibroblast cells. The treatment procedure is discussed and presented in this chapter.

3.1 Experimental setup

3.1.1 Planar Dielectric Barrier Discharge (DBD)

The Planar DBD configuration was assembled using two stainless steel electrodes with an area of 84.82 x 10^{-2} m^2. They were placed parallel to each other. Stainless steel was chosen since it neither oxidizes nor corrodes upon treatment. A pyrex glass of 2.0 mm was inserted between the two electrodes. The glass was placed on top of the bottom electrode. It acts as a dielectric to enhance the capacitance between the gap. The configuration of the planar DBD is shown in Figure 3.1.

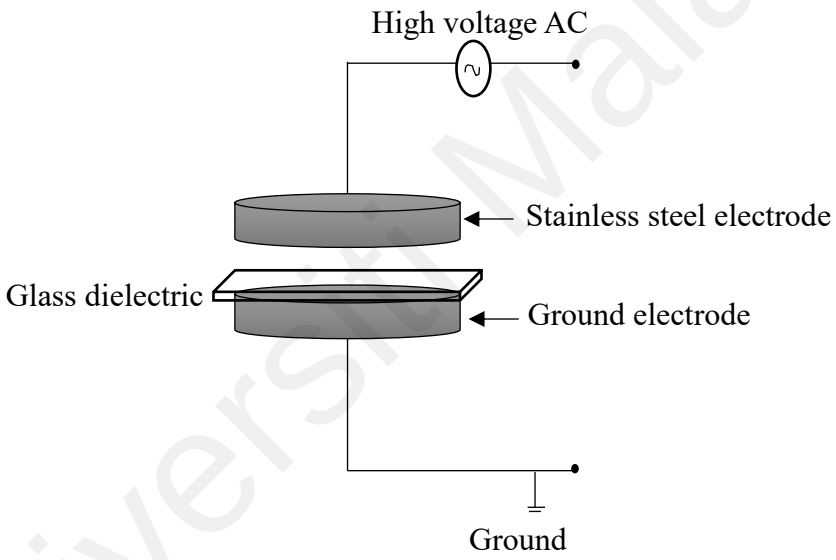

Figure 3.1: Diagram of Planar DBD setup

The top electrode was connected to a 50 Hz high voltage power supply while the bottom electrode was grounded. The applied voltage was set from 5 kV and increased until the microdischarges were initiated between the electrodes. The current-voltage (IV) signal from the oscilloscope was recorded and analysed. The analysis was more focused on the relationship between the numbers of filaments with the applied voltage. Suitable voltage was required for the treatment of chronic wound bacteria samples.

3.1.2 Capillary Guided Corona Discharge (CGCD)

The CGCD configuration consisted of a 200 μm diameter enamel copper wire and a 10 x 10 cm in dimension square metal plate electrode. It was assembled in a pin to plane configuration. A quartz tube with an outer diameter of 6 mm and inner diameter of 1 mm was used to enclose the copper wire. It also functions to disseminate plasma into a wider area. This process occurs by trapping the residual charges on the inner surface of the quartz tube. Figure 3.2 shows the configuration for the CGCD.

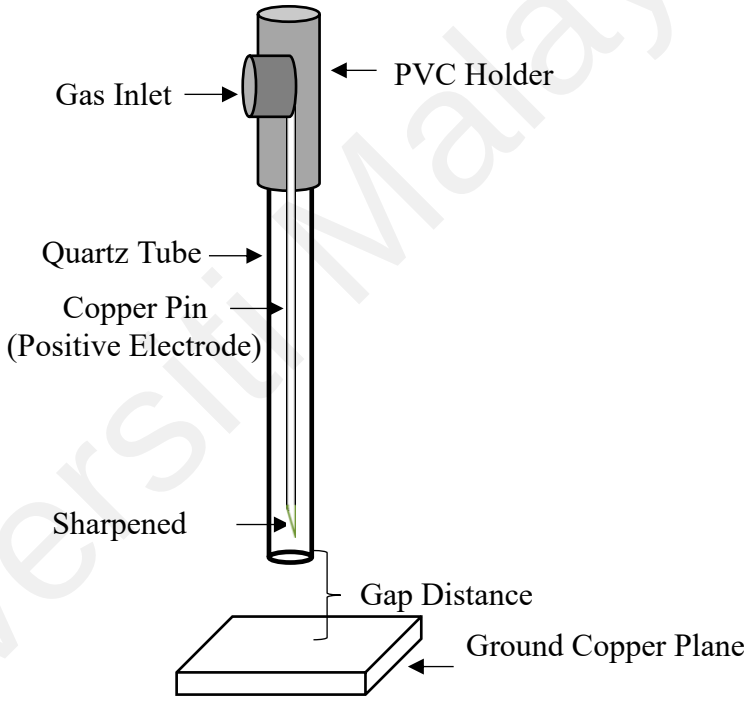

Figure 3.2: Diagram of CGCD configuration

The copper wire was connected to a high voltage direct current with a maximum output of 15 kV. A ballast resistor with a resistance of 26 MΩ was introduced between the power supply and the high voltage electrode. The usage of the ballast resistor is to prevent the transition from glow to arc discharge. A high voltage cable was used in the connection to ensure no current leakage during discharge.

3.1.3 AC plasma Jet at Ambient Air

Results from the bacterial treatment using planar DBD and CGCD configuration suggested that capillary configuration was more suitable for further investigations. A plasma jet configuration was constructed from the capillary configuration. This plasma jet configuration was adopted from pin to plane configuration. This configuration was first tested by Walsh et al in 2008. According to Walsh et al, this configuration is more favored due to the high electric field strength along the pin electrode. It has a tendency to generate a longer plasma plume. Plasma jet configuration is more favored and convenient for further treatment. This plasma jet can easily be designed to be more portable. Geometrical parameters in the capillary configuration was similar to the parameters in the construction of the plasma jet. A copper wire of 200 μm was connected to an AC power supply of 40 kHz maximum frequency. The copper wire was fixed at 2 mm from the end of the quartz nozzle. It was enclosed in a quartz tube measuring 6 mm outer diameter and 1 mm inner diameter. A new ground electrode was introduced. A copper tape of 0.5 cm width wrapped around the quartz tube at a suitable distance to the end of the quartz capillary tube. This distance is labelled as gap distance of the configuration. The copper pin was connected in series with a step-down transformer connected in series with the AC source. The schematic diagram of the setup is shown in Figure 3.3

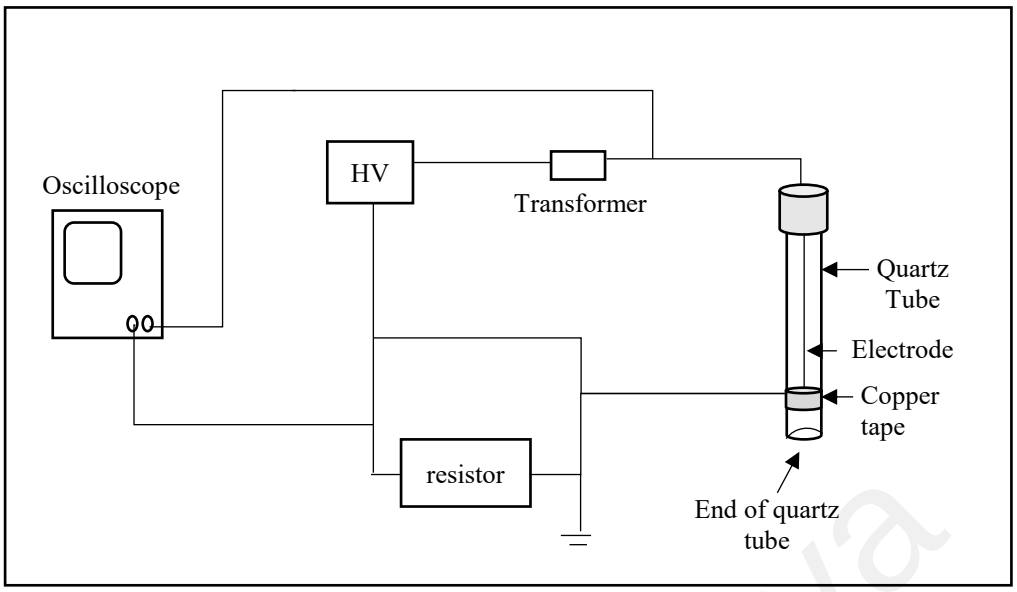

Figure 3.3 : Schematic Diagram of Plasma jet

The suitable gap distance was determined by varying the distance of the copper ring to the end of the quartz nozzle tube. The copper pin was set at 2 mm from the end of the quartz tube. The distance of the copper ring was varied from 2 mm to 5 mm from the end of the quartz tube. The applied voltage was varied from 10 to 25 kV for each gap distances aforementioned. The generation of plasma was observed and the current voltage (IV) signal waveform was recorded using a high end oscilloscope.

3.1.4 DC plasma Jet With Nitrogen Gas

A suitable gap distance was determined from the configuration of AC plasma jet. The copper pin was fixed at 2 mm from the end of the quartz tube. This suits the ability of plasma generated at 15 kV to 25 kV applied voltage. This geometrical parameter was maintained through out. A direct current (DC) power supply of maximum output of 15 kV was able to generate plasma jet. The DC power supply was tested in order to determine the availability of the plasma jet to be set in portable mode. In this case, nitrogen was introduced into the quartz tube via the gas inlet. Plasma could not be generated at ambient air. Industrial nitrogen gas with 99.999% purity which serve as the feed gas was

introduced into the quartz tube to accelerate the generation of the plasma jet and increase the gas ionization. Lotfy et al., (2019) had introduced nitrogen gas into plasma jet configurations where they have reported a plasma jet with relatively high energy excited states. It was found that nitrogen gas particles are able to enhance the growth of germination seeds. The gas flow was determined by connecting a flow rate meter to the nitrogen gas inlet. Gas flow was controlled by using valves as well as a gas regulator. The gas was fed through the gas inlet connected by a gas tubing connector to ensure no leakage during flow. The amount of gas fed into the quartz tube was determined by using a flow meter (Dwyer RMA-221-SSV) where it was connected from the gas tank to the gas inlet of the quartz tube. The schematic diagram of the DC plasma jet configuration setup shown in Figure 3.4.

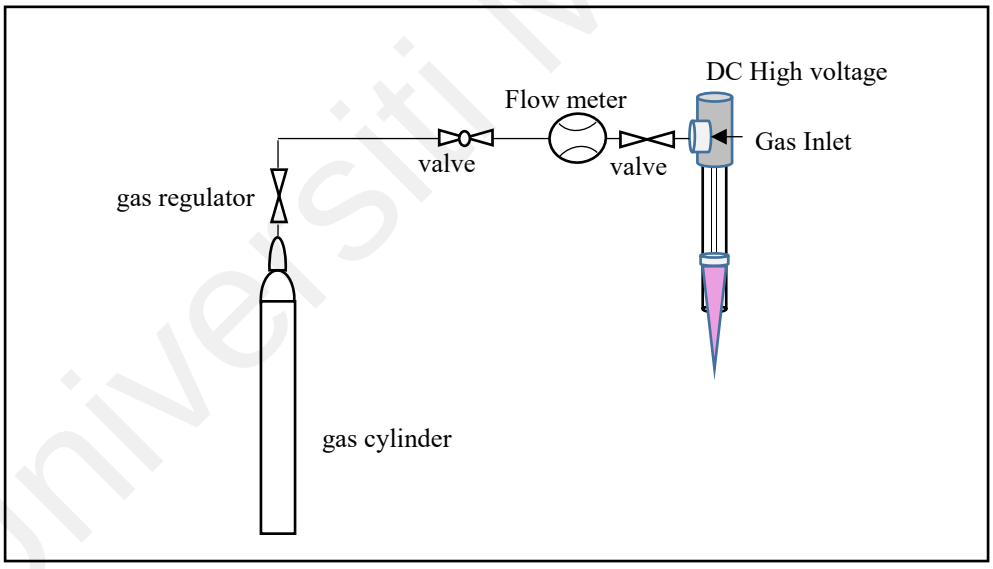

Figure 3.4 : Gas system connection for DC plasma jet

Most of the previous research introduced feed gas for many reasons, such as increasing the length of the plasma jet. The longest plasma jet ever generated was from Pfender et al., (1989). It has been reported as the longest plasma plume of 11 of 23.6 Litre/minute of argon gas. To date, most of the plasma jet design introduced feed gas as the carrier gas, (Lofty et al., 2019).

On top of that, feed gas also act as components that affects the generated reactive species, Adhikari et al., (2018).

3.2 Diagnostic Technique

3.2.1 Current Voltage (IV) Measurement

Measurements were carried out on the characteristics of the generated AC and DC plasma jet discharge such as current-voltage (IV). IV signals of both plasma jet were measured using a Tektronix high voltage probe, a current probe and a high-end oscilloscope. The P6015A high voltage probe is a ground-referenced 100 MΩ, 3.0 pF capacitance with 1000X attenuation. Due to its resistance, the high voltage probe will bypass some of the currents during the experiment. The upper maximum bandwidth of 75 MHz indicates the highest signal that can be detected. This signal will be attenuated to 70.7% of its original magnitude. The fastest rise time of this probe is 3.33 ns. It will ensure that the bandwidth is sufficient and suitable to be used in obtaining the plasma discharge signal. Shunt resistor of 1 kΩ was introduced for both AC and DC circuit for the measurement of discharge current. The schematic diagram of the IV signals is shown in Figure 3.5.

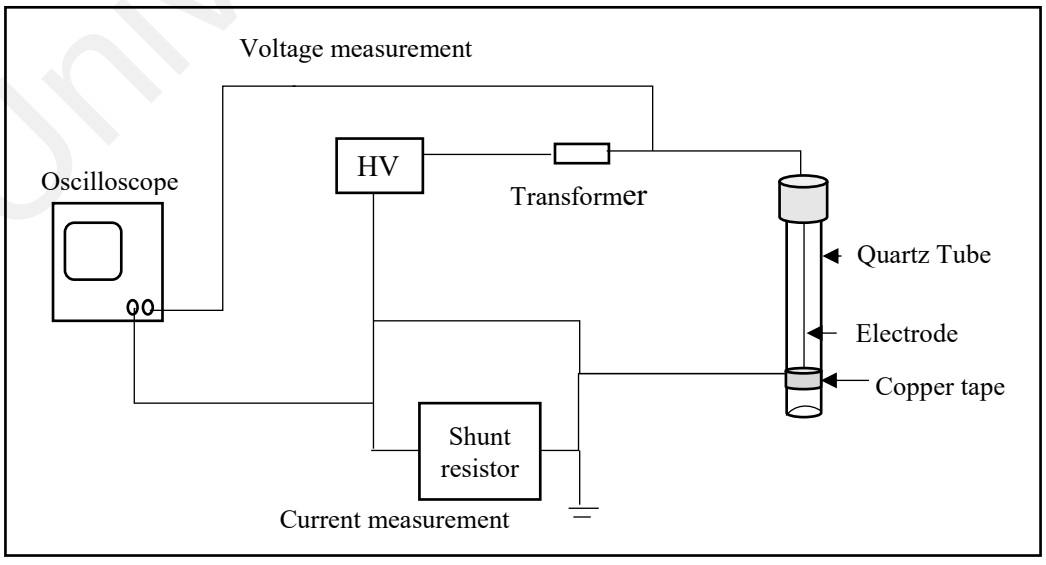

Figure 3.5 : Schematic diagram of IV signal measurement setup for AC and DC plasma jet

Currents passing through the resistor will develop a potential difference across it where a 1 Kohm resistor was introduced as a sensing resistor suited for the measurement of discharge current. The range of 1 V of sensing voltage was appropriate to be used. Discharge current can be calculated by the following equation,

$$I(\mathrm{t}) = \frac{V(t)}{R} \tag{3.1}$$

Discharge current was recorded by using a high-speed oscilloscope Tektronix TDS 2024B which has a maximum bandwidth of 200 MHz. This oscilloscope is suitable to capture the plasma discharge waveforms that typically occurs in a few hundreds of nanoseconds. The time base for this oscilloscope is 2.5 ns. Besides the highest bandwidth, it is also able to detect signal waveform with a sampling rate of 2.0 Gigasamples/second. The primary signal recorded by the oscilloscope will be the discharge current and discharge voltage waveforms. Signal waveform from both power supplies were collected and analysed. Most of the previous research reported that an AC plasma jet would have a typical waveform of filamentary discharge or microdischarges. The DC discharge will consist of series of pulses in nanosecond.

3.2.2 Plasma jet Discharge Power

A common practice of getting the discharge power of a plasma jet is by plotting a charge, *Q* and voltage, *V* figure. This QV figure is also known as the Lissajous Figure. A typical Lissajous figure is shown in Figure 3.6 (Peeters et al., 2018).

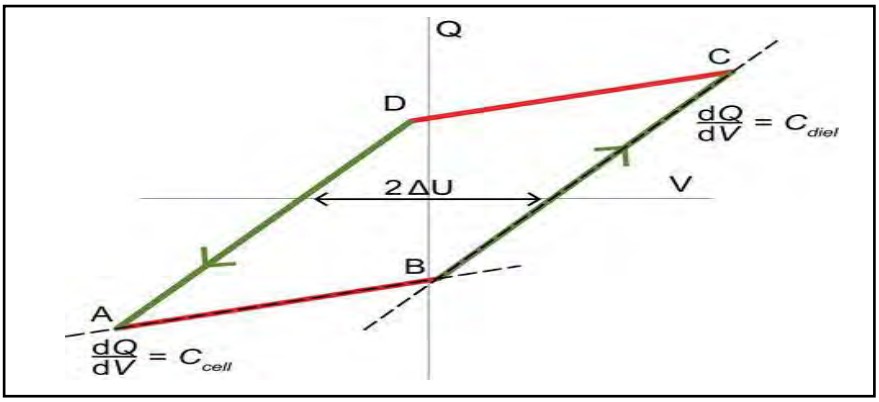

Figure 3.6: Typical QV Lissajous figure

Total discharge power was obtained by the product of the enclosed area of the QV Lissajous figure with the frequency of the discharge. The value of charges transferred across the gap between the electrodes, Q was calculated to plot the QV figure using the the $Q = CV$ relationship. C is the total capacitance and V is the voltage across capacitors. A series of capacitors with a total capacitance of 0.66 µF was used to determine the voltage drop across it. Considering that the two parallel plates as two capacitors in series, C total or regarded as C_{gap} can be determined as follows.

$$\frac{1}{C_{cell}} = \frac{1}{C_{diel}} + \frac{1}{C_{gap}} \tag{3.2}$$

Peeters et al., (2018) suggested that the C_{cell} can be obtained from the gradient of lines AB and CD while the gradient of BC lines and DA lines correspond to C_{diel}. The discharge power for DC plasma jet was obtained by using a simple operational method. The discharge power was calculated using the common equation,

$$E = VIT \tag{3.3}$$

Given that the E is the discharge energy, V is equivalent to discharge voltage, I is the discharge current and T is the discharge time. For every signal pulses recorded by the oscilloscope, the product of equation 3.3 was averaged. The discharge power is the

product of the average energy with the frequency of the DC plasma discharge obtained from the reciprocal of the discharge period.

3.3 Spectroscopy Technique

3.3.1 Plasma Emission

The Optical Emission Spectroscopy (OES) method is commonly practiced in the determination of the elemental composition of a plasma discharge. OES is a spectroscopic technique which does not require invasive methods. It can also be implemented in the observation of function and wavelength form of photons emitted from atoms or molecules. These photons will be emitted as atoms or ionized molecules. Emitted photons for every transition of each excitation level are associated with certain or discrete wavelengths, whereas specific electronic structure represents the types of the compositions. The reliable and excellent HR 4000 OES spectrometer was employed to determine electron temperature. In addition, the spectrometer came together with a fibre optic which has the ability to detect a range of 200 nm to 1100 nm of wavelength with a sensitivity of 100 photons per count at 800 nm. The OES technique was conducted together with a Spectra Suite software used to analyze the recorded spectra. The technique was implemented to obtain the electron temperature for both plasma jet in the AC and DC mode. It is important to emphasis on an accurate alignment during the emission spectrum of plasma jet where the optical fibre must be aligned with the frontal part of the plasma plume to ensure it can capture most of the emission generated. One way to improve the alignment is by using lens. It is also essential to note that the distance between the optical fibre is set not too close to the surface of the plasma jet plume. This is to ensure no conductive path is created to the optical fibre that might cause distortion to the spectrum. The optical fibre tip was placed around 1 cm to the surface of plasma jet. In this experiment, it was found that when the distance was less than 1 cm, the emission

could hardly be detected and led to the formation of a conductive path between the frontal part of the fibre optic with the plasma plume tip. The entire setup was placed in a dark condition throughout the emission spectroscopy detection experiment to ensure that the background noise is eliminated.

3.3.2 Plasma Electron Temperature

Evaluation of the plasma performance is based on the determination of electron temperature. Electron temperature is commonly obtained from the density of spectral lines. These lines are dependent on the electron temperature and proportional to the electron density. Therefore these parameters can be determined using Boltzmann plot (Shrestha et al. 2015; Tyata et al. 2013). The equation is shown below.

$$\frac{I_1}{I_2} = \frac{g_1}{g_2}\frac{A_1}{A_2}\frac{\lambda_2}{\lambda_1} e^{\left[-\left(\frac{E_1-E_2}{kT_{el}}\right)\right]} \quad (3.4)$$

I_{em} is the intensity, g is the statistical weight which is equivalent to $2J+1$ in nitrogen SPS, A is the transition probability, λ is the wavelength, E is the energy of the excited state in ev and k is the Boltzmann constant. The subscript 1 and 2 refer to the spectral lines of the same element selected. This method can only be applied when the plasma is in a complete local thermodynamic equilibrium (LTE). According to Shreshta et al., (2016), plasma jet is not in complete LTE and therefore the Boltzmann plot method is not a valid method to determine the exact value of the electron temperature. It is only able to give the estimation value of the electron temperature with various working condition of plasma discharge. In this study, this method was applied in order to estimate the electron temperature. The values of E, g and A were obtained from the National Institute of Standards and Technology (NIST) atomic spectra datasheet using the Boltzmann plot method. The

electron temperature of AC and DC plasma jets were estimated by applying the Boltzmann plot.

3.4 Samples for Treatment

3.4.1 Pure Culture Bacteria

Three different bacterial strains were used in the plasma treatment. Chronic wound bacteria samples, *Staphylococcus aureus* (MRSA) and *Pseudomonas aeruginosa* (PA) strains were treated using planar DBD and CGCD configurations. *E coli* bacteria was tested using both AC and DC plasma jet. All strains were cultured from pure cultures of *S. aureus*, *P. aeruginosa* and *E coli* strains respectively. The strains were collected from culture collections in the Biomedical Science and Molecular Microbiology laboratory, Institute of Postgraduate Studies, University of Malaya. Strains were isolated from various specimens including nasal swab, tissue swab, bone swab and also wound swab (Ling, 2012). The clinical specimens collected from wound swab were used to culture *E coli* strains using MacConkey agar. MRSA and PA strains were cultured using blood agar. Cultured agar was inoculated overnight at 35^{o} C. The suspected *S. aureus* colonies in blood agar (showed b-haemolysin with golden-yellow colonies) was further tested with coagulase test and cefoxitin disk diffusion test following Clinical and Laboratory Standards Institute, CLSI guidelines (2010). MRSA was identified as MRSA if zone diameter is less than 21 mm and tested positive in coagulase test. *E coli* was identified as pure *E coli* as it yielded pink-coloured colonies and displayed uniform gram-negative rods (Pondei et al., 2013). The purity of the bacterial cultures was determined by streaking on mannitol-salt agar. All the bacterial cultures of the strains were stored in Tryptone Soy Broth (TSB) supplemented with 50% glycerol at 20 ^{o}C and 85 ^{o}C. Tryptone Soy Agar (TSA) stab cultures were also stored at room temperature (Ling, 2012). Swabbed agar plates were stacked upside down before conducting the treatment process. All samples

were prepared in replicates of two for each treatment. Wound healing process involves three overlapping stages, inflammation, proliferation and remodeling (Gurtner et al., 2008). It is important in playing a key role in the deposition of extracellular matrix (ECM) components, wound contraction and remodeling of new ECM (Zielins et al., 2014). Fibroblasts are responsible for most collagen and elastin synthesis and organization of the ECM components. They are indispensable in determining how well the wound will ultimately heal.

3.4.2 Serial Dilution

Serial dilution was conducted before the treatment process began. The amount of bacterial colonies can be determined before the treatment process through serial dilution by applying the following equation.

$$CFU = \left(\frac{(No\ Of\ Colonies\ on\ Plate) * (Dilution\ Factor)}{Amount\ of\ Plated\ suspension}\right) \quad (3.5)$$

The amount of bacteria colonies before the treatment is labelled as control. The efficacy of the discharge configuration can be determined by comparing the bacterial viability. A suspension of 900 μL phosphate buffered solution (PBS) solution was prepared before the treatment process. An aliquot of 100 μL of overnight bacterial suspension was serially diluted by three folds before treatment. Serial dilution method was only conducted for MRSA and PSA strains. This is to ensure a better comparison of the CFU between the control samples and the treated bacteria.

3.5 Arrangement for Bacteria Treatment

50 µL of the 10^{-3} fold serially diluted bacteria culture was pipetted on a glass slide. The slide was placed under plasma exposure at different durations. MRSA and PSA strains were tested using planar DBD. The time of treatment was varied from 10 minutes to 60 minutes. After treatment, all samples including control samples were washed in 0.85%. phosphates buffered saline (PBS) solution to remove bacterial strain from the glass. The suspension was shaken for homogeneity. 100 µL of homogenous bacterial suspension of each treated samples was pipetted on agar. Surface agar was uniformly spread through the spread plate method for colonies enumeration. Spread agar plates were incubated overnight at 37 °C. Bacterial colonies were enumerated after overnight incubation. Controlled samples and treated samples data were recorded. Similar steps were repeated for the treatment with CGCD configuration. However, treatment time under CGCD was limited until 40 minutes. Luria Bertani (LB) agar was used as nutrient agar for the MRSA bacteria growth. Tripticase Soy agar (TSA) was used to grow PA strains. All strains were prepared with a total replicates of 6 from three different trials. The treatment under planar DBD and CGCD configuration are summarized in Table 3.1.

Table 3.1 : Treatment parameter for planar DBD and CGCD configurations

	Planar DBD	**CGCD**
Discharge Source	AC power supply	DC power supply
Type of Bacteria	MRSA and PA	MRSA and PA
Time of exposure (MRSA)	10, 20, 30, 60 minutes	10, 20, 30 and 60 minutes
Time of exposure (PA)	10, 20, 30, 40 minutes	10, 20, 30, 40 minutes
Gap distance	2 mm	10 mm

Suitable DBD configurations, plasma jet efficacy was tested on *E coli* bacteria lawn. Bacteria lawn was prepared in order to identify the effect of plasma on the sterilisation area upon treatment. Pure culture of *E coli* was swabbed on LB agar by using sterilized cotton swab. Bacteria lawn was exposed to both AC and DC plasma jet. Bacteria lawn was placed at the tip of the plasma jet. The treatment of the plasma jet is summarized in Table 3.2

Table 3.2: Treatment parameter for AC and DC plasma jet

	AC Plasma jet	**DC Plasma jet**
Type of bacteria	*E coli* lawn	*E coli* lawn
Distance of treatment	Tip of Plasma plume	Tip of Plasma Plume
Applied Voltage	25 kV	15 kV
Time of exposure	5, 10, 30, 60, 120 seconds	5, 10, 30, 60, 120 seconds

Treated bacteria lawn was immediately incubated overnight at 37 °C. The sterilized area under plasma treatment was compared for both AC and DC plasma jet. The data for both treatment was recorded. Graph of comparison was plotted for both AC and DC plasma jet.

3.6. Arrangement for Fibroblast Treatment

Normal Human Dermal Fibroblasts (NHDF) cells (C-12302) was purchased from PromoCell (Germany) and maintained in a commercial fibroblast growth medium (PromoCell, Germany) supplemented with 1 ng/mL basic fibroblast growth factor, 5 µg/mL insulin, 2% (v/v) fetal bovine serum (FBS), 100 U/mL penicillin, and 100 µg/mL streptomycin and incubated in humidified air containing 5% CO_2 at 37 °C. 3-(4,5-dimethylthiazol-2-yl)-5-(3-carboxymethoxyphenyl)-2-(4-sulfophenyl)-2H-tetrazolium

(MTS) solution (Cell Titer 96 Aqueous One Solution, #G3582, Promega, WI, USA) was purchased to measure the cell proliferation rate of NHDF. 5,000 NHDF per well (400 µL/well) were seeded onto a 24-well plate and incubated overnight at 37 °C in a 5% CO_2 incubator. The seeded cells were exposed to atmospheric pressure plasma powered by AC at 15 kV. The time of treatment were varied from 10 s, 20 s, 40 s and 60 s. The parameter is listed in Table 3.3

Table 3.3: Different parameter of AC plasma jet on fibroblast cells treatment at a different time of exposure

Applied voltage (kV)	Distance to the samples (From the plasma tip) (mm)
25 kV	5
15 kV	10
15 kV	15
15 kV	20

Cells were exposed to the plasma at short duration of exposure of 10 seconds, 20 seconds, 40 seconds to 60 seconds. This treatment time was applicable to all the listed parameters in Table 3. Treated cells were also incubated with different incubation time from 24 hours, 48 hours to 72 hours. This incubation time is to ensure the growth of the cells is sufficient. Treated fibroblast cells were analysed based on the absorbance rate. For treated samples at each time point, 40 µL MTS reagent per well was added into the plate and incubated for additional 3 h at 37 ◦C in the 5% CO_2 incubator. The optical density (OD) was then measured at 490 nm using a multimode microplate reader (Tecan, Switzerland). Graph of cells absorbance at different time of exposure was plotted. The effect of incubation hour on the cells absorbance also investigated and displayed in the graph.

CHAPTER 4: RESULTS AND DISCUSSION

In this study, two dielectric barrier discharge (DBD) configurations have been employed to generate plasma at atmospheric pressure. One is planar DBD while the other configuration is capillary guided corona discharge (CGCD). Both DBD configurations were operated in transferred mode. Their suitability for bacteria treatments have been tested. Capillary configuration was found to be more suitable, thus this configuration was used for bacteria treatment. The capillary configuration was improvised by changing the mode of operation from transferred mode to non-transferred mode. This improved mode was used to generate plasma jet at atmospheric pressure. Alternating current (AC) and Direct current (DC) power supply were employed to power the improved mode of operation. Plasma jet was successfully generated at atmospheric pressure when powered by AC and DC power supply. The efficacy of the generated plasma jet has been identified from bacteria samples treatments. Bacteria samples were isolated from wound swab cultures. It was found that plasma jet powered by AC power supply is more effective in bacterial inactivation. The effect of AC plasma jet on the proliferation process of fibroblast cells was also investigated.

4.1: Characteristics of plasma discharge for Planar DBD

Plasma can be generated at atmospheric pressure by using corona discharge, dielectric barrier discharge (DBD) and arc discharge, (Xu et al., 2008). Atmospheric pressure plasma is commonly generated using DBD configurations since the generated plasma is at a low temperature. Low-temperature plasma is suitable to be employed in biomedical applications, (Xu et al., 2008). In this study, a planar DBD configuration was employed to generate plasma at atmospheric pressure. It was powered by a 50 Hz AC with a maximum voltage of 40 kV peak to peak.

It was found that the plasma generated consisted of current filaments or filamentary discharge in between the gap. The schematic diagram of the filamentary discharge is shown in Figure 4.1.

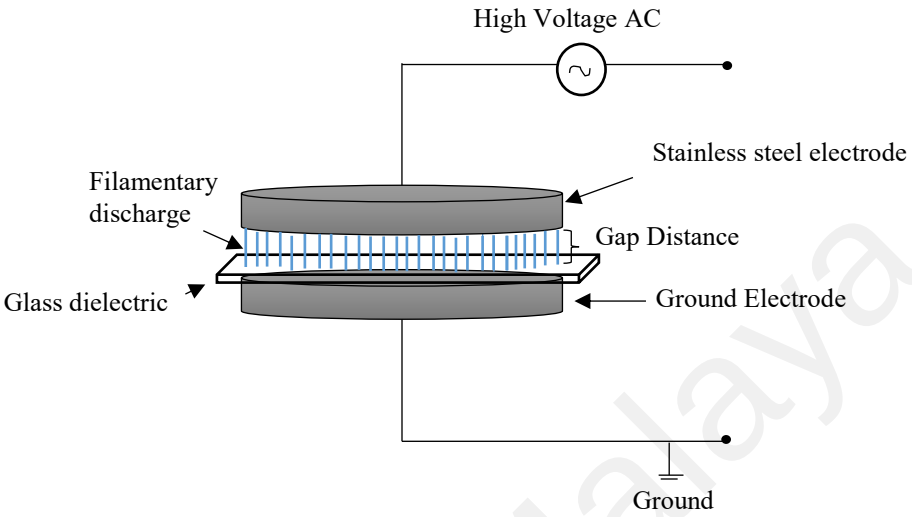

Figure 4.1: Filamentary Discharge between plates of Planar DBD setup.

A glass dielectric was placed between the gap to prevent the discharge transition to arc discharge. This will limit the number of current filaments bridging the gap. Charges will build up on the surface of the electrode and form arc discharge. Arc discharge is a high-temperature discharge which is unsuitable for bacteria treatment. Gap distances of 1 mm and 2 mm were tested for this DBD configuration. Suitable gap distance is required for the plasma to be generated. It was observed that as the gap distance increased, a higher discharge voltage is required to generate plasma. When the applied voltage was set at 15 kV peak to peak at 1 mm gap, filamentary discharge started to generate. Current filaments were observed once the applied voltage reached more than 7 kV peak to peak. As the applied voltage increased, the number of current spikes increased. As the gap distance was increased to 2 mm, plasma started to be initiated at 7 kV peak to peak. The current voltage of the DBD is shown in Figure 4.2

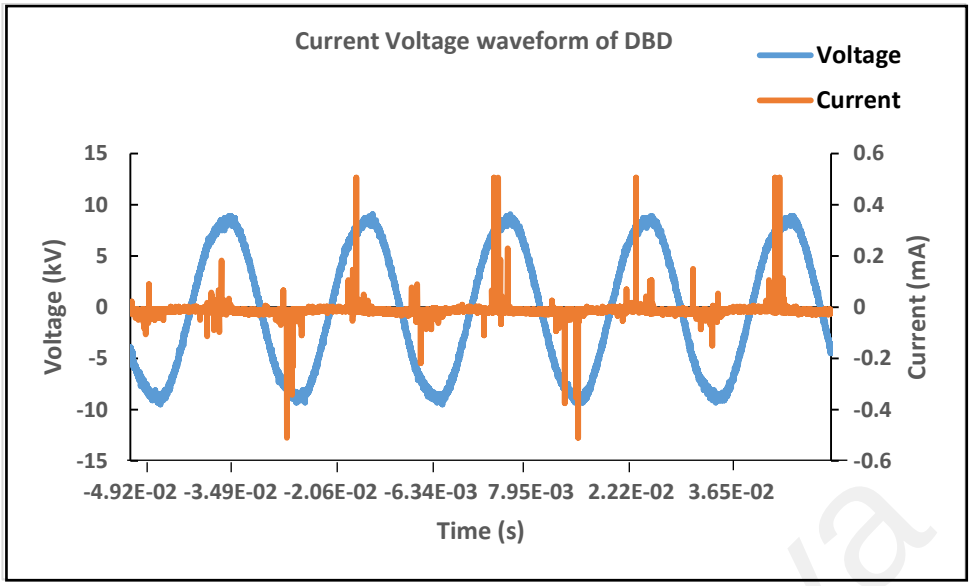

Figure 4.2: Current Voltage waveform of DBD configuration

The number of current spikes increase as the applied voltage is increases from 7 kV peak to maximum peak to peak of 26 kV. Analysis of the number of current spikes for the planar DBD is shown in Figure 4.3.

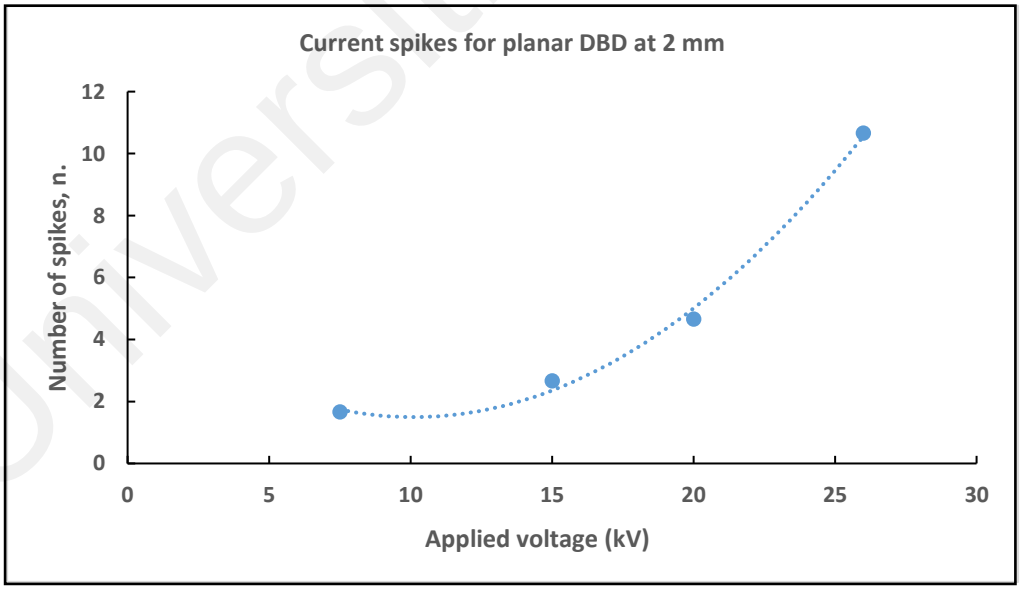

Figure 4.3: Number of current spikes for planar DBD at 2 mm gap for planar DBD

Higher applied voltage was required to generate the plasma causing more spikes to occur. This condition might have occurred due to the presence of higher electric field strength required to generate plasma.

4.2: Characteristics of plasma discharge of Capillary Guided Corona Discharge (CGCD)

Plasma at atmospheric pressure was generated using other configurations of DBD. Capillary configuration or capillary guided corona discharge (CGCD) configuration was used to generate plasma at atmospheric pressure. CGCD configuration was powered by a direct current (DC) supply with a maximum voltage of 15 kV. A quartz capillary tube was introduced in the configuration as a dielectric. Plasma is commonly generated in streamer form for capillary configurations. It is similar to what has been reported by (Chang et al., 1991). According to Chang et al, (1991) during the formation of the plasma, charges build up on the quartz surface and the capillary tube guides the charges out to the end of the capillary tube. As a result, it was observed that plasma discharge is generated in streamer form. The schematic diagram of the streamer form generated by the CGCD configuration is shown in Figure 4.4.

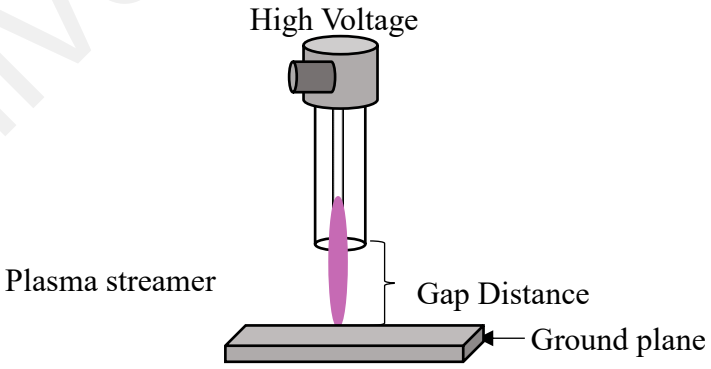

Figure 4.4: Generated plasma in streamer form for CGCD configuration

Plasma streamer is also known as filamentary discharge where it consists of a large number of current filaments. The current voltage waveform of the CGCD is shown in Figure 4.5

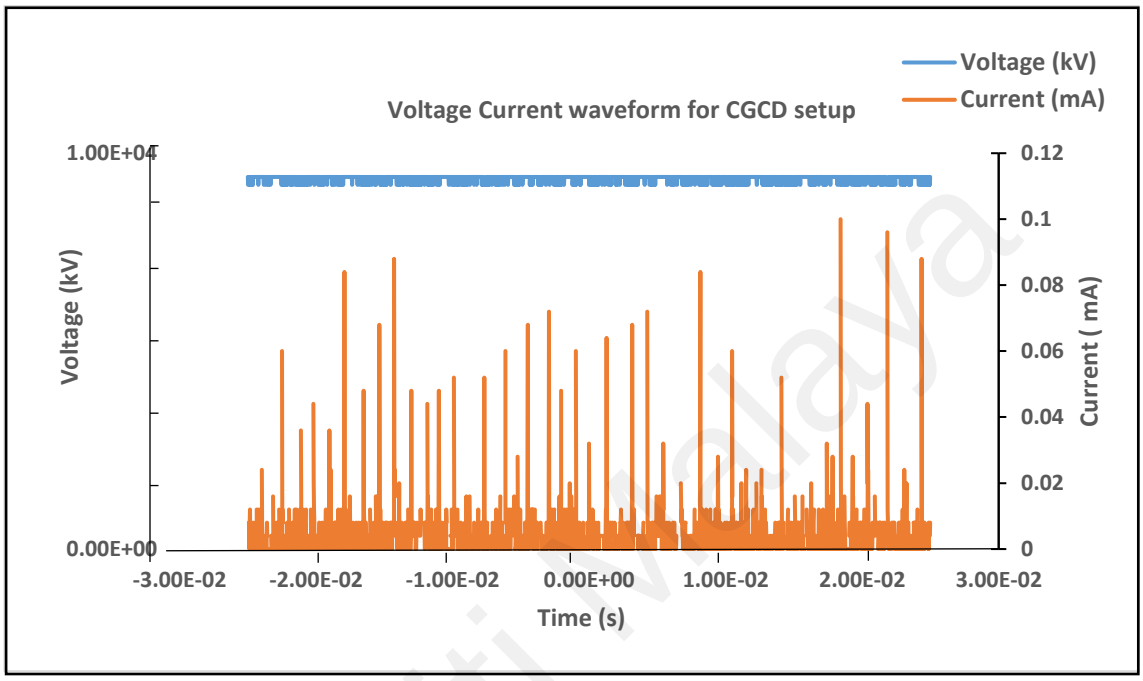

Figure 4.5: Current Voltage waveform of CGCD configuration

Gap distance of 6 mm to 10 mm was tested for the generation of plasma. The current voltage analysis of results is shown in Figure 4.6. It is shown that as the gap distance increases, higher applied voltage is required to generate plasma.

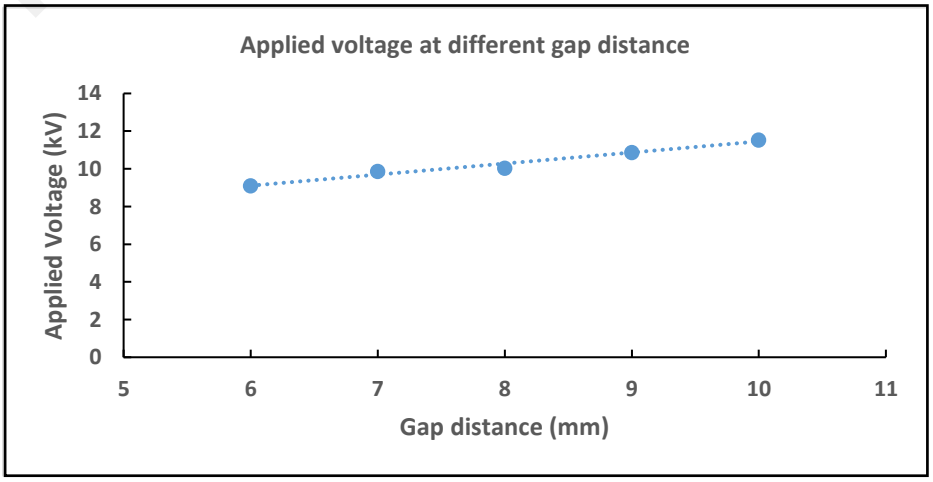

Figure 4.6: Applied voltage at different gap distance for CGCD configurations

Higher applied voltage is required to generate plasma as the gap distance increases. This is due to the higher electric field at the sharp tip of the copper electrode.

4.3: DBD configuration suitability on bacterial treatment

Suitable DBD configuration on bacteria treatment was determined using both planar DBD and CGCD on bacteria treatments. Bacteria samples were collected from the culture collection of Biomedical Science laboratory University of Malaya. The bacteria samples were isolated from chronic wound swab. The isolated bacteria samples were Meticilin Resistant *Staphyloccus aureus* (MRSA) and *Pseudomonas aeruginosa*, (PA) strains. The strains are MRSA 0704-18, MRSA 0704-3, MRSA 0408-34 and PA 04, PA 18, PA 19, PA 2 respectively. According to Werdin et al., 2009, MRSA and PA bacteria have been identified in most of the chronic wound cases. It can be found in about 20% to 50% of chronic wound cases. MRSA and PA bacteria strains were cultured by a streak plate method and incubated overnight. The image of the single colony of a bacteria control is shown in Figure 4.7.

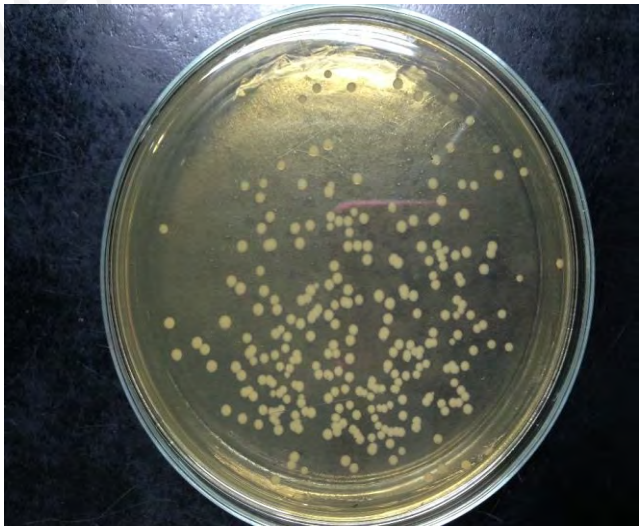

Figure 4.7 : Single colony of bacteria control

It is important that the bacteria culture is a single colony in order to ensure that the bacteria is a pure culture.

4.4 Treatment of Bacteria strains by Planar DBD

A suitable gap distance was chosen for the treatment of chronic wound bacteria samples using planar DBD configuration. A gap distance of 2 mm was applied to generate the plasma. The gap distance was chosen due to the consistency of the number of filaments between the gap. It is also important to ensure that no arcing is generated between the gap during the treatment. The treatment time was varied from 10 mins to 60 mins on the MRSA and PA strains with a total of 6 replicates for each time of exposure. When the time of treatment was varied, the suitability of the configuration on the bacterial treatment can be determined. Inactivated bacterial colonies on agar plates after treatment was counted through the plate count method. The data is plotted in the form of a log graph as shown in Figure 4.8.

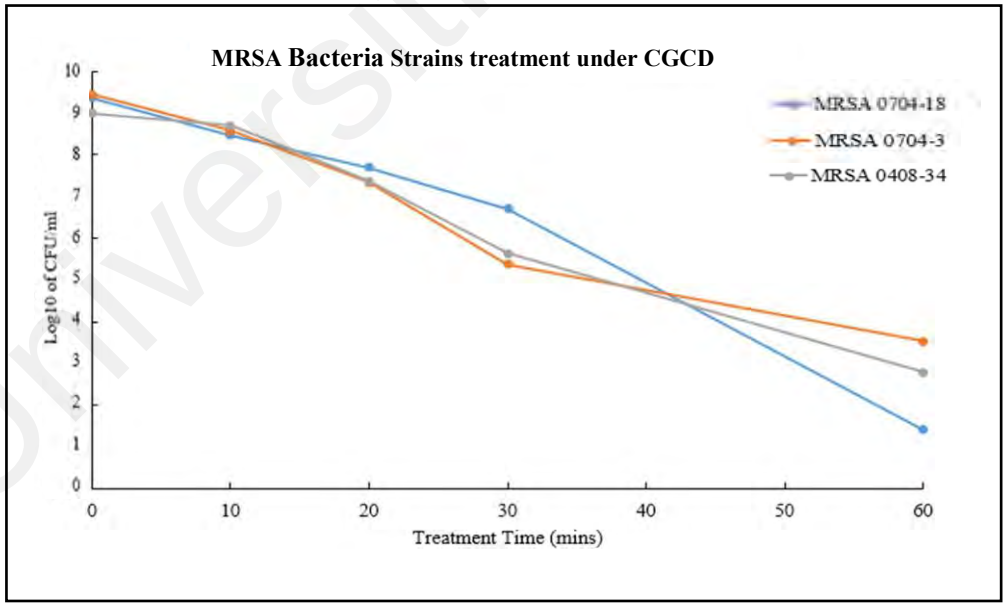

Figure 4.8: Log form graph of MRSA strains under DBD treatment at different treatment time

The graph in Figure 4.8 shows that MRSA populations reduced to 5 Log_{10} in colony-forming unit (CFU)/ ml after 30 minutes of planar DBD treatment. When the duration of treatment time was extended to 60 minutes, more than 80 percent of the bacteria

population was inactivated. Treatment time was not extended to avoid excessive heating to the DBD setup. PA bacteria treatment with planar DBD configuration showed similar results with MRSA strains. 5 $\log_{10}$ reduction in the populations were achieved after more than 30 minutes of treatment time. When the time of exposure was extended to 40 minutes, all bacteria strains population were inactivated. Results are shown in Figure 4.9.

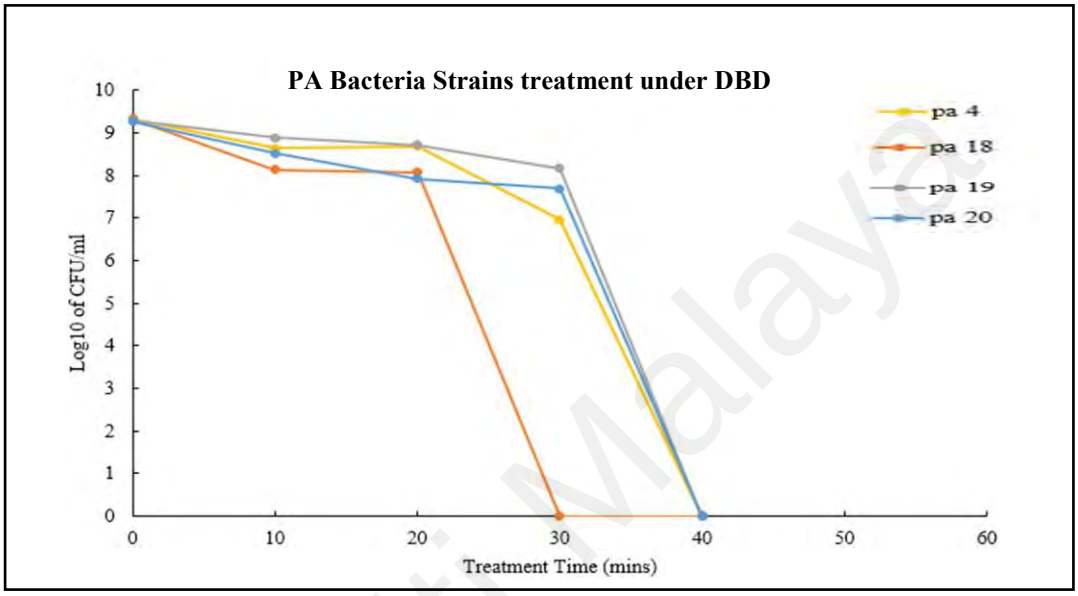

Figure 4.9: Log form graph of PA bacteria strains using DBD setup at different treatment time

4.5 Treatment of Bacteria strains by CGCD

Treatment on the same bacteria strains were repeated with a different DBD configuration. This was to identify the suitability of the configuration to the treatment. CGCD configuration was employed on the same bacteria as planar DBD. MRSA and PSA bacteria strains were tested at a gap distance of 8 mm. This gap distance was chosen due to the stability of the plasma streamer. Similar time of exposure was maintained with the CGCD configuration throughout the treatment. This is to ensure a better comparison on the suitability of both DBD configurations. After plasma treatment, the colonies were counted and the data were plotted in the log form graph. The graph is presented in Figure 4.10.

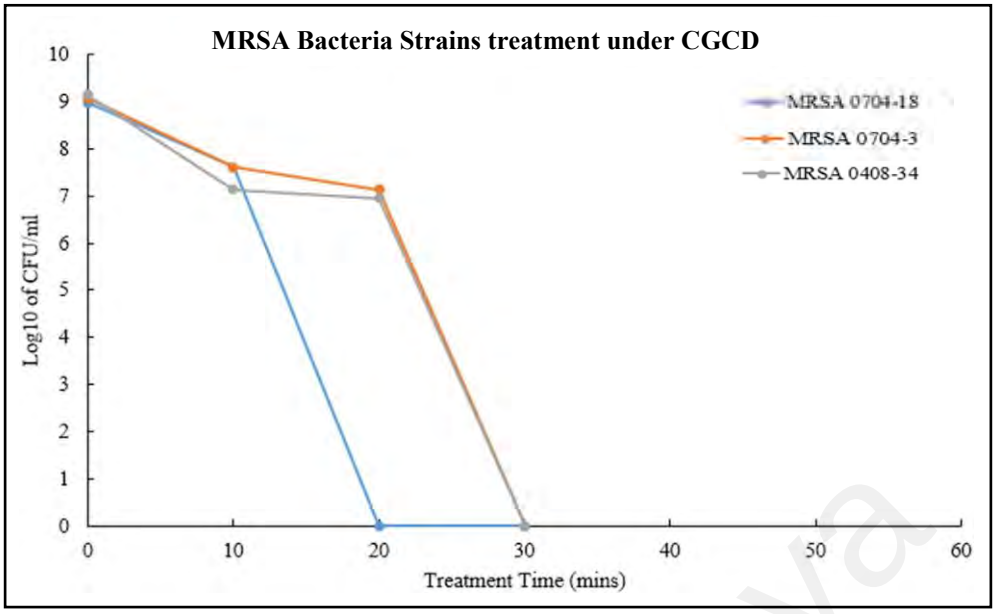

Figure 4.10: Log form of MRSA bacteria strains under CGCD setup at different treatment time

The log graph shows that MRSA strains required 10 minutes of plasma treatment to reduce to 7 $\log_{10}$ in its populations. Prolong treatment time of 20 to 30 minutes was required for full inactivation of all MRSA strains. Treatment time of 20 to 30 minutes shows complete inactivation's of PA strains. The plotted graph is shown in Figure 4.11

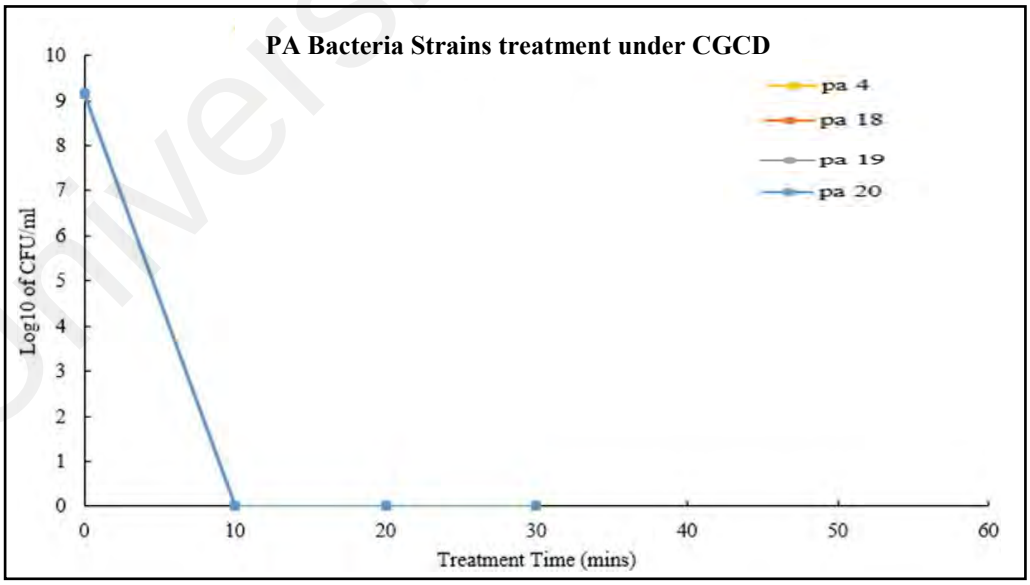

Figure 4.11: Log form of PA bacteria strains under CGCD setup at different treatment time

4.6 Bacterial Treatment comparison of Planar DBD and CGCD

To identify the suitability of the DBD configurations, treatment data for both configurations were analyzed and a log form graph was plotted. The plotted graph is shown in Figure 4.12.

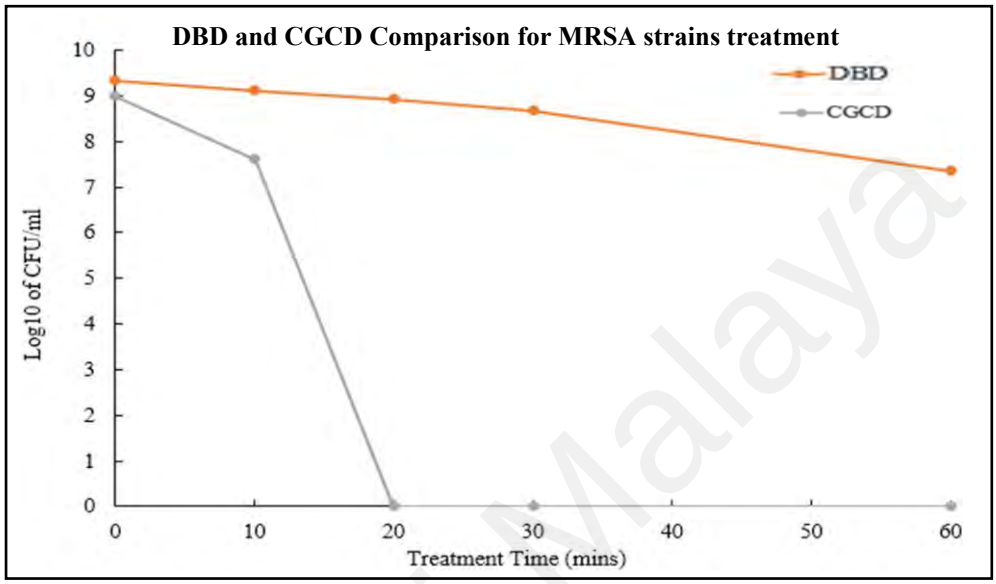

Figure 4.12: Log form of planar DBD and CGCD setups efficacy on MRSA strains at different treatment time

From the plotted graph, data for the CGCD configuration reduce to almost 7 $\log_{10}$ in less than 10 minutes for all MRSA strains. Complete inactivation of all MRSA strains after 20 minutes. However, planar DBD requires more time to decrease to 9 $\log_{10}$ in the population for all MRSA strains. A similar analysis was performed on the PA bacteria strains. Both DBD configuration treatment data on PA bacteria strains were analysed. Graph of the analysed data is shown in Figure 4.13. Raw data for bacteria treatment for both configurations are presented in appendix B1-B4.

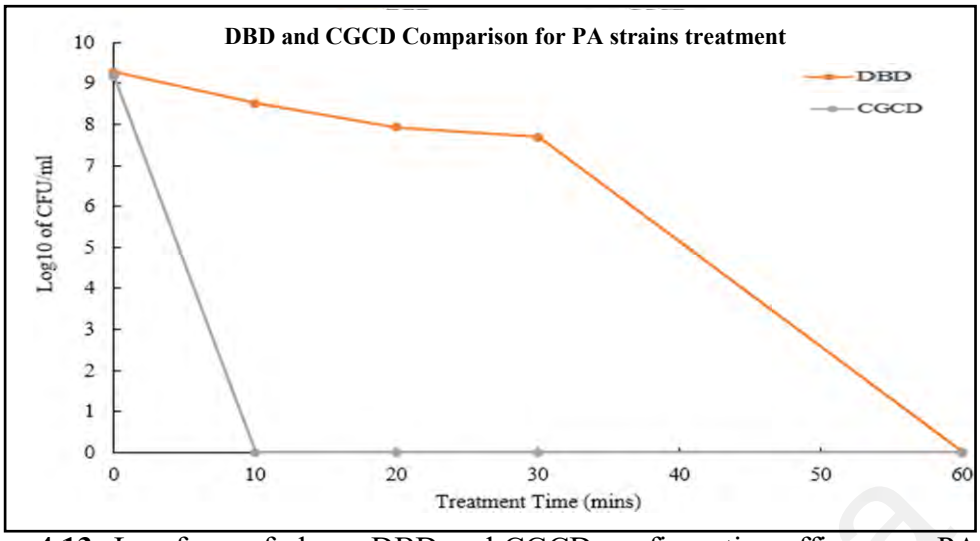

Figure 4.13: Log form of planar DBD and CGCD configuration efficacy on PA strains at different treatment time

Under planar DBD configuration treatment, all PA strains achieve full inactivation after 60 minutes. This observation can be explained based on the nature of the plasma generated. Planar DBD was generated in filamentary form where the current filaments distributed randomly on the electrode surface. Random reaction with the bacteria samples caused discrepancies in the bacterial effect. CGCD configuration generated a plasma streamer followed by corona wind. These corona winds turn to be more diffused upon reaching the bacteria, providing a better reaction between the plasma and the bacteria samples. The inactivation results are in accordance with previous works which suggested that gram-negative bacterium (PA) inactivates faster than positive bacterium (MRSA).

4.7 AC Plasma jet

The treatment of bacterial strains results suggested that capillary configuration is more efficient and convenient than planar DBD for further implementations. Therefore, the capillary configuration was improvised by changing to a new configuration. Pin to ground ring configuration was implemented to generate plasma jet. The new configuration diagram is shown in Figure 4.14.

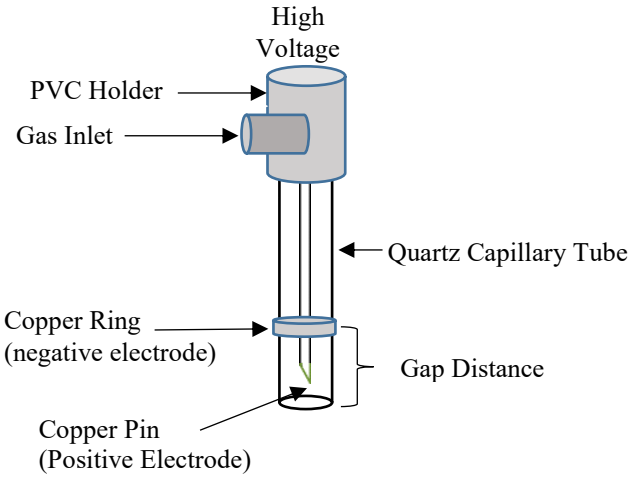

Figure 4.14: A pin to ring configuration for the generation of plasma jet

In the new configuration, the capillary geometrical parameter was maintained together with the same diameter of quartz capillary tube. Prior to the generation of the plasma jet, a suitable gap distance was determined. The gap distance is defined as the distance from the copper ring to the end of the quartz capillary tube (Figure 4.14). The copper pin was fixed at 2 mm from the end of the tube while the copper ring was varied from 2 mm to 5 mm from the end of the tube. No plasma was observed when the applied voltage was set at 10 kV. This might be due to insufficient energy to initiate the ionization. When the applied voltage was increased from 15 kV to 25 kV, generation of plasma started. Plasma was generated without any feed gas. It was generated in ambient air. This is to ensure further improvement of the configurations is able to operate in portable mode. The image of the plasma jet generated is shown in Figure 4.15

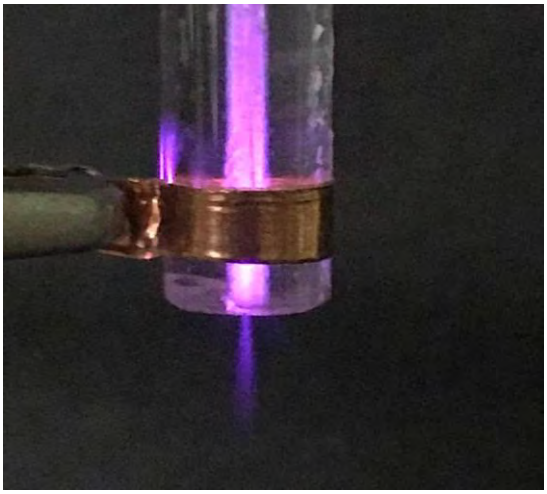

Figure 4.15 : AC plasma jet at atmospheric pressure at ambient air

4.7.1 Characteristics of The AC Plasma jet

Diagnostic methods was performed to determine the electrical characteristics of the generated plasma jet. The electrical characteristics of the AC plasma jet are as follows:

a) Voltage-Current measurement

b) Discharge Power

c) Spectroscopy

When the plasma jet was generated using an AC source, the current voltage (IV) was recorded. Recorded IV is shown in Figure 4.16

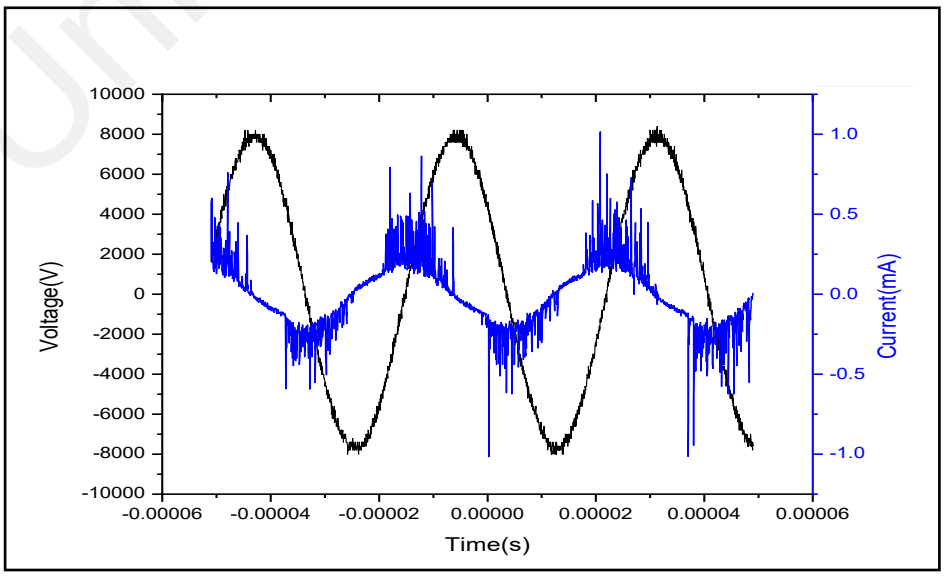

Figure 4.16: IV waveform for AC plasma jet at 15 kV applied voltage

Figure 4.16 shows an IV waveform of the generated plasma as the applied voltage was set at 15 kV. Diagram shows that for every cycle of positive and negative, it consists of microseconds current spikes. These current spikes lie on top of the voltage signals. It was a capacitive discharge as the current spikes led the voltage signals. Each spike is built of a numerous number of discharge filaments. The current spikes are observed at positive cycles when the discharge voltage reaches more than 4 kV. Discharge voltage started to increase until maximum discharge of around 6 kV peak to peak voltage. It shows a consistent number of spikes for every cycle of positive and negative. When the applied voltage increases to 20 kV, more intense plasma are observed. This is indicated by more number of current spikes generated. The current spikes are shown in Figure 4.17.

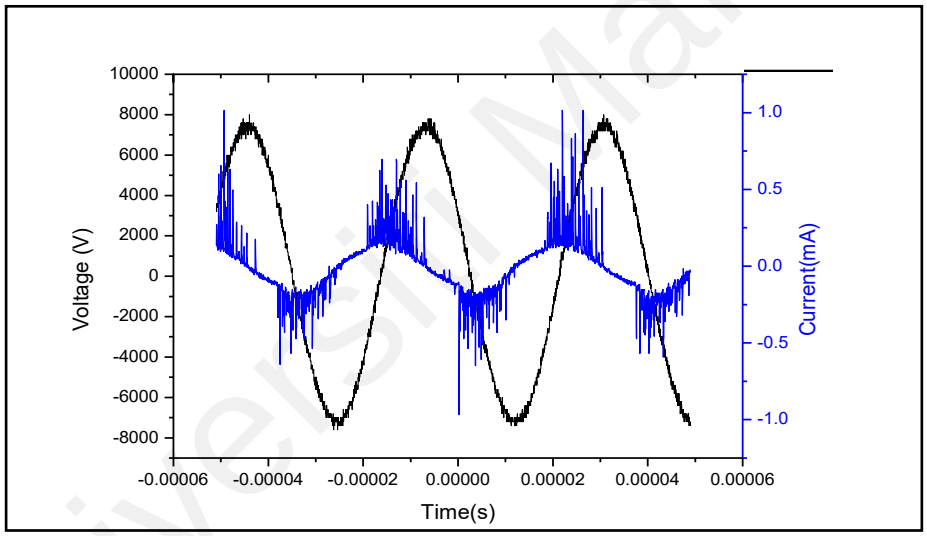

Figure 4.17: IV waveform of AC plasma jet at 20 kV applied voltage

Current spikes start to be initiated at the same discharge voltage and gradually increase until maximum 8 kV peak to peak voltage. It is observed that discharge current is in the miliamperes magnitude. This low current discharge indicates that it is in the DBD current range. As the applied voltage is set to 25 kV, there are no significant changes with IV signals. Results in Figure 4.16 show that current spikes occur once the applied voltage reaches 4 kV. Maximum discharge of 8 kV peak to peak voltage is attainable. Memory effect needs to be considered for the negative cycle discharge. Higher discharge voltage

is observed for the first negative cycles. Furthermore, it can be concluded that plasma discharges consist of plasma ON and plasma OFF regions. Plasma ON and OFF regions are shown in Figure 4.18.

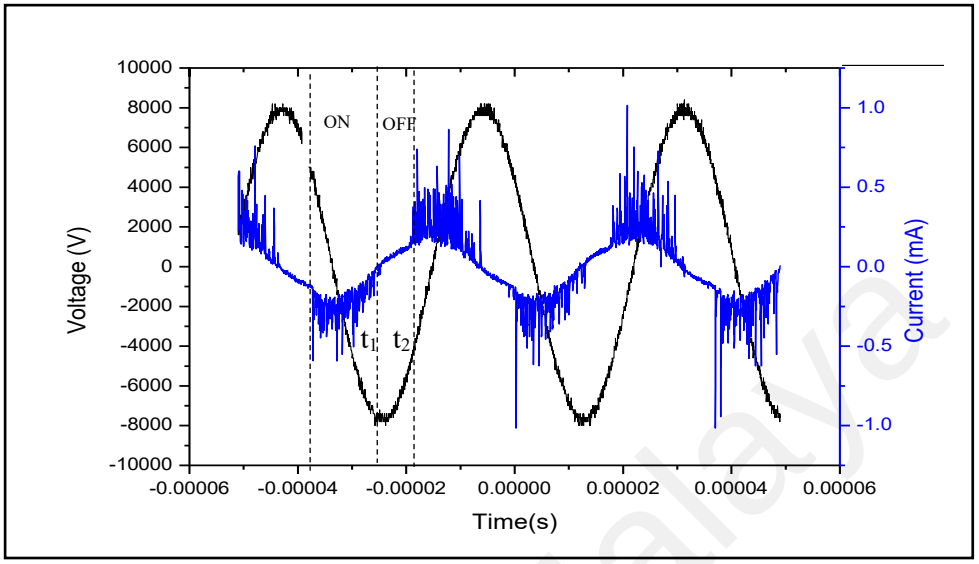

Figure 4.18: IV waveform for plasma jet at 25 kV

Plasma ON region is referred to as the region where the plasma is generated. While the OFF region indicates that no discharge was generated. This is due to insufficient energy where it does not follow the Paschen Law of ionization. Moreover, when the applied voltage was increased from 15 kV to 25, it shows that the number of current spikes increases. The results are as shown in Figure 4.19.

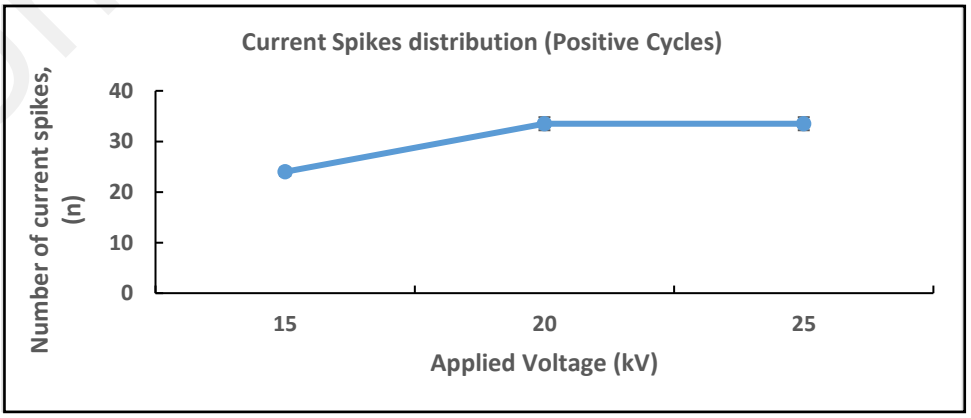

Figure 4.19 : Number of current spikes, n at positive cycles

From the diagram in Figure 4.19, it shows that the number of spikes for positive cycles increases as the applied voltage increases from 15 kV to 25 kV. This might be due to the sufficient energy for more energetic electrons to be ionised. Moreover, as the applied voltage is set to 25 kV, no changes to the number of current spikes are observed. Thus, it indicates the limitation of electron avalanche for these geometrical parameters. Hence, applied voltage was not extended beyond 25 kV. For the negative cycles, similar observation with positive cycles are observed. The number of spikes increases as the applied voltage increases from 15 kV to 25 kV. Plume length is a crucial parameter in bacteria strain treatment. Longer jet plumes will make the treatment at different depths of tissues possible. The longest jet plume ever reported for biomedical samples treatment is about 11 cm by Pfender et al in 1989. The jet plume was produced at 23.6 litre/min of feed gas. The AC plasma jet length reached 5 mm when the applied voltage was set to 20 kV and 25 kV. Results of plasma jet length at different applied voltages are presented in Figure 4.20

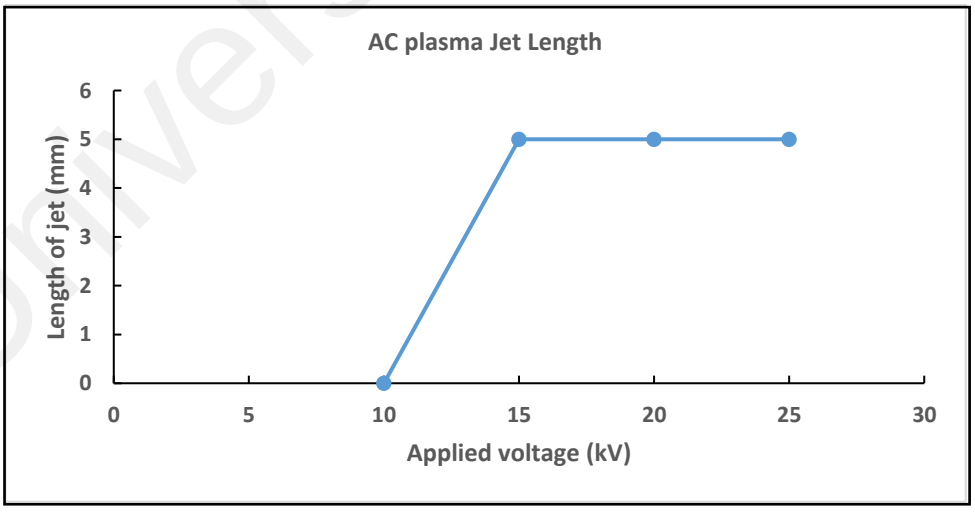

Figure 4.20: Length of AC Plasma jet at different applied voltage

According to Lau et al., 2014, the electric field strength is higher when applying higher V_{pp}. Subsequently, it will induce higher electrical excitation energy. This will cause more ionization and thus brighter jet emission and longer jet occurs. (Lau et al., 2014).

4.7.2 Discharge Power

Determination of the discharge power of plasma jet is to identify the power efficiency of the treatment. A report from Manley in 1943 suggested a method in calculating the total charge transported for DBD configurations. The widely used method in obtaining discharge power is conducted by plotting a graph of charge against discharge voltage (Q-V). This figure is also known as the Lissajous Figure. From the parallelogram shape of a Lissajous figure, the total charge transfer as well as the capacitance between the gap distance, C_{gap} can also be determined. According to Peeters et al., 2018 Q-V diagrams can sometimes deviate from its ideal shape. This might be due to the real, physical characteristics of the reactor, or experimental error (Peeters et al., 2018). Before a Q-V figure can be plotted, a suitable capacitor is needed. Hence, using an appropriate capacitor is crucial. The capacitance of the capacitor should greatly exceed the capacitance of the reactor, i.e. Cm $\gg$ C_{cell} (Peeters et al., 2018). In this case, capacitors of 0.66 micro Farad was employed in series by assuming that the capacitance of the discharge is in the magnitude of picofarad. Figure 4.21 depicts the shape of the Q-V plot which slightly deviates from the ideal parallelogram shape.

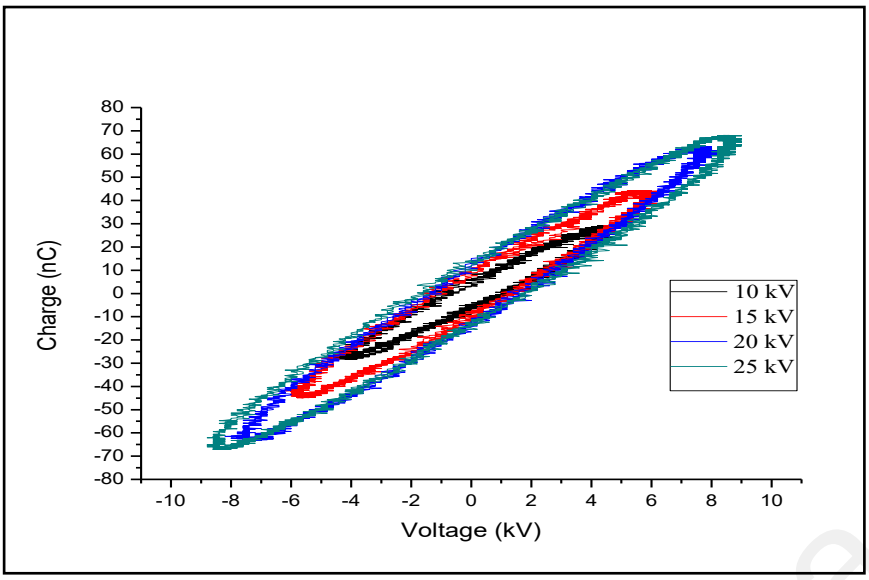

Figure 4.21: Q-V plot for AC plasma jet at 10 kV to 25 kV of applied voltage

Referring to the types of Q-V shape suggested by Peeters et al., the shape of the Q-V plots in Figure 4.21 resembles the noisy Q-V diagrams. According to Peeters et al., (2018) this is a common phenomenon and almost unavoidable. It occurs due to the interference from the microplasma discharges themselves (Peeters et al., 2018). Moreover, as the applied voltage was increased from 10 kV to 25 kV, the shape of the parallelogram becomes longer but not wider. This observation is similar to what has been reported by Manley. As it can be observed from Figure 4.21, the enclosed area of the Q-V plot indicates an increment of the applied voltage. The area is associated with mean energy deposited, hence the discharge power of the plasma jet. At a lower voltage, the area signifies smaller discharge power. As the applied voltage was increased, the discharge power increased exponentially. Calculation of discharge power includes 10 kV applied voltage to assure the relationship of discharge power with the applied voltage. Results of discharge power are shown in Figure 4.22.

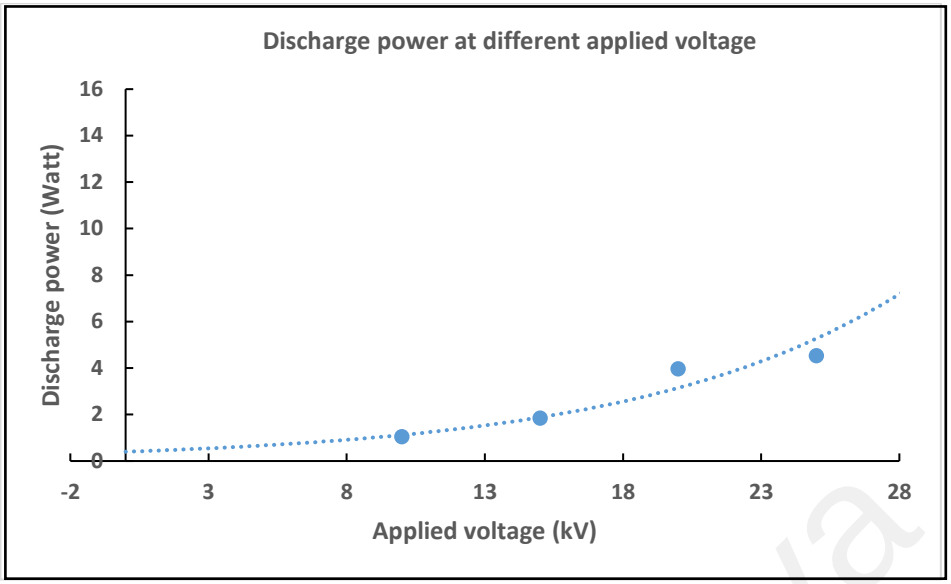

Figure 4.22: Discharge power for AC plasma jet at different applied voltage

From the trend of the graph, it shows that the discharge power generated from the discharge system can be increased further for higher discharge power. In this study, the discharge voltage was limited to 25 kV for treatment purposes. The raw data for both AC and DC plasma jet are presented in appendix A.1 and A.2 respectively.

4.7.3 Emission Spectroscopy and AC Electron Temperature

In this study, the ratio method was employed in order to calculate the plasma electron temperature. This method is an estimation value for the electron temperature. The determination of electron temperature is important to ensure that the system is safe to be employed for treatment. Figure 4.23 shows the emission spectrum for AC plasma jet at optimized parameter selected for further treatment.

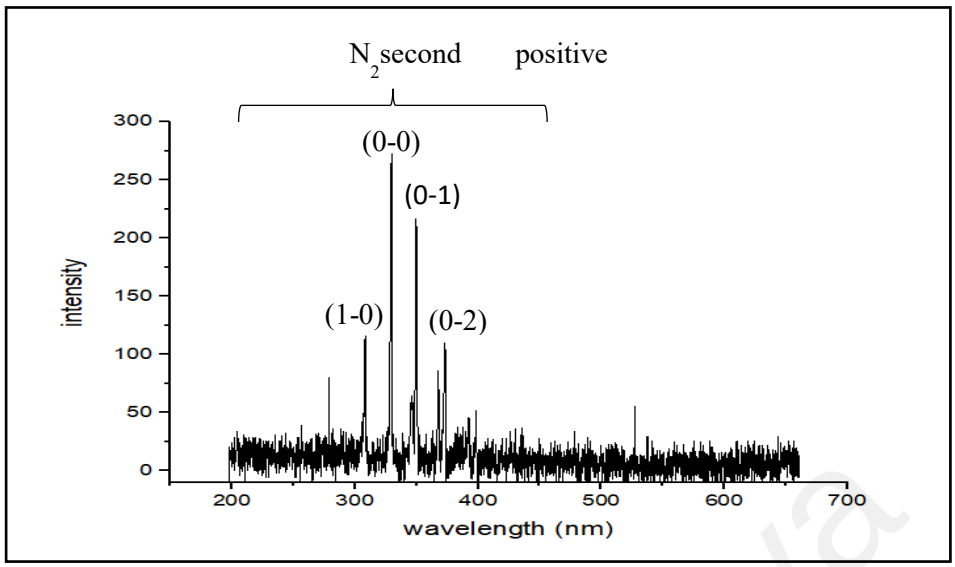

Figure 4.23: Optical Emission Spectrum of atmospheric pressure AC plasma jet

Figure 4.23 shows the emission spectrum of the AC plasma jet generated at ambient air. It shows a strong emission between 300 nm to 400 nm of wavelength. It corresponds to nitrogen second positive system which is equivalent to one of the emission spectra of nitrogen emission. Background emission was collected for apparent differences between the emission spectrum. The noise was reduced by repeating the emission for a few times. The electron temperature was calculated by referring to the rotational band of (1-0), (0-0), (0-1) and (0-2) mainly represented by 379.26 nm, 691.92 nm, 472.18 nm and 294.30 respectively. During the excitation of nitrogen second positive system, collisions occur between excited species with the surrounding causing the species to become thermalized to room temperature. A similar observation was obtained by Dudek et al., (2007) where they had suggested that the electron temperature is higher near the active electrode and eventually becomes lower as it approached the negative electrode. Therefore, from the line emission obtained, it can be suggested that the temperature of the plasma jet is almost room temperature. For a quick comparison, a thermocouple exposed near the surface of the plasma jet confirms the plasma jet temperature to be at room temperature.

4.8 DC plasma Jet

DC power source was employed to generate plasma jet at atmospheric pressure. In order to generate plasma jet, nitrogen gas was employed as the feed gas. Nitrogen gas was fed into the quartz capillary tube at different gas flow. It was observed that, as the capillary tube was fed with different gas flow, applied voltage increased and reached up to a maximum of 15 kV. Result is shown in Figure 4.24.

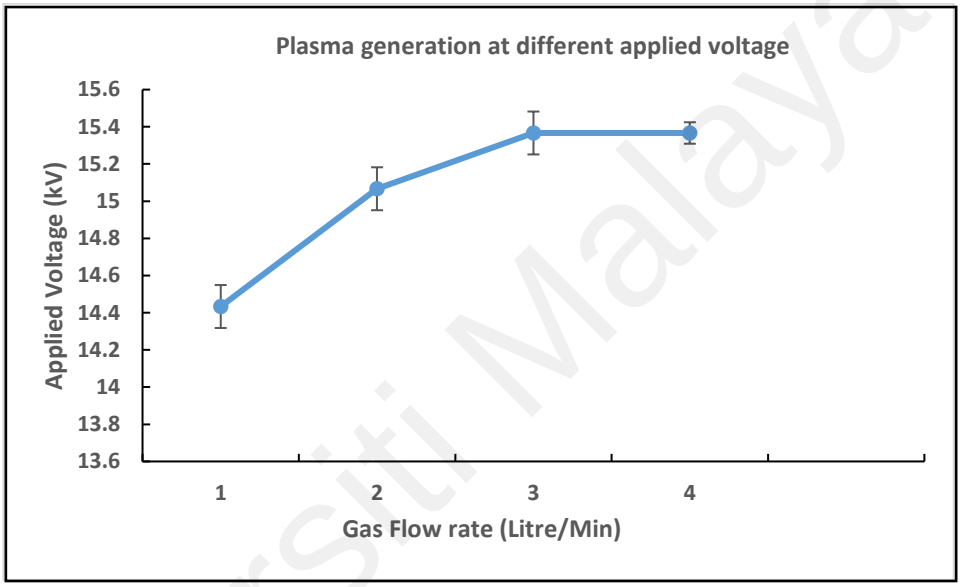

Figure 4.24 : Plasma Generation with different applied voltage

As the gas flow was set at 1 litre/min, applied voltage applied exceeded 14 kV but no plasma was observed. As the gas flow rate was increased, higher applied voltage was needed to generate the plasma jet. The image of the plasma jet powered by DC power supply is shown in Figure 4.25.

Figure 4.25: DC plasma jet generated with nitrogen as feed gas at atmospheric pressure

4.8.1 Characteristics of The DC Plasma jet

DC Plasma jet was generated with nitrogen gas as the feed gas, and the IV waveform consist of a combination of short and long spikes. The result is shown in Figure 4.26.

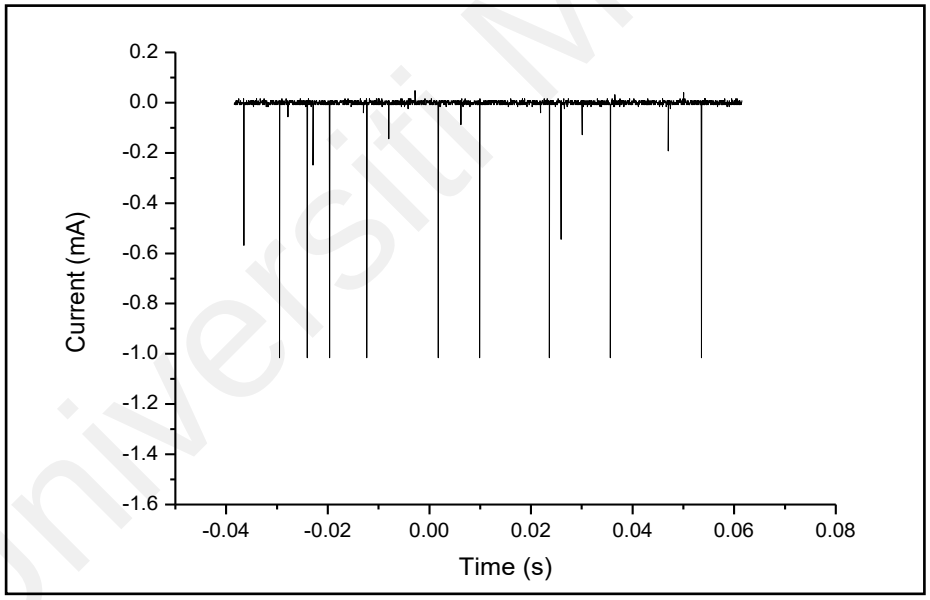

Figure 4.26: Current spikes for 2 litre/min of nitrogen feed gas of DC plasma jet

The discharge operates in the form of periodic current pulses. It was synchronized with the frequency of the power supply. Figure 4.26 shows that the current spikes consist of short and long current pulses. The current pulses occurs at 3 mA at certain operating time with the longest current spike reaching up to almost 5 mA. The amplitudes of the current pulses are in miliamperes. DC plasma jet generated current pulses mode due to the

hindering of electric field strength near the high voltage (HV) electrode, (Shashurin., 2017). Moreover, discharge will be initiated when the electric field on the HV electrode reaches the threshold value. Discharge occurs to compensate the electric field near the electrode. (Shashurin., 2017). The field near the electrode recovers as gas moves downstream and prepares conditions for the next discharge initiation. The faster the local electric field is recovered, the more frequent the streamers are fired (Shashurin., 2017). When the gas flow rate increases to 3 litres/min, the number of current pulses increase. Results are presented in Figure 4.27

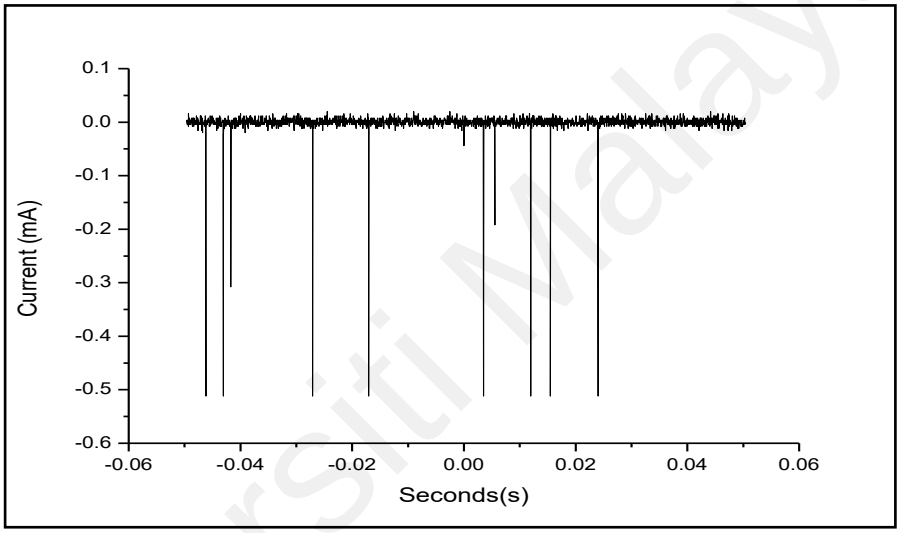

Figure 4.27 : Current spikes for 3 litre/min of nitrogen feed gas of DC plasma jet

As the gas flow increases from 2 litre/min to 3 litre/min, it shows that higher applied voltage is required to generate plasma. It is most likely that at a higher flow rate, the number of gas particles flowing in is greater than those flowing out from the quartz tube. Therefore, a higher applied voltage is required to ionize the gas particles. This causes the velocity of gas particles to continuously change in magnitude and direction. The gas swirls and eddies but the overall bulk of the gas still moves along a specific direction. The plume is forced out from the mouth of the quartz tube. On the other hand, when the gas flow is set to 4 litre/min, it can be observed that the polarity of the current pulses change. The current waveform is presented in Figure 4.28.

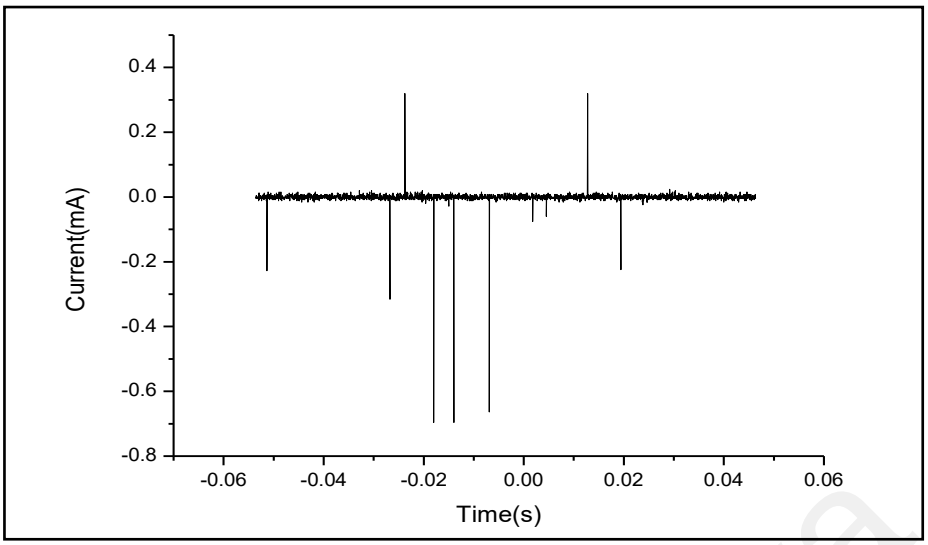

Figure 4.28: Current spikes for 4 litre/min of nitrogen feed gas for DC plasma jet

From the diagram, the direction of travel of the active species can be observed. Few spikes are observed on the positive polarity. This might be due to the changes to the polarity of the species during discharges, Moreover, the number of current spikes reduces as the gas flow increases. A lesser number of current spikes indicates less discharge generation and it may be due to the turbulence effect of the discharge. Thus, fewer gas particles can be ionised during the discharge process. Length of the generated DC plasma jet length was observed and plotted. The plotted graph of the length is presented in Figure 4.29. The graph shows that there is no plasma jet generation at 1 litre/ min of nitrogen gas flow. As the gas flow increases to 2 litre/ min, plasma jet starts to be generated. However, further increases in the gas did not increase the plasma jet length.

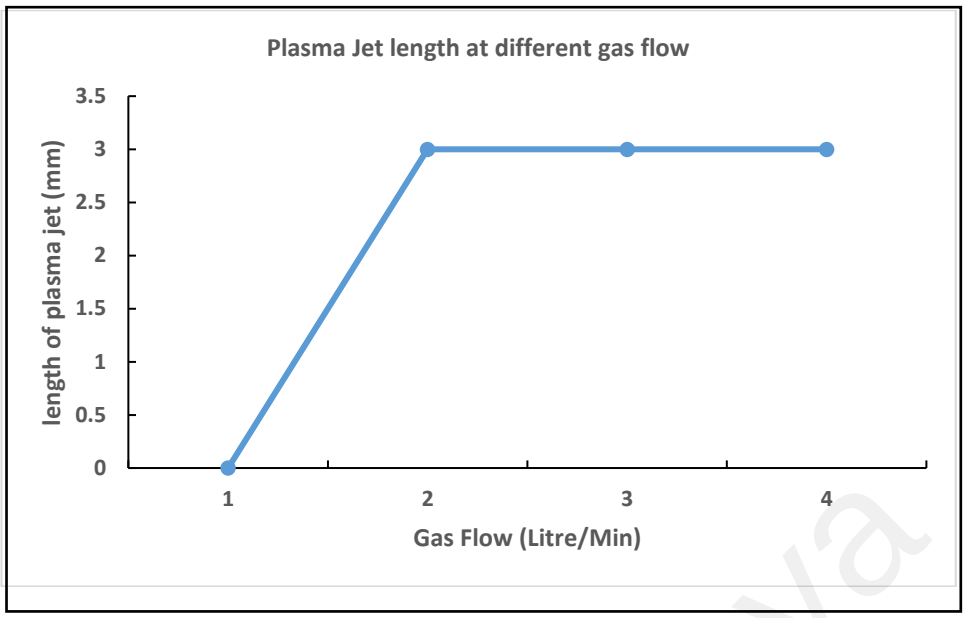

Figure 4.29: DC plasma jet length at a different gas flow

Initially, the length of plasma increases with the increase of flow rate up. Plasma length reaches the maximum value of 3.0 mm when the gas flows at 2 litre/ min. However, further increase of the gas flow to 4 litre/ min is not followed by any changes to the length of the plasma jet. This might be due to the turbulence effect. The jet length decreases when the flow rate is further increased as the flow becomes more turbulent, (Lau et al., 2014). When the flow rate increases gradually, more gas particles are available to be ionized. Therefore higher applied voltage is needed and higher discharge is observed. Number of charged particles forced out from the quartz tube would be higher.

4.8.2 Discharge Power

DC plasma jet generated a small value of power discharge of about 0.01 Watt to 1.7 Watt at different gas flow. Figure 4.30 displays the relationship between discharge power for the DC power supply with the flow gas rate.

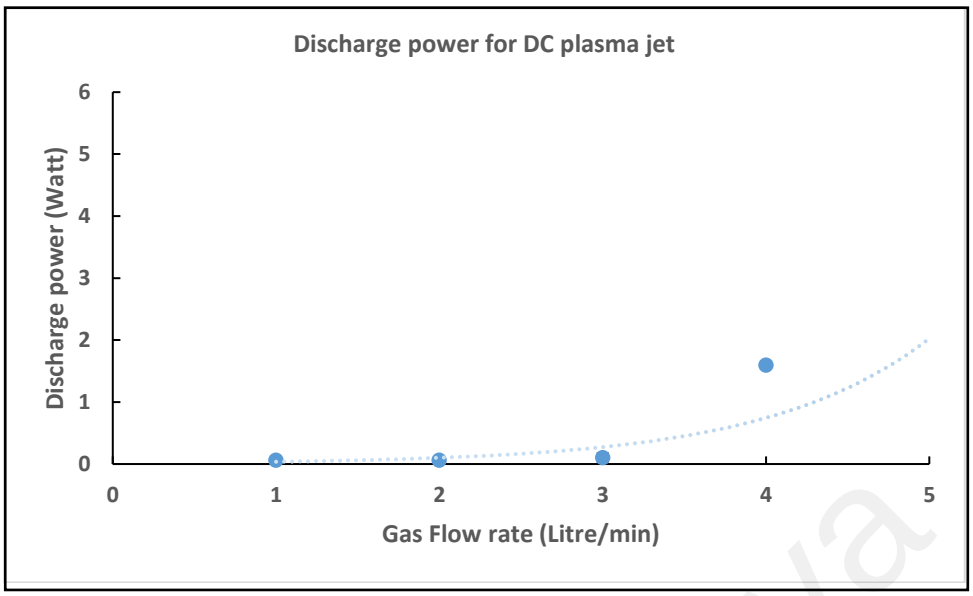

Figure 4.30 : Discharge power at different gas flow for DC plasma jet

When the gas flow extends to more than 3 litre/min, the discharge power increases drastically. Further increment of gas flow rate should generate greater discharge power.

4.8.3 Emission Spectroscopy and Electron temperature

Emissions of DC plasma jet was obtained at different gas flow. The emission of the plasma jet graph is used to determine the electron temperature of the DC plasma jet as shown in Figure 4.31.

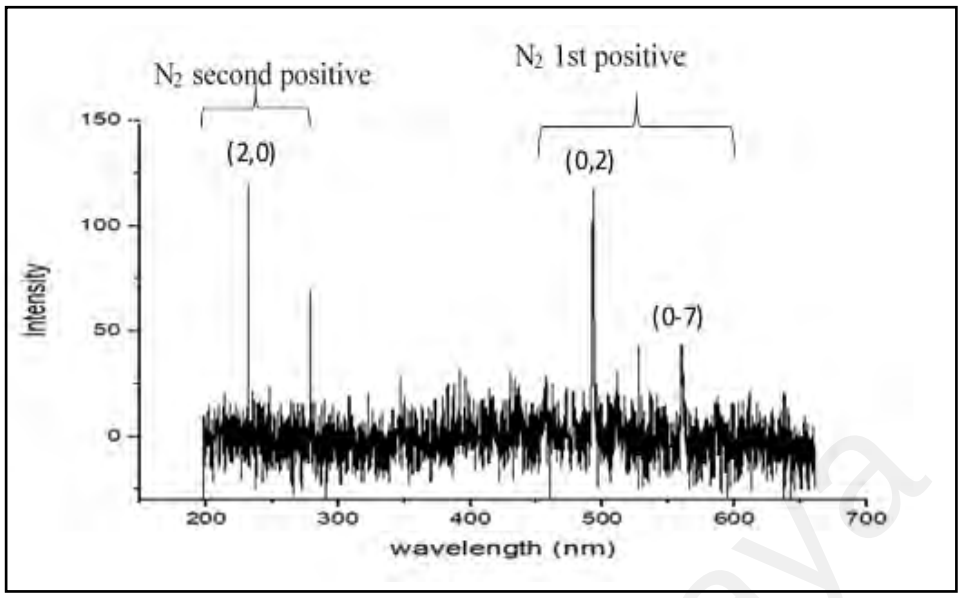

Figure 4.31: Optical Emission Spectrum of atmospheric pressure DC plasma jet at 2 litre/min nitrogen gas flow

The electron temperature is calculated by applying the rotational band of (2,0), (0,2), (0-7) which particularly corresponds to 231 nm, 494 nm and 560 nm respectively. This indicates that the electron temperature of the DC plasma jet is similar to those in the AC plasma jet. Thus, it can be concluded that, the exposure of DC plasma jet to biomedical samples is as safe as the AC plasma jet.

4.9 Atmospheric pressure Plasma Jet treatment on Wound Bacteria samples

4.9.1 AC Plasma Jet bacteria lawn treatment

The efficacy of the generated plasma jet has been identified from bacteria samples treatments. *E coli* lawn bacteria was exposed under AC plasma jet with different time of exposure. The samples were prepared on agar lawn where it can quickly determine the effect of the treatment on the size of treatable area. The result after treatment is presented in Figure 4.32

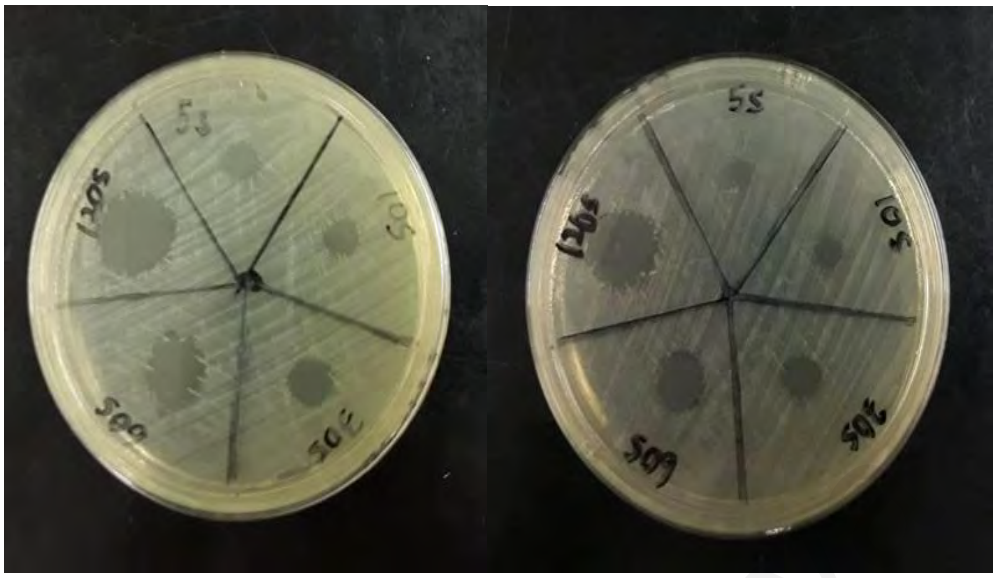

Figure 4.32: *E coli* lawn treatment under AC plasma jet and its replicate

Figure 4.32 clearly shows the effect of inactivation after 5 seconds of treatment with AC plasma jet. Another replicates shows similar effects. Moreover, size of the treatable area is bigger than the diameter of the AC plasma jet

4.9.2 DC Plasma Jet bacteria lawn treatment

E coli bacteria lawn was also exposed to DC plasma with different time of exposure. Results are presented in the images shown in Figure 4.33

Figure 4.33 : *E coli* lawn treatment under DC plasma jet and it replicate

Images show that the effect of DC plasma jet is clearly observable when the time of exposure is more than 60 seconds.

4.9.3 Comparison between AC and DC Plasma jet on *E coli* Lawn Treatment

As can be observed from Figure 4.32 and 4.33, treated size area increases as the treatment time is increased. The same observation has been reported by Deng et al in 2008 where the sterilized zone is much bigger than plasma treatment area. Similar results are observed for both AC and DC plasma jet. According to Deng at al., plasma diffusion over the surface area causes the plasma to inactivate nearby bacteria. Moreover, we can observe that the effect of both plasma jet is more significant on AC plasma jet compared to DC plasma jet. A bigger size of treatable area is observed within less treatment time for AC plasma jet than DC plasma jet. These data are presented in Figure 4.34 where it shows the differences in terms of its efficacy on *E coli* treatment

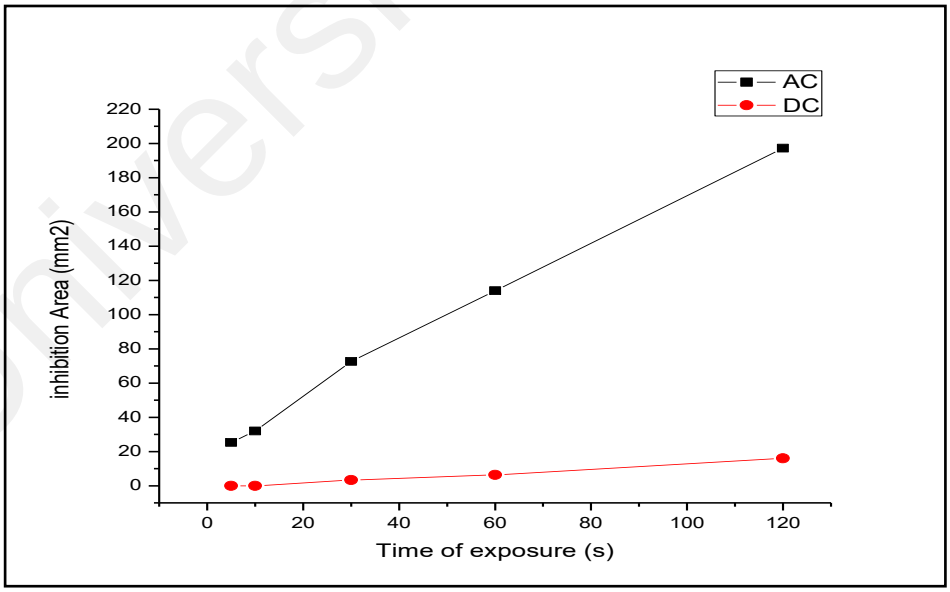

Figure 4.34: Comparison between AC and DC plasma jet on *E coli* lawn treatment

Non-thermal plasma jet has been found effective in inactivating various microorganisms including *E coli* (Hong *et al.*, 2009). Comparing the two graphs in Figure 4.34, both AC

and DC plasma jet are capable of inactivating *E coli*. Furthermore, AC plasma jet is more effective whereby the time required to clear out the same size of area is less than DC plasma jet. Higher time of plasma exposure indicates greater size of treatable area. AC plasma jet is more effective in killing the *E coli* bacteria due to its higher discharge power compared to DC plasma jet.

4.10 Atmospheric pressure AC plasma jet treatment on Fibroblast Cells

Further treatment was conducted on fibroblast cells. This treatment was done in order to determine the effect of AC plasma jet on the proliferation of fibroblast cells. AC plasma jet was applied for the treatment of the fibroblast cells due to the efficacy of AC plasma jet which was greater than DC plasma jet. Fibroblast cells were seeded in 24-well plate and exposed to AC plasma jet with different time of exposure. Results depicting treatment of fibroblast cells are shown in Figure 4.35.

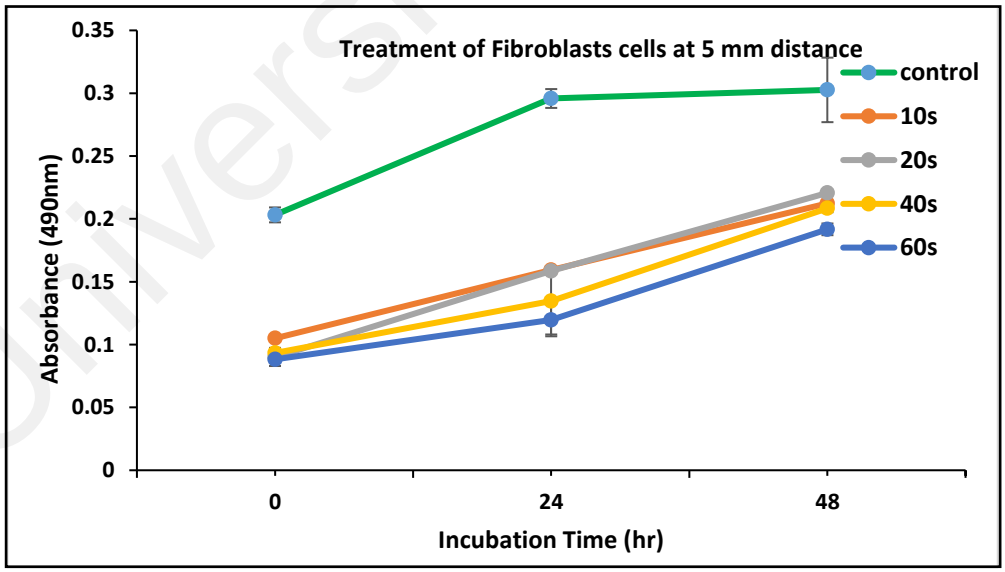

Figure 4.35: Treated Fibroblast cells at 25 kV at a distance of 5 mm from quartz nozzle

The fibroblasts viability reduces (about 50%) after the plasma treatment (including the minimum 10s treatment). The fibroblasts went through repairing mechanism and slowly re-grew for 48 hr. The growth rate is lower compared to the untreated control cells. Cells

treated for 40 seconds and 60 seconds have a lower recovery rate especially in the first 24-hr compared to cells treated for 10s and 20s. Treatment at a fixed applied voltage of 25 kV at a distance of 5 mm from the end of quartz capillary tube indicates that the amount of plasma exposure is too excessive. It kills almost 50% of the cells populations. As the incubation rate is increased to 72 hrs while maintaining the same time of exposure, cells did not proliferate better than the normal cell does. When the voltage is reduced to 15 kV with the cells exposed at 10 mm distance, results show that proliferation rates increase compared to the 25 kV applied voltage. This result is presented in Figure 4.36

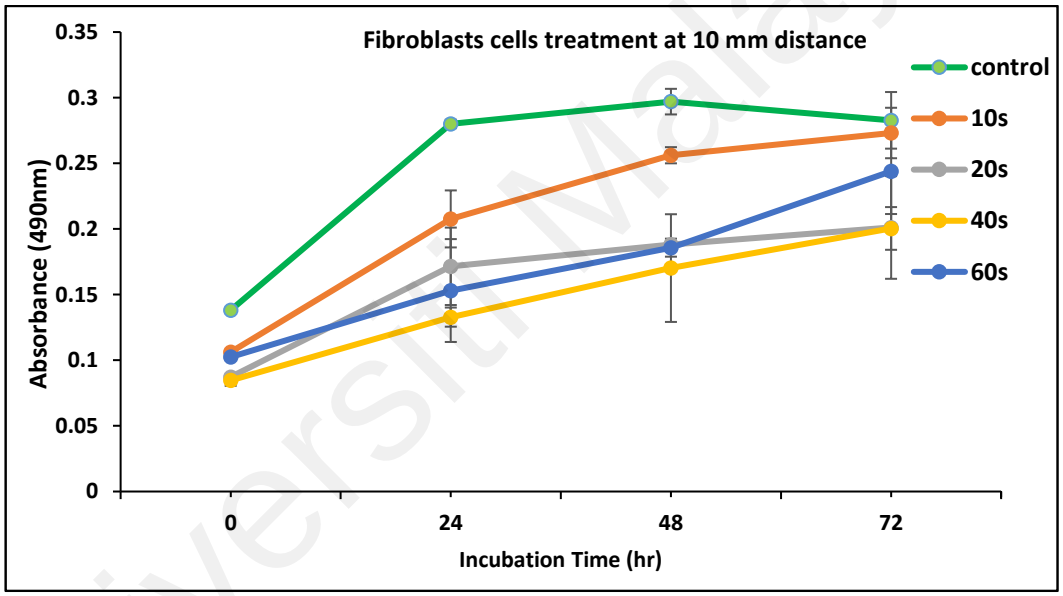

Figure 4.36: Treated Fibroblast cells at 15 kV at a distance of 10 mm from nozzle

Figure 4.35 shows a consistent trend with the previous data where it shows dose-dependent reduction of growth. Cells require a low dosage of plasma for the proliferation to occur. The test was repeated for 15 mm and 20 mm distance from the tip of the plasma jet plume. Results for both distances are presented in Figure 4.37.

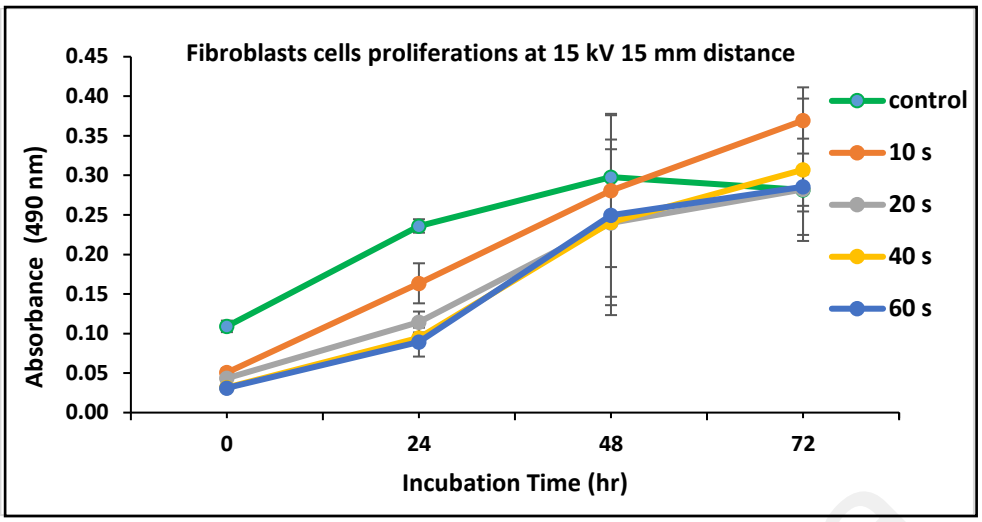

Figure 4.37 : Treated Fibroblast cells at 15 kV at a distance of 15 mm from nozzle

Better proliferation rate is observed when the applied voltage is set at 15 kV at a distance of 15 mm. Once the incubation rate reaches 72 hours, it can be seen that the 10 seconds treatment time has a higher absorbance rate compared to normal cell (control). When the distance is increased to 20 mm, results shows a better proliferation rate. Graph is shown in Figure 4.38.

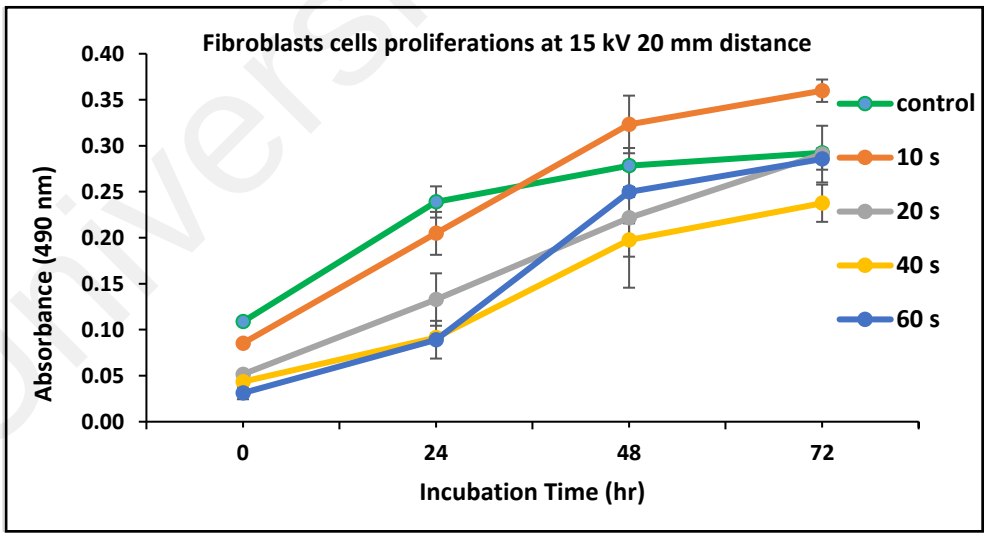

Figure 4.38 : Treated Fibroblast cells at 15 kV at a distance of 20 mm from nozzle

Less incubation time is required for the absorbance rate to increase compared to the normal cells. Cells proliferate better than the control cells as the line of absorbance shows a steeper line than the normal cell does. This is observable after 48 hours of incubation. Without incubation, it can be observed that normal cells have a greater absorbance than other treatment time.

4.11 Comparison between different treatment time of AC Plasma jet on Fibroblast cells

Data from the experiment demonstrates no cells proliferation were observed for all treatment times (10 s, 20 s, 40 s and 60 s) at a distance of 10 mm from the tip of the plasma at 25 kV applied voltage. No significant cells proliferation can be observed for all treatment time at a distance of 10 mm from the plasma jet tip when the applied voltage was reduced to 15 kV too. No significant effect were observed after the incubation time was extended from 24 hours to 72 hrs. Greater proliferation rate compared to normal cell was observable after 72 hours of incubation time when the distance from the tip was increased to 15 mm, at 10 seconds of treatment. Once the distance increased to 20 mm, less incubation time of 48 hours was required for the 10 seconds treatment time of the proliferation rate to be observable. Greater treatment time of more than 10 seconds induces apoptosis to the fibroblast cells. According to Shi et al., (2018), plasma at atmospheric pressure promotes the proliferation process of fibroblast cells. This proliferation process occurs when inducing the generation of ROS, upregulating the expression of P-p65, downregulating the expression of IκB, and activating the NF-κB signaling pathway and consequently altering cell cycle progression. Fibroblast toxicity under plasma jet treatment reduced after applying low dosage of plasma. This was achievable when the applied voltage was reduced from 25 kV to 15 kV. Moreover, the distance also affects the dosage of the plasma jet. Higher distance from the tip of the

plasma lowers the plasma dosage. It can be concluded that by lowering the applied voltage and increasing the distance to the samples, the absorbance rate or proliferation can be increased. Kalghatghi et al., (2019) reported that using low dose of plasma is suffice to promote cell proliferation.

4.12 Plasma Jet Dosage

Plasma dosage is an important parameter be defined to compare the results on cells proliferation. A simple operation involving regression method was conducted to determine the plasma dosage. Results for cell proliferation was tabulated and the results are presented in Table 4.1.

Table 4.1: Tabulated Data for Model Summary

Regression Statistics	
Multiple R	0.902015413
R Square	0.813631806
Adjusted R Square	0.800924884
Standard Error	0.042616137
Observations	48

By referring to the table, approximately 81% of the observed variation can be explained by the model inputs. It also explains all the variability of the response data around its mean. Both independent variables in the model are significant (< 0.05) whereas plasma dosage is dependent to the time of treatment, distance as well as the time of incubation. Table 4.2 displays data set for plasma dosage dependence variable. From Table 4.1 and 4.2, we can figure out that the relationship of plasma dosage was as follows:

Table 4.2 : Results of the plasma dosage dependence variable

	Coefficients	Standard Error	t Stat	P-value	Lower 95%	Upper 95%	Lower 95.0%	Upper 95.0%
Intercept	0.076884	0.026928	2.85518	0.006539	0.022614	0.131153	0.022614	0.131153
X Variable 1	-0.00069	0.00032	-2.15172	0.036947	-0.00133	-4.4E-05	-0.00133	-4.4E-05
X Variable 2	8.62E-05	0.001507	0.057244	0.95461	-0.00295	0.003123	-0.00295	0.003123
X Variable 3	0.003139	0.000229	13.69155	1.82E-17	0.002677	0.003601	0.002677	0.003601

$$\textit{Plasma Dosage} = 0.077 - (0.00068)T_T + (8.625E\text{-}05)d + (0.1)/T_I$$

Where T_T = Time of treatment, d = Distance from the nozzle T_I = Time of Incubation

Data analysis shows that the plasma dosage is dependent on the time of treatment, distance and time of incubation at specific applied voltage (15kV). The results is similar with the previous study conducted by Cheng et al in 2014 where they concluded that major factors in plasma dosage are the gas flow rate, output voltage difference at the electrodes and the duration of exposure to the plasma. In another study, Wang et al., 2015 stated that the plasma dosage is dependent on the time of plasma exposure. Thus, time of incubation is very crucial to ensure the cells obtain a sufficient amount of time for the proliferation process to occur. Data for fibroblast treatment for different distant are presented in appendix C.

CHAPTER 5: CONCLUSION AND RECOMMENDATION

5.1 CONCLUSION

In this study, an empirical investigation on the design of plasma jet specifically on plasma characteristics, plasma diagnostics as well as its effect on the wound healing samples treatment were investigated. The plasma jet is designed in such a way that it is suitable to be used for treatment as well as the prospect to be improvised into a portable mode design. The study started with a preliminary treatment using two different configurations of DBD. From the results, the final design of the plasma discharge was outlined. A portable and easy handling device, plasma jet powered by AC and DC power supply was successfully generated where the applied voltage is around 15 kV to 25 kV and 15 kV respectively. The plasma jet was generated at ambient air with jet plume length of around 5 to 6 mm. Nevertheless, DC requires nitrogen gas in order to promote the ionization process to generate the jet plume. AC plasma ionization started off with weak ionization along the pin as the applied voltage is set to 15 kV. While, at 25 kV it generates a longer plume. A diagnostic technique was implemented for the analysis of the signals by using various methods such as current-voltage measurement, plasma spectroscopy as well as signal analysis. The temperature of the electron plasma jet can be inferred from the estimation of Boltzmann plot. It also has been tested by using Fluke thermometer which confirms that the plasma jet temperature is in the range of 37 to 40°C and safe to be tested on biomedical samples. Finally the effect of plasma jet is investigated on bacteria samples and also fibroblast cells where this will be the main criteria of the effectiveness of the plasma jet. Treatment with different time of exposure was conducted at 25 kV AC power supply on *E coli* lawn while treatment using DC at applied voltage at around 15 kV has resulted in the inactivation of a bigger bacteria lawn area after 10 s treatment for both supplies. The reactive species diffusion and the UV irradiation produced in plasma jet

made the sterilized zone much bigger than plasma treatment area. In comparison, the effect of treatable area is clearer on AC mode power supply to DC power supply. Nevertheless, both plasma jets are effective in killing *E coli* bacteria in 5 to 10 seconds of treatment. The following part of the treatment involve cells proliferations where the AC plasma jet was selected due to its better results in bacteria treatment. Normal fibroblast cells were seeded in 24-well plate overnight before undergoing plasma treatment at different exposure. Findings suggest that the plasma jet should be operated with a low dosage of plasma where in this case plasma generated at 25 kV at 5 mm distance from the tip of the plasma jet resulted in higher toxicity to the cells compared to the normal cells without treatment. Meanwhile, as the gap distance is increased to 10 mm from the tip at 15 kV the cells proliferate better than the high applied voltage. Further tests at different distances from the plasma tip has resulted in a better proliferation effect of cells. It is observed that treatment time of 10 seconds is sufficient to enhance proliferation rate. Distance of 20 mm in 48 hours of incubation time has resulted in a higher proliferation rate than normal cells does. The results indicate that introducing a low voltage proliferates more than high dosage of plasma. Similar findings have been reported by Shi et al in 2018 where the introduction of low dosage plasma to wound healing promotes cells proliferation by activating the NF-kB signaling factor. From this study, it can be understood that in generating plasma jet at atmospheric pressure, correct and suitable comparison makes it easier to generate plasma plume in ambient air without a complex gas system. However, of the jet plume generated in this study is short as compared to previous studies carried out in ambient air. Kim et al., (2009) generated longer plasma plumes in ambient air by employing oxygen gas as the feed gas. In the long run, this study have successfully shown that plasma jet can be simply generated with a suitable power supply and prepared in portable mode. The latest technology of plasma jet in portable has been investigated by Usta et al., (2019) where they have designed a

portable battery-powered non-thermal atmospheric plasma device and determine the characterization of its antibacterial efficacies. In this study, plasma jet powered by two modes of power supply seems to be a convenient design. A group of researchers invented a low-cost dual-mode portable power jet in 2018 where the device mainly consists of a pen electrode, high-frequency ac power supply, ac/dc module and a dc air pump. The device is a low-cost device with a dimension of 280 mm × 190 mm × 180 mm. Alternative in conventional wound management required some advanced technologies in inhibiting wound bacteria, mitigate the chances of developing chronic wound and promote rapid healing. The use of non-thermal plasma operates at atmospheric pressure emerge as a promising approach. Non-thermal plasma has been widely used in bacteria disinfection and potentially harmless to be used on living tissues. Its antiseptic effect on bacteria inhibition on patient wound has to be investigated while the effect on cells proliferations also required some careful research. In this study, two dielectric barrier discharge (DBD) configurations, planar DBD and capillary configuration were employed. The effects on meticilin resistant *Staphylococcus aureus* (MRSA) and *Pseudomonas aeruginosa* (PA) isolated from chronic wound bacteria strains have been confirmed. The atmospheric plasma jet powered by (AC) and direct current (DC) were used on bacteria lawn treatments. The efficacy of the plasma treatment on *E coli* lawn at depends on the time of exposure. The current-voltage (IV) measurement, discharge power and spectroscopy results were used to characterize the properties of the plasma jets. The effect of the plasma jet on fibroblast cells were investigated, and the results obtained shown improved cell proliferation with AC plasma jet at applied voltage of 15 kV to 20 kV at a distance of 20 mm. The dosage of plasma treatment was determined using the multiple linear regression method based on the absorption results at 490 nm. High dosage was determined that may have negative effect on the fibroblast cells when the treatment distant was at 5 mm, 10 mm and 15 mm. Cells proliferation only increased at the low voltage discharge and at

distant of 20 mm, indicate the potential of using this condition of non-thermal plasma in wound management. High dose of plasma could have incurred toxicity in the cells causing the reduction in cell culture. These results are important references when the plasma jet is considered as a tools to accelerate wound healing process. According to Lu et al. (2008), Uhm et al. (2007) and Eto et al. (2008), plasma device-generated at ambient air contains a mixture of air, RONS such as oxygen atom, O, ozone, O_3, nitrogen oxide, NO, nitrogen dioxide, NO_2, hidroxil, OH and hydrogen peroxide, H_2O_2 it is believed that these highly active species have a high impact on the plasma treatment processes. The exact effect or the contribution of each reactive species is yet to be revealed. Nevertheless, cold atmospheric plasma jet remains as the latest and most promising techniques for potential wound healing treatment (Lu et al., 2019). Various parameters and geometrical conditions have been explored, where some have been proven effective in laboratory scale. Implementation of plasma treatment however is yet to be widely utilized. Beside the challenge of finding suitable condition in each situation, the other concern is the needs of complex equipment with skills in plasma technology. The economic efficiency as well as the treatment related issues like efficacy and safety are to be considered too.

5.2 Limitation of the study

The main limitation in this study is the determination of the exact value of electron temperature of the plasma jet by using Stark Broadening method. In applying that method, hydrogen gas should be feed into the quartz tube to produce the OH α & β lines. The suggested method cannot be implemented due to some constraints. Another limitation of the design is time where in better time, one can improve the design for the betterment of results.

5.3 Recommendation

Several improvements can be made on the setup of the plasma jet to escalate the performance of generated plasma in future works. Another design with a different geometrical parameter can be further tested which might include the different types of pin electrodes instead of copper electrode. This has been reported by Liu et al in 2018 where they have implemented three different types of high voltage pin., with various insulations including completely covered needle with insulating dielectric, partially covered needle (PCN) with insulating dielectric, and non-covered needle with any insulating dielectric have been investigated and compared. It has shown promising results of consolidating the chemical reaction of the plasma jet. Other than that, simulation of the generated plasma jet might enhance the understanding behavior of the plasma jet as such it was investigated by a group of researcher (Bischof et al., 2019; Shigeta., 2019., and Wen et al., 2019). Generating plasma by applying lower applied voltage might be a crucial improvement that can be done to ensure no conductive path occurs during direct contact where it has been successfully investigated by various researchers generating plasma jet with input voltages as low as 10 V (Shigeta, 2018), and 2-12 kV (Cordaro et al., 2019).

REFERENCES

Adhikari, E. A., Samara, V., & Ptasinska, S. (2018). Influence of O_2 or H_2O in a Phys. plasma jet and its environment on plasma electrical and biochemical Performances. *Journal of Physics D: Applied Physics, 51*, 1361-1371.

Akatsuka, H., & Suzuki, M. (1993). Arc-heated magnetically trapped expanding plasma jet generator. *Review of Scientific Instruments, 64,* 1734-1739.

Aldea, E., Peeters, P., Vries, H. D., & Van De Sanden, M. C. M. (2005). Atmospheric glow stabilization. Do we need pre- ionization? *Surface and Coatings Technology, 200,* 46-50.

Anghel, S. D., & Simon, A. (2007). An alternative source for generating atmospheric pressure non-thermal plasmas. *Plasma Sources Science Technology, 16,* 1-4.

Balzer, J., Heuer, K., Demir, E., Hoffmanns, M. A., Baldus, S., Fuchs, P. C., Awakowicz, P., Suschek, C. V., & Opländer, C. (2015). Non-thermal dielectric barrier discharge (DBD) effects on proliferation and differentiation of human fibroblasts are primary mediated by hydrogen peroxide. *Plos ONE, 10,* 1-18

Baldanov, B. B., Ranzhurov, T. V., Semenov, A. P., & Gomboeva, S. V. (2019). Bacterial inactivation using atmospheric pressure single pin electrode microplasma jet with a ground ring. *Journal of Theoretical and Applied Physics, 13,* 95-99.

Bartnikas, R. (1968). Note on the discharges in helium under AC conditions. *Journal of Physics D: Applied Physics*, *1,* 659-661.

Baum, C. L., & Arpey, C. J. (2005). Normal cutaneous wound healing: Clinical correlation with cellular and molecular events. *Dermatologic Surgery: Official Publication for American Society for Dermatologic Surgery*, *31,* 674-686.

Benocci, R., Esena, P., Galassi, A., Piselli, M., & Sciascia, M., (2004). Study of the thermal plasma etching at atmospheric pressure on silica rods. *Journal of Physics D: Applied Physics, 37,* 1206-1213.

Birmingham, J. G., & Hammerstrom, D. J. (2000). Bacterial decontamination using ambient pressure nonthermal discharges. *IEEE Transactions on Plasma Science, 28,* 51-55.

Bischoff, L., Hübner, G., Korolov, I., Donkó, Z., Hartmann, P., Gans, T., Held, T. V., BisGathen, S. V. D., Liu, Y., Mussenbrock, T., & Schulze, J. (2018). Experimental and computational investigations of electron dynamics in micro atmospheric pressure radio-frequency plasma jets operated in He/N_2 mixtures. *Plasma Sources Science Technology, 27,* 1361-1386.

Blackert, S., Haertal, B., Wende, K., Von, W. T., & Lindequist, U. (2013). Influence of Non-thermal atmospheric pressure plasma on cellular structures and processes in human keratinocytes (HaCaT). *Journal of Dermatological Science, 70,* 173-181.

Block, S. S. (1992). Sterilization. *Encyclopedia of Microbiology, 4,* 87-103.

Boffa, C., Heberlei, J., & Pfender, E. (1970). Criterion for establishing deviations from Lte in atmospheric pressure argon plasma jets. *Journal of Mechanical Engineering, 4,* 213-221.

Boudam, M., Moisan, M., Saoudi, B., Popovici., C., Gherardi, N., Massines, F. (2006). Bacterial spore inactivation by atmospheric-pressure plasmas in the presence or absence of UV photons as obtained with the same gas mixture. *Journal of Physics D: Applied Physics, 39,* 3494-3507.

Brownrigg, J. R., Apelqvist, J., Bakker, K., Schaper, N. C., & Hinchliffe, R. J. (2013). Evidence-based management of PAD & the diabetic foot. *European Journal of Vascular and Endovascular Surgery, 45,* 673-681.

Buss K., Arch. (1932). *Journal of Elektrotechnic*, *26,* 261-265.

Chang, M. B., Balbach, J. H., Rood, M. J., & Kushner, M. J. (1991). Removal of SO_2 from gas streams using a dielectric barrier discharge and combined plasma photolysis. *Journal of Applied Physics*, *69,* 4409-4417.

Chang, M. B., Kushner, M. J., & Rood, M. J. (1992). Gas phase removal of NO from gas streams via dielectric barrier discharges, *Journal of Environmental Science and Technology, 26,* 777 – 781.

Chirokov, A., Gutsol, A., Fridman, A., Sieber, K., Grace, J., & Robinson, K. (2005). Self-organization of microdischarges in dielectric barrier discharge, *IEEE Transactions Plasma Science, 33,* 300-301.

Chen, Z., & Mathur, V. K. (2002). Non-thermal plasma for gaseous pollution control. *Journal of Industrial & Engineering Chemistry Research*, *41,* 2082-2089.

Cheng, X., Sherman. J., Murphy. W., Ratovitski. E., Canady, J. & Keidar, M. (2014). The effect of tuning cold plasma composition on glioblastoma cell viability. *Plos One*, *9,* 2082-2089.

Clinical and Laboratory Standards Institute, (CLSI). (2010). Performance standards for antimicrobial susceptibility testing, twenty informational supplement. approved standard. Retrieved on Jan 10, 2019, from https://clsi.org/media/2663/m100ed29_sample.pdf.

Cordaro, L., Masi, G. D., Fassina, A., Mancini, D., Cavazzana, R., Desideri, D., Sonato, P., Zuin, M., Zaniol, B., & Martines, E. (2019). On the electrical and optical features of the plasma coagulation controller low temperature atmospheric plasma jet. *Journal of Applied in Biological Systems, 2,* 156-167.

Daeschlein, G., V., Woedtke, T., Kindel, E., Brandenburg, R., Weltmann, K. D., & Jünger, M. (2010). Antibacterial activity of an atmospheric pressure plasma jet against relevant wound pathogens in-vitro on a simulated wound environment. *Journal of Plasma Process Polymer*, *7,* 224–230.

Darby, I. A., & Hewitson, T. D. (2007). Fibroblast differentiation in wound healing and fibrosis. *Journal of International Review of Cytology, 257,* 143-179.

Das, S. P., Dalei, G., & Barik, A. (2018). A dielectric barrier discharge (DBD) plasma reactor: An Efficient Tool to Measure the Sustainability of Non- Thermal Plasmas through the Electrical Breakdown of Gases. *IOP Conference Series Materials Science and Engineering, 410,* 1-12.

Davydov, A. I., Kuchukhidze, S. T., Shekhter, A. B., Khanin, A. G., Pekshev, A. V., & Pankratov, V. V. Clinical evaluation of intraoperative application of air-plasma flow enriched by nitrogen monoxide in operations on the uterus and adnexa. (2004). *Journal of Problems of Gynecology, Obstetrics and Perinatology, 3,* 12-17.

Davis, S. C., Ricotti, C., Cazzaniga, A., Welsh, E., Eaglstein, W. H., & Mertz, P. M. (2008). Microscopic and physiologic evidence for biofilm-associated wound colonization in vivo. *Wound Repair Regenerative*, *16,* 23-29.

Deng. S., Ni. G., & Cheng, C. (2008). Bacterial inactivation by atmospheric pressure dielectric barrier discharge Plasma Jet. *Japanese Journal of Applied Physics, 47,* 7009-7012.

Desmouliere, A. (1995). Factors influencing myofibroblast differentiation during wound healing and fibrosis. *Journal of Cell Biology International*, *19,* 471-476.

Desmouliere, A., Chaponnier, C., & Gabbiani, G. (2005). Tissue repair, contraction, and the myofibroblast. *Journal of Wound Repair Regeneration*, *13,* 7–12.

Dresvin, S. V., & Klubniki, V. S. (1971). Disequilibrium in an argon plasma-jet from a high-frequency induction discharge at atmospheric-pressure. *Journal of High Temperature, 9,* 437-445.

Dobrynin, D., Fridman, G., Friedman, G., & Fridman, A. (2009). Physical and biological mechanisms of direct plasma interaction with living tissue. *New Journal Physics, 11,* 1367-1392.

Dudek, D., Bibinov, D., Awakowicz, P., & Engemann, J. (2007). Characterization of an atmospheric pressure dc plasma jet. *Journal of Physics D: Applied Physics, 40,* 7372-7378.

Eliasson, B., & Kogelschatz, U. (1991). Modeling and applications of silent discharge. Plasmas. *IEEE Transactions on Plasma Science*, *19,* 309-323.

Eliasson, B., Hirth, M., & Kogelschatz, U. (1987). Ozone synthesis from oxygen in dielectric barrier discharges. *Journal of Physics D: Applied Physics, 20,* 1421-1437.

Eto, H., Ono, Y., Ogino, A., & Nagatsu, M. (2008). Low-temperature sterilization of wrapped materials using flexible sheet-type dielectric barrier discharge. *Applied Physics Letters, 93,* 221-226.

Etufugh, C. N., & Phillips, T. J. (2007). Venous ulcers. *Clinical Dermatology*, *25,* 121-30.

Freeman, M. P. (1968). A quantitative examination of local thermodynamic equlibrium condition in effluent of an atmospheric pressure Argon plasma jet. *Journal of Quantum Spectroscopic Radiatation*, *8,* 435-436.

Fröhling, A., Baier, M., Ehlbeck, J., Knorr, D., & Schlüter, O. (2012). Atmospheric pressure plasma treatment of *listeria innocua* and *escherichia coli* at polysaccharide surfaces: Inactivation kinetics and flow cytometric characterization. *Innovative Food Science & Emerging Technologies*, *13,* 142-150.

Fridman, G., Friedman, G., Gutsol, A., Shekhter, A.B., Vasilets, V. N., & Fridman, A. (2008). Applied plasma medicine. *Plasma Processes and Polymers*, *5,* 503-533.

Gabbiani, G. (2003). The myofibroblast in wound healing and fibrocontractive diseases *Journal of Pathology*, *200,* 500-503.

Garate, E., Evans, K., Gornostaeva, O., Alexeff, I., Kang, W., Rader, M., & Wood, T. (1998). Atmospheric plasma induced sterilization and chemical neutralization. *In Proceedings of the IEEE International Conference on Plasma Science,* 1-4 June, Raleigh NC, USA.

Gianinni, G. M., & Ducati, A. C. (1960). Plasma steam apparatus and methods U S P Office US2922869 A.

Giannini, G. M. (1957). The plasma jet and its applications. *High Intensity Arc Symposium*, *197,* 80-90.

Gerber, I. C., Mihaila, I., Hein, D., Nastuta, A. V., Jijie, R., Pohoata, V., & Topala, P. (2017). Time behaviour of helium atmospheric pressure plasma jet electrical and optical parameters. *Journal of Applied science, 7,* 812-828.

Gherardi, N., & Massines, F. (2001). Mechanisms controlling the transition from glow silent discharge to streamer discharge in nitrogen. *IEEE Transactions on Plasma Science*, *29,* 536-544.

Gibalov, V. I., & Pietsch, G. J. (2000). The development of dielectric barrier discharges in gas gaps and on surfaces. *Journal of Applied Physics*, *33,* 280-289

Glocker, B., Nentwig, G., & Messerschmid, E. (2000). 1–40 kW steam respectively multi gas thermal plasma torch system. *Vacuum*, *59,* 5-46.

Gobrecht, H., Meinhardt, O., & Hein, F. (1964). About the silent electrical discharge in ozonizers. *Physical Chemistry, 68,* 55-63.

Golubovskii, Y. B., Maiorov, V. A., Behnke, J. F., Tepper, J., & Lindmayer, M. (2004). Study of the homogeneous glow-like discharge in nitrogen at atmospheric pressure. *Journal of Physics D: Applied Physics*, *37,* 1346-1356.

Gosbell, I. B. (2002). The significance of MRSA and VRE in chronic wounds, *Australian Journal of Wound Management, 10,* 15-19.

Gui-Min, X., Yue, M., & Guan-Jun, Z. (2008). DBD plasma jet in atmospheric pressure argon. *IEEE Transactions on Plasma Science, 36,* 1352-1353.

Grundmann, H., Aires-de-Sousa, M., Boyce, J., & Tiemersma, E. (2006). Emergence and resurgence of methicillin resistant *staphylococcus aureus* as a public-health threat. *The Lancet*, *368,* 874-875.

Hähnel, M., Woedtke, V. T., & Weltmann, K. D. (2010). Influence of the air humidity. on the reduction of *bacillus* spores in a defined environment at atmospheric pressure using a dielectric barrier surface discharge. *Plasma Process Polym*er, *7,* 244-249.

Heinlin, J., Isbary, G., Stolz, W., Morfill, G., Landthaler, M., & Shimizu, T. (2011). Plasma applications in medicine with a special focus on dermatology. *Journal of the European Academy* of *Dermatology* and *Venereology, 25,* 1-11.

Heinlin, J., Morfill, G., Landthaler, M., Stolz, W., Isbary, G., & Zimmermann, J. L. (2010). Plasma medicine: possible applications in dermatology. *Journal of Dermatology, 8,* 968–976.

Hermann, H. W., Henins, I., Park, J., & Selwyn, G. S. (1999). Decontamination of jet chemical and biological warfare (CBW) agents using an atmospheric pressure plasma (APPJ). *Physic Plasmas, 6,* 2284-2296.

Hinz, B. (2007). Formation and function of the myofibroblast during tissue repair. *Journal of investigative Dermatology, 127,* 526-537.

Hirth, M. (1981). Beitr. *Plasma physics, 20,* 1-27.

Honda, K., & Naito, Y. (1955). On the nature of silent electrical discharge. *Journal of the Physical Society of Japan, 10,* 1007-1011.

Hong, Y. F., Kang, J. G., Lee, H. Y., Uhm, H. S., Moon, E., Park, Y. H. (2009). Sterilization effect of atmospheric plasma on *escherichia coli* and *bacillus subtilis* endospores. *Letter Applied Microbiol*ogy, *48,* 33-37.

Hubicka, Z., Cada, M., Sicha, M., Churpita, A., Pokorny, P., Soukup, L., & Jastrabik, L. (2002). Barrier torch discharge plasma source for surface treatment technology at atmospheric pressure. *Plasma Sources Science Technology, 112,* 195-202.

Isbary, G., Shimizu, T., Li, Y. F., Stolz, W., Thomas, H. M., & Morfill, G. E. (2013). Cold atmospheric plasma devices for medical issues. *Expert Revision Medicine Devices*, *10,* 367–377.

Janca, J., Klima, M., Slavicek, P., &Zajickova, L. (1999). HF plasma pencil- new source for plasma surface processing. *Surfing Coating Technology, 116,* 547-551.

Jeong, J. Y., Babayan, S. E., TúG, V. T. C., Selwyn, S., Robert, S., Hicks, F., & Henins, I. (1999). Etching materials with an atmospheric-pressure plasma jet. *Plasma Sources Science and Technology*, *7,* 1699-1789.

Jones, S. G., Edwards, R., & Thomas, D. W. (2004). Inflammation and wound healing: the role of bacteria in the immuno-regulation of wound healing. *International Journal Low Extreme Wounds, 3,* 201-208.

Jin, R. L., Gui, M. X., Xing, M. S., & Guan, J. Z. (2017). Low temperature plasma promoting fibroblast proliferation by activating the NF-κB pathway and increasing cyclinD1 expression. *Scientific Reports*, *7,* 1-12.

Kalghatgi, S., Fridman, A., Friedman, G., & Clyne, A. M. (2009a). Cell proliferation following non-thermal plasma is related to reactive oxygen species induced fibroblast growth factor-2 release. *IEEE Engineering in Medicine and Biology Society*, *10,* 6030-6033.

Kalghatgi, S., Friedman, G., Fridman, A., & Clyne, A. M. (2009b). Endothelial cell proliferation is enhanced by low dose non-thermal plasma through fibroblast growth factor-2 Release. *Analysis of Biomedical Engineering, 38,* 748-757.

Kalghatgi, S., Kelly, C., Cerchar, E., Torabi, B., Alekseev, O., Fridman, A., Friedman, G., & Azizkhan, C. J. (2011). Effects of nonthermal plasma on mammalian Cells. *Plos ONE*, *6,* 1-11.

Kim, S. J., Chung, T. H., Bae., S. H., & Leem, S. H. (2009). Cold atmospheric argon plasma jet source and its application for bacterial inactivation. *Applied Physics letters*, *94,* 1415-1427.

Kim, D. W., Kim, T. H., Park, H. W., & Park, D. W. (2011). Synthesis of nanocrys talline magnesium nitride (Mg_3N_2) powder using thermal plasma. *Applied. Surface Science, 257,* 5375-5379.

Kim, G. C., Kim, G. J., Park, S. R., Jeon, S. M., Seo, H. J., Iza, F., & Lee, J. K. (2009). Plasma coupled with antibody-conjugated nanoparticles: A new weapon against cancer. *Journal of Physics D: Applied Physics*, *42,* 3205-3311.

Kim, S. J., Chung, T. H., Bae, S. H., & Leem, S. H. (2009). Bacterial inactivation using atmospheric pressure single pin electrode microplasma jet with a ground ring. *Applied Physics Letters*, *94,* 1415-1418.

Kirkpatrick, M. J., Dodet, B., & Odic, E. (2007). Atmospheric pressure humid argon DBD plasma for the application of sterilization-measurement and simulation of hydrogen, oxygen, and hydrogen peroxide formation. *International Journal Plasma Environment Science Technology*, *1,* 96–101.

Klein, L., & Gibbs, R. (2004). Use if microbial cultures and antibiotics in the prevention of infection-associated preterm birth. *American Journal of Obstetrics and Gynecology, 190,* 493-502.

Klemenc, A., Hintenberger, H., & Höfer, H. (1937). About the discharge process in a Siemens ozone apparatus. *Electrochemistry*, *43,* 1503-1517.

Kogelschatz, U. (2002). Filamentary, patterned, and diffuse barrier discharges. *IEEE Transactions on Plasma Science, 30,* 1400-1408.

Kogelschatz, U. (2003). Dielectric-barrier discharges: Their history, discharge physics, and industrial applications. *Plasma Chemistry and Plasma Processing, 23,* 1-47.

Kogelschatz, U. (2005). "Industrial ozone generation: Historical perspective, current status and future Prospects". *CDROM Proceedings IOA 17th Ozone World Congress, Strasbourg F*, *11,* 1-16.

Kogelschatz, U. (2010). Collective phenomena in volume and surface barrier discharges. *Journal Physics: Conference Series, 257,* 38-43

Koinuma, H., Ohkubo, H., Hoshimoto, T., Inomata, K., Shiraishi, T., Miyanaga, A., & Hayashi, S. (1992). Development and application of microbeam plasma generator. *Applied Physics Letter, 60,* 816-817.

Kurihara, K., Sasaki, K., Kawarada, M., & Koshino, N. (1988). High-rate synthesis of diamond by DC plasma-jet chemical vapor-deposition. *Applied Physics Letter*, *52,* 437-438.

Lamb, C. M., & Garner, P. (2014). Selective non-operative management of civilian gun-shot wounds to the abdomen: A systematic review of the evidence. *International Journal of Quality for health Care, 45,* 659-666.

Langmuir, I. (1928). Oscillation in Ionized gases. *Proceedings of the National Academy of Sciences of the United States of America*, *14,* 627-637.

Laroussi, M. (1996). Sterilization of contaminated matter with an atmospheric pressure plasma. *IEEE Transactions on Plasma Science, 24,* 1188-1191.

Laroussi, M. (2005). Low temperature plasma based sterilization: Overview and state of-the-art. *Plasma Processes and Polymers, 2,* 391-400.

Laroussi, M., Alexeff, I., & Kang, W. (2000). Biological Decontamination by Non thermal Plasma. *IEEE Trans. Plasma Science, 28,*184-188.

Laroussi, M., Richardson, J. P., & Dobbs, F. C. (2002). Effects of non-equilibrium atmospheric pressure plasmas on the heterotrophic pathways of bacteria and on their cell morphology. *Applied Physics Letter, 81,* 772-783.

Laroussi, M., Sayler, G., Galscock, B., McCurdy, B., Pearce, M., Bright, N., Malott, C. (1999). Images of biological samples undergoing sterilization by a glow discharge at atmospheric pressure. *IEEE Transactions on Plasma Science, 27,* 34-35.

Lau, Y. T., Jayapalan, K. K., Pam, M. E., Chin, O. H., and Wong, C. S. (2014). Dependence of dielectric barrier discharge jet length on gas flow rate and applied voltage, *Journal of Science Technology in the Tropics*, *10,* 131-138.

Lee, H. W., Kim, G. J., Kim, J. M., Park, J. K., Lee, J. K., & Kim, G. C. (2009). Tooth bleaching with nonthermal atmospheric pressure plasma. *Journal of Endodontics*, *35,* 587-591.

Li, B., & Wang, J. H. (2011). Fibroblasts and myofibroblasts in wound healing: Force generation and measurement. *Journal of Tissue Viability, 20,* 108-120

Lin, L., Lyu, Y., Trink, V ., Canady, J*, &* Keidar, M. (2019). Cold atmospheric helium plasma jet in humid air environment. *Journal of Applied Physics*, *125,* 1250-1260.

Liu, D., Zhang, Z., Liu, Z., Wang, B., Li, Q., Wang, X., & Kong, M. G. (2018). Plasma jets with needle-ring electrodes: The insulated sealing of the needle and its effect on the plasma characteristics. *IEEE Transactions on Plasma Science*, 46, 2942-2948.

Liu, J. R., Xu, G. M., Shi, X. M., & Zhan, G. J. (2017). Low temperature plasma promoting fibroblast proliferation by activating the NF-κB pathway and increasing cyclinD1 expression, *Scientific Reports, 7,* 107-114.

Ling, K. T. (2012). Genetic and phenotip characterization of clinical methicillin stapyloccus. University Malaya. Retrieved from http://studentsrepo.um.edu.my/4333/

Lofty, K. (2017). Cold plasma jet construction to use in medical, biology and polymer applications. *Journal of Modern Physics*, *8,* 1901-1910

Lotfy, K. El-Raheem, H. A., & Al-Harbi, N. A. (2019). Cold atmospheric pressure nitrogen plasma jet for enhancement germination of wheat seeds. *Plasma Chemistry and Plasma Processing, 39,* 897-912.

Lu, Z. P., Stachowicz, L., Kong, P., Heberlein, J. & Pfender, E. (1991). Diamond synth esis by DC thermal plasma cvd at 1 atm. *Plasma Process*, *11,* 387-394.

Lu, X. P., Jiang, Z. H., Xiong, Q., Tang, Z. Y., Hu, X.W., & Pan, Y. (2008). An 11 cm long atmospheric pressure cold plasma plume for applications of plasma medicine. *Applied Physics Letter, 92,* 1502-1505.

Lu, X. P., Zhiyuang, T., & Zhonghe, J. (2008). A single electrode room-temperature plasma jet device for biomedical applications. *Applied Physics Letter*, *92,* 1504-1515.

Maisch, T., Shimizu, T., Li, Y. F., Heinlin, J., Karrer, S., & Morfill, G. (2012). Decolonisation of MRSA*, S. aureus* and *E. coli* by cold-atmospheric plasma using a porcine skin model in vitro. *Plos One*, *7,* 1-9.

Lu, X. P., Tao, Ye., Cao, Y. G., Sun, Z. Y., Xiong, Q., Tang, Z. Y., Xiong, Z. L., Hu, J., Jiang, Z. H., & Pan, Y. (2008). The roles of the various plasma agents in the inactivation of bacteria. *Journal of Applied Physics*, *104,* 1-6.

Manley, T. C. (1943). The electric characteristics of the ozonator discharge. *Transactions of Electrochemical Society*, *84,* 83-96.

Massines, F., Gherardi, N., Naude, N., & Segur, P. (2009). Recent advances in the understanding of homogeneous dielectric barrier discharges. *European Physical Journal Applied Physics*, *47,* 1-10.

Massines, F., Messaoudi, R., & Mayoux, C. (1998). Comparison between air filamentary and helium glow dielectric barrier discharges for the polypropylene surface treatment. *Plasmas Polym*er, *3,* 43-59.

Masuda, S., Akutsu, K., Kuroda, M., Awatsu, Y., & Shibuya, Y. (1988). A ceramic based ozonizer using high frequency discharge. *IEEE Transactions on Industry Applications*, *24,* 223-231.

Mendis, D. A., Rosenberg, M., & Azam, F. (2000). A note on the possible electrostatic disruption of bacteria. *IEEE Transactions on Plasma Science*, *28,* 1304-1306.

Mizuno, A. (2007). Industrial applications of atmospheric non-thermal plasma in environmental remediation. *Plasma Physics and Controlled Fusion*, *49,* 1-15.

Morfill, G. (2009). Nosocomical infections: A new approach towards preventive medicine using plasmas. *New Journal Physics*, *11,* 1367-1370.

Nagai, T., & Kawakami, M. (1991). Reduction of NOx emission from medium speed Diesel engines. *Bulletin of the M.E.S.J, 19,* 325-330.

Nan, X., Cui, X., Fang, Z., & Shi, Y. (2018). A two-mode portable atmospheric pressure air plasma jet device for biomedical applications. *IEEE Transactions on Plasma Science*, *99,* 1-7.

Ngo, M. H. T., Liao, J. D., Shao, P. L., Weng, C. C., & Chang, C. (2014). Increase fibroblast cells proliferation and migration using atmospheric N_2/Ar micro-plasma for the stimulated release of fibroblast growth factor-7. *Plasma Processes and Polymers*, *11,* 80-88.

Okazaki, S., Kogoma, M., Uehara, M., & Kimura, Y. (1993). Appearance of stable glow discharge in air, argon, oxygen and nitrogen at atmospheric pressure using 50 Hz source. *Journal of Physics D: Applied Physics, 26,* 889-892.

Osawa, N., Takashi, A., Yoshioka, Y., & Hanaoka, R. (2013). Generation of high pressure homogeneous dielectric barrier discharge in air. *European Physical Journal Applied Physics, 61,* 1-7.

Osawa, N., Yoshioka, Y. (2012). Generation of low-frequency homogeneous dielectric barrier discharge at atmospheric pressure. *IEEE Transactions on Plasma Science*, *40,* 2-8.

Papageorghiou, L., Panousis, E., Loiseau, J. F, Spyrou, N., & Held, B. (2009). Two-dimensional modelling of a nitrogen dielectric barrier discharge (DBD) at atmospheric pressure: Filament dynamics with the dielectric barrier on the cathode. *Journal of Physics D: Applied Physics*, *42,* 1-10.

Paschen, F. (1889). Analytical Physics. *273,* 69-75.

Peeters, F. J. J., Yang, R., & Van De Sanden, M. C. M. (2015). The relation between the production efficiency of nitrogen atoms and the electrical characteristics of a dielectric barrier discharge. *Plasma Sources Science and Technology*, *24,* 1-9.

Peeters, F., & Butterworth, T. (2018). Electrical diagnostics of dielectric barrier discharge. *Intech Open*, *7,* 1-27.

Pfender, E., & Capetti, A. (1989). Probe measurements in argon plasma jets operated in ambient argon. *Plasma Chemistry and Plasma Processing, 9,* 329-341.

Pieraggi, M. T., Bouissou, H., Angelier, C., Uhart, D., Magnol, J. P., & Kokolo, J. (1985). The fibroblast. *Ann Pathology*, *5,* 65-76.

Pondei, K., Fente, B. G., & Oladapo, O. (2013). Current microbial isolates from wound swabs. *Tropical Medical Health*, *41,* 49-53.

Rice, J. B., Desai, U., Cummings., A. K., Birnbaum, H. G., Skornicki, M., & Parsons, N. B. (2014). Burden of diabetic foot ulcers for medicare and private insurers. *Diabetes Care*, *37,* 651-658.

Sergey, A. S., Stefan, W., Yaoge, L., Bernadette, V. D. V. S., Jan, B. B., Mauritius, C. M., Van, D. S., & Hindrik, W. D. V. (2015). Dynamics of the atmospheric pressure diffuse dielectric barrier discharge between cylindrical electrodes in roll-to- roll PECVD reactor, *The European Physical Journal Applied Physics*, *71,* 1-6.

Sharkey, M. A., Chebbi, A., McDonnell, K. A., Staunton, C., and Dowling, D. P. (2015). Evaluation of the sensitivity of bacterial and yeast cells to cold atmospheric plasma jet treatments. *Biointerphases, 10,* 1-9.

Shashurin, X. & Wang, A. (2017). Study of atmospheric pressure plasma jet parameters generated by DC voltage driven cold plasma source. *Journal of Applied Physics, 122,* 1-6.

Shekhter, A. B., Serezhenkov, V.A, Rudenko, T.G., Pekshev, A.V, Vanin, A.F. (2005). Beneficial effect of gaseous nitric oxide on the healing of skin wounds. *Elsevier, 12,* 210-219.

Shekhter, A., B. Kabisov, R. K., Pekshev, A. V. Kozlov, N. P., & Perov, Y. L. (1998). Experimental and clinical validation of plasma dynamic therapy of wounds with nitric oxide. *Bulletin of Experimental Biology and Medicine, 126,* 829-839.

Shi, X. M., Xu, G. M., Zhang, G. J., Liu, J. R, Wu, Y. M., Gao, L. G., Yang, Y., Chang, Z. S., & Yao, C. W. (2018). Low temperature plasma promotes fibroblast proliferation in wound Healing by ROS-activated NF-κB signaling Pathway. *Current Medical Science*, *38,* 107-114.

Shigeta, M. (2018). Modeling and simulation of a turbulent-like thermal plasma jet for nanopowder production. *IEEJ Transactions on Electrical and Electronic Engineering*, 14, 16-28.

Shin, D., & Minn, K. W. (2004). The effect of myofibroblast on contracture of hypertrophic scar. *Plastic Reconstructive Surgery, 113,* 633–640.

Shrestha, R., Gurung, J. P., Subedi, D. P., & Wong, C. S. (2015). Atmospheric pressure single electrode argon plasma jet for biomedical applications. *International Journal of Emerging Technology and Advanced Engineering*, *5,* 193-198.

Siemens, W. (1857). Poggendorfs Ann. *Physical Chem*ical, *102,* 66-122.

Smith, R. S., Smith, T. J., Bliden, T. M., & Phipps, R. P. (1997). Fibroblasts as sentinel cells: Synthesis of chemokines and regulation of inflammation. *Journal of Pathology, 151,* 317–322.

Starostin, S. A., ElSabbagh, M. A. M., Aldea, Vries, H. D., Creatore, M., & Van De Sanden, M. C. M. (2008). Formation and expansion phases of an atmospheric pressure glow discharge in a PECVD reactor via fast ICCD imaging. *IEEE Transactions on Plasma Science*, *36,* 968-969.

Starostin, S. A,. Premkumar, P. A., Creatore, M., Van Veldhuizen, E. M, De Vries, H., Paffen, R. M. J, & Van de Sanden, M. C. M. (2009). On the formation mechanisms of the diffuse atmospheric pressure dielectric barrier discharge in CVD processes of thin silica-like films. *Plasma Sources Science and Technology*, *18,* 1-11.

Stoffels, E., Flikweert, A. J., Stoffels, W. W., Kroesen, G. M. W. (2003). Plasma Needle: A non destructive atmospheric plasma source for fine surface treatment of biomaterials. *Plasma Sources Science and Technology, 11,* 1-168.

Stollenwerk, L., Amiranashvili, S., Boeuf, J. P., & Purwins, H. G. (2007). Formation and stabilisation of single current filaments in planar dielectric barrier discharge. *European Physical Journal D: Atomic, Molecular, Optical and Plasma Physics*, *44,* 133-139.

Tanaka, M., Yagi, S. & Tabata, N., (1978). The observations of silent discharge by image intensifier. *Transaction IEE of Japan*, *98,* 57-62.

Thomas, E. S. (2014). A global perspective on wound care. *Advanced Wound Care*, *3,* 548-552.

Tipa, R. S., & Kroesen, G. M. W. (2011). Plasma-stimulated wound healing. *IEEE Transactions on Plasma Science*, *39,* 2978-2979.

Toda, K., Takaki, K., Kato, S., & Fujiwara, T. (2001). Removal of NO and NOx using a multipoint-type dielectric barrier discharge at a narrow gap. *Journal of Physics D: Applied Physics*, *34,* 2032-2029.

Tyata, R. B., Subedi, D. P., Shrestha, R., & Wong, C. S. (2013). Generation of uniform atmospheric pressure argon glow plasma by dielectric barrier discharge. *Pramana-Journal of Physics, 80,* 507-517.

Townsend, J. (1910). The theory of ionization of gases by collision. Retrieved from https://archive.org/details/theoryofionizati00townuoft/page/n6

Townsend, J. (1915). Electricity in Gases *(Oxford: Oxford University Press).*

Uhm, H. S., Lim, J. P., & Li, S. Z. (2007). Sterilization of bacterial endospores by an atmospheric pressure argon plasma jet. *Applied Physics Letters*, *90,* 1-4.

Usta, Y. H., Cukur, E. Yıldırım, C., & Ercan, U. K. (2019). Design of a portable, battery-powered non-thermal atmospheric plasma device and characterization of its antibacterial efficacies. *Journal of Electrostatics*, *99,* 1-8.

Veldhuizen, E. M., & Van. D. (2000). Electrical discharges for environmental purposes: Fundamentals and Applications. *New York: Nova Science*, *18,* 1-432.

Wagner, H. E., Yurgelenas, Y. V., & Brandenburg, R. (2005). The development of microdischarges of barrier discharges in N_2/O_2 mixtures-Experimental investigations and modelling. *Plasma Physics and Controlled Fusion*, *47,* 159-163.

Wang, C., Zhang, H., Xue, Z., Yin, H., Niu, Q., & Chen, H. (2015). The relation between doses or post-plasma time points and apoptosis of leukemia cells induced by dielectric barrier discharge plasma. *AIP advances*, *5,* 1-9.

Weltmann, K-D., Kindel, E., Brandenburg, R., Meyer, C., Bussiahn, R., Wilke C & Von, W. T. (2009). Atmospheric pressure plasma jet for medical therapy: plasma parameters and risk estimation. *Contribution Plasma Physics, 49,* 631-640.

Wang, M., Holmes, B. Cheng, X., Zhu, W., Keidar, M., & Zhang, L. G. (2013). Cold atmospheric plasma for selectively ablating metastatic breast cancer cells. *Plos one*, *8,* 1-11.

Wen, K., Liu, X. Zhou, K., Liu, M., Zhu, H., Huang, J., Zhang, Z., Huang, R., Mao. J., Liu, M., Yan, X., & Liao, H. (2019). 3D time-dependent numerical simulation for atmospheric plasma spraying. *Surface and Coatings Technology*, *371,* 344-354.

Werdin, F., Tennenhaus, M., Schaller, H. E & Rennekampff, H. O. (2009). Evidence-based management strategies for treatment of chronic wounds. *Eplasty, 9,* 169-179.

Werner, V. S. (1857). Poggendorfs Ann. *Physical Chemistry*, *102,* 1-10

Winter, J., Wende, K., Masur, K., Iseni, S., Dünnbier, M., Hammer, M. U., Tresp, H. (2013). Feed gas humidity affecting a cold atmospheric-pressure plasma jet and plasma-treated. *Journal of Physics D: Applied Physics, 46,* 29-38.

Xin, P. L. (2008). The roles of the various plasma agents in the inactivation of bacteria. *Journal of Applied Physics*, *5,* 11-16.

Xu, N., Cui, X., Fang, X., Senior Member, IEEE, Shi, Y., & Zhou, R. A two-mode portable atmospheric pressure air plasma jet device for biomedical applications. *IEEE Transactions on Plasma Science*, *46,* 947-953.

Xudong, Xu., & Kushner, M. J (1998). Multiple microdischarge dynamics in dielectric barrier discharges. *Journal of Applied Physics*, *84,* 4153-4150.

Yasuda, H., Iriyama, Y., (1989). Plasma polymerization. *Comprehensive Polymer Science and Supplements, 4,* 357-375.

Yoshie, K., Kasuya, S., Eguchi, K., & Yoshida, T. (1992). Novel Method for C-60 synthesis-a thermal plasma at atmospheric-pressure. *Applied Physics Letter, 61,* 2782-2783.

Wu, S., Lu, X., Xiong, Z., & Pan, Y. (2010). A touchable pulsed air plasma plume driven by DC power supply. *IEEE Transactions on Plasma Science*, *38,* 3404-3408.

LIST OF PUBLICATIONS AND PAPERS PRESENTED

1. **Norhayati, M. N**., Yap, S. L., Yap, S. S., Lee, B. K., & Thong, K. L. (2016). Cold plasma inactivation of chronic wound bacteria. *Archives of Biochemistry and Biophysics*, *605*, 76-85.

PAPERS PRESENTED

1. **Norhayati, M. N**., Yap, S. L., Yeang, T. S., Thong, K. L., & Partha, S. (2019). Effect of Atmospheric Pressure Plasma Jet in wound bacteria and cell proliferation. *XXXIV International Conference on Phenomena in Ionized Gases (XXXIV ICPIG) and the 10th International Conference on Reactive Plasmas, (ICRP-10).*

2. Yap, S. L., Lee, B. K, **Norhayati, M. N**., & Yap, S. S. (2015). Characteristics of Parallel-Plate Dielectric Barrier Discharge and Capillary-Guided Corona Discharge at Atmospheric Pressure. *10th Anniversary Asian-European International Conference on Plasma Surface Engineering, (AEPSE2015).*